**JOÃO PAULO HERRERA DA SILVA**

# ECOLOGICAL AND EVOLUTIONARY ASPECTS OF BEGOMOVIRUS POPULATIONS IN WILD HOSTS

Tese apresentada à Universidade Federal de Viçosa, como parte das exigências do Programa de Pós-Graduação em Fitopatologia, para obtenção do título de *Doctor Scientiae*

Orientador: Francisco Murilo Zerbini

**VIÇOSA**
**MINAS GERAIS – BRASIL**
**2024**

**Ficha catalográfica elaborada pela Biblioteca Central da Universidade Federal de Viçosa - Campus Viçosa**

T
S586e
2024

Silva, João Paulo Herrera da, 1987-
Ecological and evolutionary aspects of begomovirus populations in wild hosts / João Paulo Herrera da Silva. – Viçosa, MG, 2024.
1 tese eletrônica (123 f.): il. (algumas color.).

Texto em inglês.
Orientador: Francisco Murilo Zerbini Júnior.
Tese (doutorado) - Universidade Federal de Viçosa, Departamento de Fitopatologia, 2024.
Inclui bibliografia.
DOI: https://doi.org/10.47328/ufvbbt.2024.500
Modo de acesso: World Wide Web.

1. Vírus de plantas - Genética. 2. Begomovírus - Plantas hospedeiras. 3. Plantas silvestres. I. Zerbini Júnior, Francisco Murilo, 1966-. II. Universidade Federal de Viçosa. Departamento de Fitopatologia. Programa de Pós-Graduação em Fitopatologia. III. Título.

CDD 22. ed. 579.28

Bibliotecário(a) responsável: Euzébio Luiz Pinto CRB-6/3317

**JOÃO PAULO HERRERA DA SILVA**

# ECOLOGICAL AND EVOLUTIONARY ASPECTS OF BEGOMOVIRUS POPULATIONS IN WILD HOSTS

Tese apresentada à Universidade Federal de Viçosa, como parte das exigências do Programa de Pós-Graduação em Fitopatologia, para obtenção do título de *Doctor Scientiae*

APROVADA: 15 de março de 2024

Assentimento:

Documento assinado digitalmente
gov.br
JOAO PAULO HERRERA DA SILVA
Data: 16/08/2024 00:08:04-0300
Verifique em https://validar.iti.gov.br

João Paulo Herrera da Silva
Autor

Documento assinado digitalmente
gov.br
FRANCISCO MURILO ZERBINI JUNIOR
Data: 16/08/2024 08:59:01-0300
Verifique em https://validar.iti.gov.br

Francisco Murilo Zerbini Júnior
Orientador

## AGRADECIMENTOS

A minha mãe Geni, ao meu irmão José Mario, a minha irmã Ana Carolina e ao meu sobrinho Luiz Felipe, por todo suporte, compreensão, lições, amor e carinho devotados durante minha mera existência.

Aos meus queridos Olímpio, Maria José e Marina, por todo apoio, suporte, confiança e por terem feito parte da minha vida de alguma forma.

A Universidade Federal de Viçosa pela formação de excelência por proporcionar uma experiencia única durante os últimos 18 anos, uma trajetória que teve início no ensino médio e agora se encerra no doutorado.

Ao Departamento de Fitopatologia, pela oportunidade, formação recebida, experiencia proporcionada e pela estrutura disponibilizada.

Ao Laboratório de Ecologia e Evolução de Vírus, minha segunda casa, agradeço pelo acolhimento, pelo sólido treinamento proporcionado ao longo últimos 11 anos.

Ao professor Murilo Zerbini, por todo conhecimento transferido, pela confiança, conselhos e críticas.

A todos colegas de laboratório pelo convívio e paciência, meu muito obrigado aos mais próximos, Patrícia Goulart, Joaquim, Gloria, Baltazar, Lucas e Roberta. Em especial ao Cesar pelo apoio em muitas parcerias e pela amizade.

O presente trabalho foi realizado com apoio da Coordenação de Aperfeiçoamento de Pessoal de Nível Superior – Brasil (CAPES) – Código de Financiamento 001.

Dedico este trabalho a minha mãe Geni, aos meus irmãos Ana Carolina e José Mario *In memoriam*.

## RESUMO

Silva, João Paulo Herrera, DSc., Universidade Federal de Viçosa, março de 2024. **Aspectos ecológicos e evolucionários de populações de begomovírus em hospedeiros não-cultivados.** Orientador: Francisco Murilo Zerbini.

Diversos eventos de emergência de vírus ocorreram nas últimas décadas, tanto em plantas como em animais. Em geral, os begomovírus possuem altas taxas de mutação e recombinação, que juntas contribuem para o alto grau de adaptabilidade destes agentes. Os begomovírus são grandes ameaças à agricultura, especialmente nos países em desenvolvimento. O surgimento de novas doenças resulta muitas vezes da proximidade dos hospedeiros selvagens com os hospedeiros domésticos. As plantas não-cultivadas ("silvestres") representam fontes de diversidade viral e contribuem para eventos de *spillover* que são uma pré-condição para a emergência de vírus em plantas cultivadas. Diversos begomovírus foram descritos em plantas do gênero *Sida*, mas estudos que exploram a dinâmica ecológica e evolutiva de vírus restritos a plantas não-cultivadas fora de contextos agrícolas ainda são incipientes. Neste trabalho, realizou-se um estudo de 12 anos sobre a comunidade de begomovírus que infecta *Sida acuta* em uma pequena área com baixa intervenção humana. Os resultados indicam que *Sida acuta* é um hospedeiro do tipo *mixing vessel*. A comunidade de begomovírus em *Sida acuta* é composta por diversos vírus, muitos deles subdivididos em estirpes e variantes. Diversas mudanças na composição de espécies e variantes foram observadas durante a amostragem. Nos primeiros anos de coleta, o Oxalis yellow vein virus (OxYVV) foi o vírus mais abundante na área. A população de OxYVV era composta por duas estirpes e uma dessas estirpes era subdividida em cinco variantes. Uma mudança drástica ocorreu em 2016, quando o OxYVV foi superado pelo Sida yellow leaf curl virus (SiYLCV) em termos de frequência. Outros vírus foram detectados na área, mas em baixas frequências. As mudanças na composição de espécies dentro da comunidade podem ser resultado de um evento aleatório que reduziu o tamanho efetivo da

população de OxYVV, permitindo o estabelecimento do SiYLCV, ou da migração de vírus de outras áreas, explicando assim oocorrência de vírus que não tinham sido detectado anteriormente. Eventos de recombinação em isolados de SiYLCV fornecem pistas sobre a origem desta população. A hipótese de adaptabilidade diferencial entre as variantes de OxYVV foi testada, avaliando-se o acúmulo viral e a taxa de transmissão das variantes OxYVV-S1a e OxYVV-S1b. A variante OxYVV-S1a apresentou maior acúmulo nas fases iniciais da infecção, mas a carga viral diminuiu ao longo do tempo, eventualmente igualando-se à do OxYVV-S1b. Os ensaios de transmissão não indicaram grandes diferenças nas taxas de transmissão entre as duas variantes. Os resultados são consistentes com a hipótese de diferenças de adaptabilidade ao nível de replicação entre variantes de OxYVV.

Palavras-chaves: Vírus de plantas, Evolução, Diversidade genética, Begomovirus

## ABSTRACT

Silva, João Paulo Herrera, DSc., Universidade Federal de Viçosa, March 2024. **Ecological and evolutionary aspects of begomovirus populations in wild hosts.** Advisor: Francisco Murilo Zerbini.

Numerous virus emergence events took place in the last decades, in both plants and animals. In general, begomoviruses are recognized for their high rates of mutation and recombination, which together contribute to the high of fitness of these agents. Begomoviruses are major threats to agriculture, especially in developing countries. The emergence of new diseases often results from the proximity of wild hosts to domestic hosts. Weed and wild plants represent sources of viral diversity and contribute to spillover events which are a pre-condition to virus emergence in crops. Numerous begomoviruses have been described in plants of the genus *Sida*, but studies exploring the ecological and evolutionary dynamics of viruses restricted to wild plants outside agricultural contexts are still in their infancy. In this work, we carried out a 12-year study of the begomovirus community infecting *Sida acuta* in a small area with little human intervention. The results indicate that *Sida acuta* is a highly permissive host. The begomovirus community in *Sida acuta* is composed of several viruses, many of them subdivided into strains and variants. Several changes in the species and variant composition were observed during the sampling. In the first years of collection, Oxalis yellow vein virus (OxYVV) was the most abundant virus in the area. The OxYVV population was composed of two strains and one of these strains was subdivided into five variants. A drastic change occurred in 2016, when OxYVV was outnumbered by Sida yellow leaf curl virus (SiYLCV). Other viruses were detected in the area but at low frequencies. The changes in species composition within the community could be the result of a random event that reduced the effective size of the OxYVV population, allowing the establishment of SiYLCV, or of migration of viruses from other areas, thus explaining the occurrence of viruses that had not been detected before. Recombination events in SiYLCV

isolates provide clues to the origin of this population. The hypothesis of differential fitness among OxYVV variants was tested, evaluating viral accumulation and transmission rate of the OxYVV-S1a and OxYVV-S1b variants. The OxYVV-S1a variant showed greater accumulation in the early stages of infection, but viral load decreased over time, eventually equaling that of OxYVV-S1b. Transmission assays indicated no major differences in transmission rates between the two variants. The results are consistent with the hypothesis of fitness differences at the level of replication between OxYVV variants.

Keywords: Plant viruses, Evolution, Genetic diversity, Begomovirus

## SUMMARY

# GENERAL INTRODUCTION

Plant pathogens represent a major threat to food security, accounting for at least 10% of losses in global food production (Strange & Scott, 2005). In some regions, such as South and Central America, losses reach up to 50% in bean, corn and potato crops (Ristaino *et al.*, 2021).

It is estimated that at least half of the plant diseases that have emerged in recent decades are viral in nature (Anderson *et al.*, 2004). The emergence of viral diseases is governed by evolutionary and ecological factors. From an evolutionary point of view, genetic variation results from high rates of mutation and recombination, culminating in rapid evolutionary dynamics that result in the emergence of new species and variants (Dolan *et al.*, 2018; Duffy *et al.*, 2008; Elena *et al.*, 2014; Lima *et al.*, 2017). From an ecological perspective, factors that favor viral dispersal and spillover to new hosts include degradation of ecosystems and loss of biodiversity (Keesing *et al.*, 2010; Roossinck & Garcia-Arenal, 2015), agricultural practices based on monoculture, with high host densities (Burdon & Chilvers, 1982), and the exchange of propagative material and introduction of polyphagous vectors into new areas (Gilbertson *et al.*, 2015).

Understanding the evolutionary and ecological dynamics of viral populations is essential for the adoption of sustainable management practices, and also to allow the anticipation of threats and prevention of new epidemics (Dolan *et al.*, 2018; García-Arenal & Zerbini, 2019). The emergence of new diseases in agroecosystems has been associated with ecological changes, and two hypotheses that associate the diversity of ecosystems with the emergence of pathogens have been proposed. The "amplification effect" hypothesis postulates that the greater the diversity of an ecosystem, the greater the risk of epidemics, as there will be more sources of inoculum for target hosts. The "dilution effect" hypothesis associates the low diversity of ecosystems with the possibility of the emergence of new diseases, as it may result

in greater abundance of target host species. The amplification effect requires more generalist pathogens, while more specialist pathogens would better fit the dilution effect (Pagán *et al.*, 2012). Human activity has led to the simplification of ecosystems, increasing the chances of contact between wild and domesticated hosts, and thus increasing the probability of host jumps (spillover) (García-Arenal & Zerbini, 2019; Keesing *et al.*, 2010; Roossinck & Garcia-Arenal, 2015).

Begomoviruses (family *Geminiviridae*) constitute an important group of plant viruses with small, single-stranded DNA genomes, transmitted in a persistent circulative manner by insects of the *Bemisia tabaci* complex, and which infect a wide diversity of dicotyledonous plants (Brown *et al.*, 2015; Fiallo-Olive *et al.*, 2021; Navas-Castillo *et al.*, 2011; Stansly & Naranjo, 2010). Between the 1980's and 1990's, begomoviruses emerged in different areas of the world. Dozens of begomoviruses emerged in Latin America and the Caribbean infecting tomatoes, peppers and legumes (Morales & Anderson, 2001; Ribeiro *et al.*, 1998), in the African continent infecting cassava (Legg & Fauquet, 2004), in the Indian subcontinent infecting cotton and a number of vegetable crops (Borah & Dasgupta, 2012; Briddon & Markham, 2000), and in the Mediterranean basin infecting vegetable crops (Navas-Castillo *et al.*, 2011). It has been hypothesized that this explosion of emergencies is, at least in part, the result of lateral transfer from wild to domesticated hosts, and that the process was mediated by the global dispersal of *Bemisia argentifolii* and *Bemisia tabaci stricto sensu* (Gilbertson *et al.*, 2015). The ecological and epidemiological role of wild hosts has also become evident (Ribeiro *et al.*, 1998; Rocha *et al.*, 2013; Rybicki, 1994).

In general, spillover events fail, and the probability of a virus establishing itself in a new host population is low (Elena *et al.*, 2014). Since most plant viruses are propagated naturally by vectors, the success of a spillover event requires a fine adjustment of this multi-layer interaction, *i.e*, the virus and its vector(s) need to be adapted, or adapt quickly, to the new

environment. Adaptation to a new environment, such as a new host, requires sufficient genetic variability to be selected by natural selection and to escape random genetic drift (Elena *et al.*, 2014; García-Arenal & Zerbini, 2019). The recent emergence of SARS-CoV-2 represents a case of zoonotic spillover and dramatically reinforces the importance of monitoring viruses in wild hosts (Lytras *et al.*, 2021).

Begomoviruses have a high degree of genetic variability, with molecular evolution rates comparable to those of RNA viruses (Duffy & Holmes, 2008; Duffy & Holmes, 2009). This high genetic variability results from high mutational rates and frequent recombination events (Crespo-Bellido *et al.*, 2021; Lefeuvre & Moriones, 2015; Lima *et al.*, 2017; Pita *et al.*, 2001; Rojas *et al.*, 2005; Xavier *et al.*, 2021), and confers a high adaptive capacity which may facilitate the emergence of new viral diseases (Elena *et al.*, 2014; García-Arenal & Zerbini, 2019).

In theory, DNA viruses that use the host's DNA synthesis machinery for replication, which is the case of begomoviruses, should have low mutation rates due to the proofreading activity of the host's DNA polymerases (Zhao *et al.*, 2019). However, the exact way in which begomoviruses interact with the host's DNA synthesis machinery has not been determined. As far as is known, at least two DNA polymerases are involved in the replication of begomoviruses. DNA polymerase α is responsible for synthesizing the complementary strand, forming double-stranded (dsDNA) replication intermediates. This enzyme does not have proofreading activity. DNA polymerase δ is responsible for synthesizing new ssDNA genomes (Wu *et al.*, 2021), and during the repair of double-strand breaks it is prone to errors (Deem *et al.*, 2011; Hicks *et al.*, 2010). Although it is possible that other polymerases are involved in viral replication, these studies suggest that begomoviruses may not use proof-reading DNA polymerases during replication (Wu *et al.*, 2021). Furthermore, high mutation rates may be a result of oxidative stress, since nitrogenous bases in ssDNA molecules are more exposed to this type of stress

compared to dsDNA (Duffy *et al.*, 2008; Zhao *et al.*, 2019). Besides their high mutation rates, begomoviruses are also higly recombinogenic (Lefeuvre & Moriones, 2015), possibly due to a recombination-dependent replication strategy (Jeske *et al.*, 2001). Recombinant begomoviruses have been associated with the occurrence of several epidemics (Belabess *et al.*, 2015; Belabess *et al.*, 2016; Crespo-Bellido *et al.*, 2021; García-Andrés *et al.*, 2007; Idris & Brown, 2002; Monci *et al.*, 2002; Pita *et al.*, 2001; Zhou *et al.*, 1997; Zhou *et al.*, 1998).

Given the high genetic variability intrinsic to viruses, it is not uncommon for populations to be composed of multi-strains or multi-variants. Exploring the temporal dynamics of viral populations allows us to understand how the composition of populations changes over generations, as well as the relative contribution of evolutionary mechanisms that modulate diversity, aspects that may determine the success of a variant and/or the extinction of others within these populations (Domingo, 2020; Makau *et al.*, 2022; Silva, 2020).

The success of a variant within a population may depend on its adaptability. Fitness is defined as the ability of an individual to produce fertile (infectious, in the case of viruses) offspring. Several variables contribute to viral fitness (Cervera *et al.*, 2016; Domingo & Perales, 2019; Wargo & Kurath, 2012). Historically, greater attention has been paid to replicative fitness, transmission fitness and epidemiological fitness, the latter of which reflects the contribution of the first two together (Wargo & Kurath, 2012). Fitness is closely linked to the context, for example, a virus may have a different adaptive value in different genotypes of the same host, or there may be variation in the transmission rate depending on the composition of the vector population (Gautam *et al.*, 2022; Makau *et al.*, 2022; Ning *et al.*, 2015). Conversely, non-deterministic events, such as founder effects and genetic bottlenecks, can contribute to the success of a variant in the population, as they translocate the population to another point within an adaptive landscape, generating new opportunities for other variants, not necessarily the best

adapted ones, to become established (Betancourt *et al.*, 2008; Fraile *et al.*, 1997; Gallet *et al.*, 2018; Sacristan *et al.*, 2003; Zwart & Elena, 2015)

A large portion of the work that explores temporal aspects of viral populations has been conducted spanning large areas, often with some areas or time periods being overrepresented, that is, with unbalanced sampling (Sánchez-Campos *et al.*, 2002). Systematic sampling (standardized over time and location) can provide insights into how populations evolve locally and whether the variability found at a small scale reflects the variability found in large areas. In addition, it may provide information about how population structure is shaped over time, expanding our understanding of the ecological relationships between individuals within viral populations and communities.

Studies exploring multi-strains or multi-variant viral communities have been widely explored in human systems but are still incipient in non-human animal and plant systems (Makau *et al.*, 2022). In 2011, Godinho (2014) described a population of the begomovirus Oxalis yellow vein virus (OxYVV) infecting the non-cultivated plant *Sida acuta*, consisting of three variants identified based on sequence comparisons and phylogenetic relationships. Silva (2020), in a more comprehensive study, explored the temporal dynamics of begomovirus communities in the same location and host and observed variations in terms of distribution of the frequency of variants in the OxYVV population over time, hypothesizing that there were adaptive differences between the variants present in the area.

The objectives of this work were: i) To monitor the temporal dynamics of the begomovirus community in *Sida acuta*, in the same area, to uncover evolutionary and ecological aspects that govern the succession of species and variants within a non-agricultural landscape; ii) To assess whether there are differences in terms of fitness among the OxYVV variants found in *Sida acuta*.

**Literature Cited**


Anderson, P. K.; Cunningham, A. A.; Patel, N. G.; Morales, F. J.; Epstein, P. R.; Daszak, P. Emerging infectious diseases of plants: Pathogen pollution, climate change and agrotechnology drivers. **Trends in Ecology and Evolution**, v. 19, p. 535-544, 2004.

Belabess, Z.; Dallot, S.; El-Montaser, S.; Granier, M.; Majde, M.; Tahiri, A.; Blenzar, A.; Urbino, C.; Peterschmitt, M. Monitoring the dynamics of emergence of a non-canonical recombinant of tomato yellow leaf curl virus and displacement of its parental viruses in tomato. **Virology**, v. 486, p. 291-306, 2015.

Belabess, Z.; Peterschmitt, M.; Granier, M.; Tahiri, A.; Blenzar, A.; Urbino, C. The non-canonical tomato yellow leaf curl virus recombinant that displaced its parental viruses in Southern Morocco exhibits a high selective advantage in experimental conditions. **Journal of General Virology**, v. 97, p. 3433-3445, 2016.

Betancourt, M.; Fereres, A.; Fraile, A.; García-Arenal, F. Estimation of the Effective Number of Founders That Initiate an Infection after Aphid Transmission of a Multipartite Plant Virus. **Journal of Virology**, v. 82, p. 12416-12421, 2008.

Borah, B. K.; Dasgupta, I. Begomovirus research in India: A critical appraisal and the way ahead. **Journal of Biosciences**, v. 37, p. 791-806, 2012.

Briddon, R. W.; Markham, P. G. Cotton leaf curl virus disease. **Virus Research**, v. 71, p. 151-159, 2000.

Brown, J. K.; Zerbini, F. M.; Navas-Castillo, J.; Moriones, E.; Ramos-Sobrinho, R.; Silva, J. C.; Fiallo-Olive, E.; Briddon, R. W.; Hernandez-Zepeda, C.; Idris, A.; Malathi, V. G.; Martin, D. P.; Rivera-Bustamante, R.; Ueda, S.; Varsani, A. Revision of *Begomovirus* taxonomy based on pairwise sequence comparisons. **Archives of Virology**, v. 160, p. 1593-1619, 2015.

Burdon, J. J.; Chilvers, G. A. Host density as a factor in plant-disease ecology. **Annual Review of Phytopathology**, v. 20, p. 143-166, 1982.

Cervera, H.; Lalić, J.; Elena, S. F. Effect of Host Species on Topography of the Fitness Landscape for a Plant RNA Virus. **Journal of Virology**, v. 90, p. 10160-10169, 2016.

Crespo-Bellido, A.; Hoyer, J. S.; Dubey, D.; Jeannot, R. B.; Duffy, S. Interspecies recombination has driven the macroevolution of cassava mosaic begomoviruses. **Journal of Virology**, v. 95, p. e00541-00521, 2021.

Deem, A.; Keszthelyi, A.; Blackgrove, T.; Vayl, A.; Coffey, B.; Mathur, R.; Chabes, A.; Malkova, A. Break-induced replication is highly inaccurate. **PLOS Biology**, v. 9, p. e1000594, 2011.

Dolan, P. T.; Whitfield, Z. J.; Andino, R. Mechanisms and concepts in RNA virus population dynamics and evolution. **Annual Review of Virology**, v. 5, p. 69-92, 2018.

Domingo, E. Long-term virus evolution in nature. *In*: Domingo, E. (Ed.). **Virus as Populations (Second Edition)**: Academic Press, 2020. p. 225-261.

Domingo, E.; Perales, C. Viral quasispecies. **PLOS Genetics**, v. 15, p. e1008271, 2019.

Duffy, S.; Holmes, E. C. Phylogenetic evidence for rapid rates of molecular evolution in the single-stranded DNA begomovirus *Tomato yellow leaf curl virus*. **Journal of Virology**, v. 82, p. 957-965, 2008.

Duffy, S.; Holmes, E. C. Validation of high rates of nucleotide substitution in geminiviruses: Phylogenetic evidence from East African cassava mosaic viruses. **Journal of General Virology**, v. 90, p. 1539-1547, 2009.

Duffy, S.; Shackelton, L. A.; Holmes, E. C. Rates of evolutionary change in viruses: Patterns and determinants. **Nature Reviews Genetics**, v. 9, p. 267-276, 2008.

Elena, S. F.; Fraile, A.; Garcia-Arenal, F. Evolution and emergence of plant viruses. **Advances in Virus Research**, v. 88, p. 161-191, 2014.

Fiallo-Olive, E.; Lett, J. M.; Martin, D. P.; Roumagnac, P.; Varsani, A.; Zerbini, F. M.; Navas-Castillo, J. ICTV Virus Taxonomy Profile: *Geminiviridae* 2021. **Journal of General Virology**, v. 102, p. 001696, 2021.

Fraile, A.; Alonsoprados, J. L.; Aranda, M. A.; Bernal, J. J.; Malpica, J. M.; Garciaarenal, F. Genetic exchange by recombination or reassortment is infrequent in natural populations of a tripartite RNA plant virus. **Journal of Virology**, v. 71, p. 934-940, 1997.

Gallet, R.; Fabre, F.; Thebaud, G.; Sofonea, M. T.; Sicard, A.; Blanc, S.; Michalakis, Y. Small bottleneck size in a highly multipartite virus during a complete infection cycle. **Journal of Virology**, v. 92, p. e00139-00118, 2018.

García-Andrés, S.; Tomas, D. M.; Sanchez-Campos, S.; Navas-Castillo, J.; Moriones, E. Frequent occurrence of recombinants in mixed infections of tomato yellow leaf curl disease-associated begomoviruses. **Virology**, v. 365, p. 210-219, 2007.

García-Arenal, F.; Zerbini, F. M. Life on the edge: geminiviruses at the interface between crops and wild plant hosts. **Annual Review of Virology**, v. 6, p. 411-433, 2019.

Gautam, S.; Mugerwa, H.; Buck, J. W.; Dutta, B.; Coolong, T.; Adkins, S.; Srinivasan, R. Differential transmission of Old and New World begomoviruses by Middle East-Asia Minor 1 (MEAM1) and Mediterranean (MED) cryptic species of *Bemisia tabaci*. **Viruses**, v. 14, p. 1104, 2022.

Gilbertson, R. L.; Batuman, O.; Webster, C. G.; Adkins, S. Role of the insect supervectors *Bemisia tabaci* and *Frankliniella occidentalis* in the emergence and global spread of plant viruses. **Annual Review of Virology**, v. 2, p. 67-93, 2015.

Godinho, M. T. **Coexistência e evolução molecular de populações de begomovírus na planta não-cultivada *Sida acuta***. Orientador: Zerbini, F. M. 2014. 71 f. Tese D.S. - Dep. de Fitopatologia, Universidade Federal de Viçosa, Viçosa, MG.

Hicks, W. M.; Kim, M.; Haber, J. E. Increased mutagenesis and unique mutation signature associated with mitotic gene conversion. **Science**, v. 329, p. 82-85, 2010.

Idris, A. M.; Brown, J. K. Molecular analysis of cotton leaf curl virus-Sudan reveals an evolutionary history of recombination. **Virus Genes**, v. 24, p. 249-256, 2002.

Jeske, H.; Lutgemeier, M.; Preiss, W. DNA forms indicate rolling circle and recombination-dependent replication of *Abutilon mosaic virus*. **EMBO Journal**, v. 20, p. 6158-6167, 2001.

Keesing, F.; Belden, L. K.; Daszak, P.; Dobson, A.; Harvell, C. D.; Holt, R. D.; Hudson, P.; Jolles, A.; Jones, K. E.; Mitchell, C. E.; Myers, S. S.; Bogich, T.; Ostfeld, R. S. Impacts of biodiversity on the emergence and transmission of infectious diseases. **Nature**, v. 468, p. 647-652, 2010.

Lefeuvre, P.; Moriones, E. Recombination as a motor of host switches and virus emergence: Geminiviruses as case studies. **Current Opinion in Virology**, v. 10, p. 14-19, 2015.

Legg, J.; Fauquet, C. Cassava mosaic geminiviruses in Africa. **Plant Molecular Biology**, v. 56, p. 585-599, 2004.

Lima, A. T. M.; Silva, J. C. F.; Silva, F. N.; Castillo-Urquiza, G. P.; Silva, F. F.; Seah, Y. M.; Mizubuti, E. S. G.; Duffy, S.; Zerbini, F. M. The diversification of begomovirus populations is predominantly driven by mutational dynamics. **Virus Evolution**, v. 3, p. vex005, 2017.

Lytras, S.; Xia, W.; Hughes, J.; Jiang, X.; Robertson, D. L. The animal origin of SARS-CoV-2. **Science**, v. 373, p. 968-970, 2021.

Makau, D. N.; Lycett, S.; Michalska-Smith, M.; Paploski, I. a. D.; Cheeran, M. C. J.; Craft, M. E.; Kao, R. R.; Schroeder, D. C.; Doeschl-Wilson, A.; Vanderwaal, K. Ecological and evolutionary dynamics of multi-strain RNA viruses. **Nature Ecology & Evolution**, v. 6, p. 1414-1422, 2022.

Monci, F.; Sanchez-Campos, S.; Navas-Castillo, J.; Moriones, E. A natural recombinant between the geminiviruses tomato yellow leaf curl Sardinia virus and tomato yellow leaf curl virus exhibits a novel pathogenic phenotype and is becoming prevalent in Spanish populations. **Virology**, v. 303, p. 317-326, 2002.

Morales, F. J.; Anderson, P. K. The emergence and dissemination of whitefly-transmitted geminiviruses in Latin America. **Archives of Virology**, v. 146, p. 415-441, 2001.

Navas-Castillo, J.; Fiallo-Olivé, E.; Sánchez-Campos, S. Emerging virus diseases transmitted by whiteflies. **Annual Review of Phytopathology** v. 49, p. 219-248, 2011.

Ning, W. X.; Shi, X. B.; Liu, B. M.; Pan, H. P.; Wei, W. T.; Zeng, Y.; Sun, X. P.; Xie, W.; Wang, S. L.; Wu, Q. J.; Cheng, J. X.; Peng, Z. K.; Zhang, Y. J. Transmission of Tomato yellow leaf curl virus by *Bemisia tabaci* as affected by whitefly sex and biotype. **Scientific Reports**, v. 5, p. 8, 2015.

Pagán, I.; González-Jara, P.; Moreno-Letelier, A.; Rodelo-Urrego, M.; Fraile, A.; Piñero, D.; García-Arenal, F. Effect of biodiversity changes in disease risk: Exploring disease emergence in a plant-virus system. **PLOS Pathogens**, v. 8, p. e1002796, 2012.

Pita, J. S.; Fondong, V. N.; Sangare, A.; Otim-Nape, G. W.; Ogwal, S.; Fauquet, C. M. Recombination, pseudorecombination and synergism of geminiviruses are determinant keys to the epidemic of severe cassava mosaic disease in Uganda. **Journal of General Virology**, v. 82, p. 655-665, 2001.

Ribeiro, S. G.; Ávila, A. C.; Bezerra, I. C.; Fernandes, J. J.; Faria, J. C.; Lima, M. F.; Gilbertson, R. L.; Zambolim, E. M.; Zerbini, F. M. Widespread occurrence of tomato geminiviruses in Brazil, associated with the new biotype of the whitefly vector. **Plant Disease**, v. 82, p. 830, 1998.

Ristaino, J. B.; Anderson, P. K.; Bebber, D. P.; Brauman, K. A.; Cunniffe, N. J.; Fedoroff, N. V.; Finegold, C.; Garrett, K. A.; Gilligan, C. A.; Jones, C. M. The persistent threat of emerging plant disease pandemics to global food security. **Proceedings of the National Academy of Sciences, USA**, v. 118, p. e2022239118, 2021.

Rocha, C. S.; Castillo-Urquiza, G. P.; Lima, A. T. M.; Silva, F. N.; Xavier, C. a. D.; Hora-Junior, B. T.; Beserra-Junior, J. E. A.; Malta, A. W. O.; Martin, D. P.; Varsani, A.; Alfenas-Zerbini, P.; Mizubuti, E. S. G.; Zerbini, F. M. Brazilian begomovirus populations are highly recombinant, rapidly evolving, and segregated based on geographical location. **Journal of Virology**, v. 87, p. 5784-5799, 2013.

Rojas, M. R.; Hagen, C.; Lucas, W. J.; Gilbertson, R. L. Exploiting chinks in the plant's armor: evolution and emergence of geminiviruses. **Annual Review of Phytopathology**, v. 43, p. 361-394, 2005.

Roossinck, M. J.; Garcia-Arenal, F. Ecosystem simplification, biodiversity loss and plant virus emergence. **Current Opinion in Virology**, v. 10, p. 56-62, 2015.

Rybicki, E. P. A phylogenetic and evolutionary justification for three genera of *Geminiviridae*. **Archives of Virology**, v. 139, p. 49-77, 1994.

Sacristan, S.; Malpica, J. M.; Fraile, A.; Garcia-Arenal, F. Estimation of population bottlenecks during systemic movement of Tobacco mosaic virus in tobacco plants. **Journal of Virology**, v. 77, p. 9906-9911, 2003.

Sánchez-Campos, S.; Diaz, J. A.; Monci, F.; Bejarano, E. R.; Reina, J.; Navas-Castillo, J.; Aranda, M. A.; Moriones, E. High genetic stability of the begomovirus tomato yellow leaf curl Sardinia virus in southern Spain over an 8-year period. **Phytopathology**, v. 92, p. 842-849, 2002.

Silva, J. P. **Evolution of a DNA virus in the natural environment - a journey through time**. 2020. (M.Sc. Dissertation) - Dep. de Fitopatologia, Universidade Federal de Viçosa, Viçosa, MG, Brazil.

Stansly, P. A.; Naranjo, S. E. ***Bemisia*: Bionomics and management of a global pest**. Amsterdam: Springer, 2010. 904812459X.

Strange, R. N.; Scott, P. R. Plant disease: a threat to global food security. **Annual Review of Phytopathology**, v. 43, p. 83-116, 2005.

Wargo, A. R.; Kurath, G. Viral fitness: Definitions, measurement, and current insights. **Current Opinion in Virology**, v. 2, p. 538-545, 2012.

Wu, M.; Wei, H.; Tan, H.; Pan, S.; Liu, Q.; Bejarano, E. R.; Lozano-Duran, R. Plant DNA polymerases alpha and delta mediate replication of geminiviruses. **Nature Communications**, v. 12, p. 2780, 2021.

Xavier, C. a. D.; Godinho, M. T.; Mar, T. B.; Ferro, C. G.; Sande, O. F. L.; Silva, J. C.; Ramos-Sobrinho, R.; Nascimento, R. N.; Assuncao, I.; Lima, G. S. A.; Lima, A. T. M.; Zerbini, F. M. Evolutionary dynamics of bipartite begomoviruses revealed by complete genome analysis. **Molecular Ecology**, v. 15, p. 3747-3767, 2021.

Zhao, L.; Rosario, K.; Breitbart, M.; Duffy, S. Eukaryotic circular rep-encoding single-stranded DNA (CRESS DNA) viruses: ubiquitous viruses with small genomes and a diverse host range. **Advances in Virus Research**, v. 103, p. 71-133, 2019.

Zhou, X.; Liu, Y.; Calvert, L.; Munoz, C.; Otim-Nape, G. W.; Robinson, D. J.; Harrison, B. D. Evidence that DNA-A of a geminivirus associated with severe cassava mosaic disease in Uganda has arisen by interspecific recombination. **Journal of General Virology**, v. 78, p. 2101-2111, 1997.

Zhou, X.; Liu, Y.; Robinson, D. J.; Harrison, B. D. Four DNA-A variants among Pakistani isolates of cotton leaf curl virus and their affinities to DNA-A of geminivirus isolates from okra. **Journal of General Virology**, v. 79, p. 915-923, 1998.

Zwart, M. P.; Elena, S. F. Matters of size: genetic bottlenecks in virus infection and their potential impact on evolution. **Annual Review of Virology**, v. 2, p. 161-179, 2015.

# CHAPTER 1

## LONG-TERM DYNAMICS OF A BEGOMOVIRUS COMMUNITY IN THE NATURAL ENVIRONMENT

Herrera da Silva JP, Xavier CAD, Oliveira PGS, Godinho MT, Lage JB, Silva JCF, Lima ATM, Zerbini FM (2024) Long-term dynamics of a begomovirus community in the natural environment. **Journal of Virology**, *in preparation*.

**Long-term dynamics of a begomovirus community in the natural environment**

João P. Herrera da Silva[1], César A.D. Xavier[1#,] Phedra G.S. Oliveira[1&,] Márcio T. Godinho[1], Júlia B. Lage[1], José C.F. da Silva[2], Alison T.M. Lima[3], F. Murilo Zerbini[1*]

[1]Dep. de Fitopatologia/BIOAGRO, Universidade Federal de Viçosa, Viçosa, MG 36570-900, Brazil

[2]Horticultural Science Department, University of Florida, Gainesville, FL, USA

[3]Instituto de Ciências Agrárias, Universidade Federal de Uberlândia, Uberlândia, MG, Brazil

[#]Present address: Dep. of Entomology and Plant Pathology, North Carolina State University, Raleigh, NC, 27695, USA

[&]Present address: Dep. de Microbiologia/BIOAGRO, Universidade Federal de Viçosa, Viçosa, MG 36570-900, Brazil

[*]Corresponding author: Phone: (+55-31) 3612-2423, E-mail: zerbini@ufv.br

**Abstract**

Studies that address the temporal dynamics of viral communities provide us with an overview of the complex relationships between different populations. We explored the dynamics of a begomovirus community infecting *Sida acuta* (Malvaceae) over 12 years (2011-2022) in a 0.3 ha area of Atlantic Forest regeneration located in the municipality of Viçosa, MG. The community comprised five viruses (Oxalis yellow vein virus, OxYVV; Sida yellow leaf curl virus, SiYLCV; Sida micrantha mosaic virus, SimMV; Sida mottle virus, SiMV; and Macroptilium yellow vein virus, MaYVV). The OxYVV population is subdivided into strains S1 and -S2, and OxYVV-S1 is subdivided into five variants (S1a-e). The proportions of individuals of each species/strain/variant fluctuated over time, with OxYVV predominating during the initial years but being outnumbered by SiYLCV in 2016. A recombination event detected in SiYLCV could have improved its fitness and contributed to its dispersal. Alternatively, a genetic bottleneck could have reduced the size of the OxYVV population, allowing SiYLCV to become predominant. The low variability of the SiYLCV population and the maintenance of the same recombination event by all sequences suggest a common evolutionary origin for these isolates. Selection analysis indicates that the SiYLCV population has undergone negative selective. Our results expand our knowledge about the dynamics of begomovirus communities in the natural environment and open new avenues for future research.

## Introduction

Begomoviruses (family *Geminiviridae*) are whitefly-transmitted viruses that infect plants and have small, single-stranded, circular DNA genomes which can be mono- or bipartite (Fiallo-Olive et al., 2021). Monopartite begomoviruses, which are predominant in Europe, Africa, Asia and Oceania (EAAO), have genomes around 2.8 kilobases (kb) in length, while the bipartite begomoviruses, which are predominant in the Americas (AM), have two components, named DNA-A and DNA-B, each approximately 2.6 kb in length. The genetic content of the DNA-A and DNA-B differ in terms of function. The DNA-A encodes genes that are associated with viral replication, suppression of host defense responses, cell cycle reprogramming and particle assembly, while the DNA-B encodes genes which are associated with cell-to-cell and long distance movement in the plant (Hanley-Bowdoin et al., 2013). Begomoviruses have twinned, quasi-icosahedral particles formed by 110 subunits of a single structural (coat) protein. In the case of bipartite viruses, each component is encapsidated in a separate particle (Hesketh et al., 2018). Begomoviruses are transmitted by insects from the *Bemisia tabaci* species complex, which is made up of more than 40 morphologically indistinguishable species and whose taxonomy is based on the divergence of the mitochondrial cytochrome oxidase subunit I gene (Campbell et al., 2023; De Barro et al., 2011; Dinsdale et al., 2010; Lee et al., 2013).

The *Begomovirus* genus is the largest in the virosphere, with 445 species currently recognized by the International Committee on Taxonomy of Viruses (ICTV) (Fiallo-Olive et al., 2021). Several epidemics caused by begomoviruses have been documented around the world, among them the epidemic of cassava mosaic in Sub-Saharan Africa, the damage caused by a begomovirus complex in tomatoes in the Mediterranean, in cotton in the Indian Subcontinent, and in legume, solanaceous and cucurbit crops in the Americas (Rojas et al., 2018). The great diversity of begomoviruses is a result of their rapid evolutionary dynamics,

driven by mutation rates which are equivalent to those of RNA viruses, as well as frequent recombination events and genomic reassortment (Crespo-Bellido et al., 2021; Duffy and Holmes, 2008; Duffy and Holmes, 2009; Lefeuvre and Moriones, 2015; Lima et al., 2017; Xavier et al., 2021).

Besides evolutionary mechanisms, ecological changes such as environmental catastrophes, ecosystem degradation and global connectivity can also affect the emergence of viruses. These events can contribute to the displacement of pathogens and/or their respective vectors to new niches, consequently increasing the chances of contact between non-cultivated and cultivated hosts and enabling the occurrence of spillover events that lead to the expansion of the virus host range (García-Arenal and Zerbini, 2019; Kilpatrick and Randolph, 2012; Pybus et al., 2015; Roossinck and Garcia-Arenal, 2015).

In Brazil, the emergence of begomoviruses in tomatoes during the 1990's was driven by the introduction of *Bemisia argentifolii* (then known as *B. tabaci* biotype B) in the country (Ribeiro et al., 1998). This polyphagous "supervector" facilitated the spillover of a large number of begomoviruses from their natural hosts to tomatoes, with at least two, tomato severe rugose virus (ToSRV) and tomato mottle leaf curl virus (ToMoLCV), becoming established as serious pathogens in that crop (Fernandes et al., 2008; Rocha et al., 2013; Souza et al., 2022). The severe epidemics of cassava mosaic in Africa between the 1980s and 1990s were driven by a series of evolutionary events and ecological interactions: synergistic interactions between African cassava mosaic virus (ACMV) and East African cassava mosaic virus (EACMV) leading to higher accumulation of these viruses in mixed infections and increasing their chances of transmission; a recombination event in the CP gene of EACMV-UG2 that increased its vector transmission efficiency, causing it to become the prevalent virus in a short time after displacing EACMV-UG1; and reassortment events between ACMV and EACMV that increased their diversity (Pita et al., 2001). A number of begomoviruses from the tomato yellow leaf curl

complex have emerged and established themselves through recombination events, some of them leading to host range amplification (Belabess et al., 2016; Fiallo-Olivé et al., 2019; Monci et al., 2002; Yan et al., 2021).

The geographical range of viral hosts as well as a host's permissiveness to infections by multiple viruses impacts the epidemiology of viral diseases (Elena et al., 2014; García-Arenal and Zerbini, 2019; McLeish et al., 2021; Roossinck and Garcia-Arenal, 2015; Zamfir et al., 2023). In this sense, non-cultivated plants are essential players in the emergence of begomoviruses in agroecosystems, acting as viral reservoirs and as sources of genetic variability. The role of non-cultivated plants as begomovirus reservoirs has long been recognized (Costa and Carvalho, 1960; Frischmuth et al., 1997; Roye et al., 1997), and studies of begomovirus diversity in non-cultivated hosts gained special attention in the 21$^{st}$ century (Barreto et al., 2013; Castillo-Urquiza et al., 2008; Ferro et al., 2017; Fiallo-Olivé et al., 2010, 2012, 2013, 2015; Lima et al., 2013; Mar et al., 2017; Passos et al., 2017; Pinto et al., 2016; Silva et al., 2012; Wyant et al., 2011). Most of these investigations have been conducted in the context of agricultural production. Understanding the evolutionary dynamics of plant viruses in natural (non-agricultural) ecosystems could provide insights into how these organisms evolve without the pressures imposed by anthropogenic activity, making it possible to draw parallels between these two contexts and eventually leading to more effective strategies to mitigate virus emergence in crops (Dolan et al., 2018; García-Arenal and Zerbini, 2019).

The spatio-temporal evolutionary dynamics of geminiviruses has been addressed in a number of studies, expanding our understanding of the process. Temporal analyses of tomato yellow leaf curl virus (TYLCV), a monopartite begomovirus that infects tomato, were conducted in China over four years in the same location (Yang et al., 2014). Genetic differences were observed between populations sampled in different years. However, calculations of genetic differentiation coefficients did not indicate any evidence of genetic structuring over

time (Yang et al., 2014). Another study was conducted in Spain over eight years with tomato yellow leaf curl Sardinia virus (TYLCSV), a close relative of TYLCV. Monitoring of viral populations in three different regions of the country indicated low genetic variability, and no increase in genetic distance over time (Sánchez-Campos et al., 2002). Duffy and Holmes (2009) investigated the temporal trajectory of the bipartite begomovirus East African cassava mosaic virus (EACMV) using sequences retrieved from GenBank. They were able to estimate the evolutionary rate and to identify patterns of temporal structuring for the DNA-A but not for the DNA-B.

As mentioned above, all these studies were carried out under an agricultural context. Moreover, most studies that explored temporal aspects spanned large areas, and with some specific locations and/or time points being overrepresented in relation to others (Duffy and Holmes, 2009; Mar et al., 2017; Ramos-Sobrinho et al., 2014; Rodelo-Urrego et al., 2013; Sánchez-Campos et al., 2002; Yang et al., 2014).

In this work we explored the temporal dynamics of the begomovirus community infecting the non-cultivated plant *Sida acuta* (Malvaceae) over 12 years in the natural environment (outside of an agricultural context). Samples were collected annually in the same place and at the same time of year, always in late spring. We seek to understand how the diversity and variability of begomoviruses are distributed in small areas and whether they reflect the patterns observed in larger areas. Furthermore, we explored aspects associated with temporal diversification, seeking to understand how these viruses evolve under low anthropogenic influence compared to agroecosystems.

## Materials and Methods

### Data sampling

*Sida acuta* plants (family Malvaceae) exhibiting symptoms of begomovirus infection (Figure 1) were collected over a period of 12 years (2011-2022). Sampling was carried out in December of each year. The sampled field covers approximately 300 $m^2$, in a transition zone between remnants of Atlantic Forest and an urban area near the city of Viçosa, Minas Gerais state (-20.780960, -42.883434; Figure 2). The collection field is outside of an agricultural context, with very little (if any) human intervention. The local vegetation is made up of different species of plants from the Malvaceae, Euphorbiaceae and Solanaceae families, as well as grasses and small shrubs. Whiteflies are present sporadically in the area, in much smaller numbers compared to agricultural fields in the region. On average, 35 plants were collected annually, totaling 360 plants collected over 12 years. Each plant was identified, photographed, press-dried and stored at the Virus Ecology and Evolution Laboratory of the Federal University of Viçosa.

### Cloning and Sequencing

Total DNA from plant samples was extracted using the protocol described by Doyle and Doyle (1987). Approximately 1 ng of total DNA was used as a template for amplification of complete genomes using rolling circle amplification (RCA) (Inoue-Nagata et al., 2004). The multimeric molecules produced by RCA were treated with restriction enzymes to obtain genomic length, linear molecules of approximately 2,600 bp which were ligated to the pBLUESCRIPT-KS+ plasmid vector (Stratagene), previously digested with the same enzyme and dephosphorylated. Recombinant plasmids were transformed by electroporation into

*Escherichia coli* DH5α. The clones were completely sequenced at Macrogen Inc. (Seoul, South Korea).

**Genome assemblies and sequence comparisons**

The contigs were assembled using the Geneious software (Kearse et al., 2012). Following convention, the genomes were oriented to start at the cleavage site at the origin of replication (TAATATT//AC). Contigs were subjected to an initial search against the GenBank database using BLASTn (Altschul et al., 1990) to determine the most closely related viruses. Taxonomic assignments were carried out by pairwise sequence comparison analysis using Sequence Demarcation Tool (SDT) v. 1.2, according to the guidelines of the *Geminiviridae* Study Group of the ICTV (Brown et al., 2015). Begomovirus sequences with >91% pairwise identity corresponds to the same species. Isolates from the same species that presented >94% identity were considered as belonging to the same strain (Brown et al., 2015). Genetic content and genomic organization analisys were carried out using ORFfinder (Sayers et al., 2022).

**Multiple sequence alignments**

Multiple sequence alignments were constructed for each of the genomic components (DNA-A and DNA-B) as well as each of the ORFs encoded by each component using the MAFFT v. 7 algorithm (Katoh and Standley, 2013), using the default parameters.

**Phylogenetic analysis**

Maximum likelihood phylogenetic analysis were performed using RaxML-NG (Kozlov et al., 2019). The most suitable evolutionary model was determined using ModelTest-NG based on the Akaike Information Criterion (AIC) (Darriba et al., 2020). The analysis was performed

using 1,000 bootstrap replicates. Phylogenetic trees were reconstructed for both the complete data set and for data sets in which recombinant sequences were excluded.

**Assessment of the diversity of begomoviruses over time**

Diversity comparisons between samples collected in different years were based on the effective number of species (Hill numbers) (Hill, 1973) using the iNEXT package of R software (Hsieh et al., 2016). This metric allows the quantification of the species richness of a system and also its evenness. Diversity orders are estimated using the scaling parameter *q* (Alberdi and Gilbert, 2019). A diversity of order zero ($q$=0) is insensitive to the frequency of species in the container, thus favoring rare species and penalizing relative abundance. A value of $q$=1 weights the frequency of species and is not inflated by either rare or abundant species. A diversity of order two ($q$=2) is inflated by more abundant species (Alberdi and Gilbert, 2019; Jost, 2006). We defined our type as the number of DNA-A sequences of a given species per year, normalized to the number of plants analyzed each year. As the number of plants analyzed was not the same each year, we carried out rarefaction and extrapolation analyzes using iNEXT.

In addition to the conventional approach for estimating Hill numbers, we monitored the temporal trajectory of species that make up the viral community using a recently developed approach named KHILL (Narechania et al., 2023). The basis of the tool is the same, but it differs from the previous approach in that it is not based on counting to calculate diversity. Instead, this strategy is based on the diversity of information contained in *k*-mer libraries obtained from genomic data. The amount of information is thus accumulated, allowing for comparisons between containers based on the KHILL curve. Very homogeneous data sets (with high information overlap) will produce a KHILL equal to 1, while complex data sets without information overlap will generate a higher KHILL. The metric takes into account relative abundance, as populations with several species distributed in uniform proportions will produce

higher KHILL values than populations where one species prevails. This method is free from sequence alignment and tree construction. As in the previously described approach, our container were defined based on the sampling years.

**Estimates of genetic variability and genetic structure**

We calculated the average nucleotide diversity index, π (Nei, 1987), for both genomic segments and for each gene. Estimates of π values were computed through pairwise comparisons using a Python script developed by Lima et al. (2017). We then computed a 95% confidence interval for the mean values of π through a bootstrap test, with 1,000 non-parametric simulations using the boot package in R software (https://cran.r-project.org/web/packages/boot/boot.pdf). Additional variability indices were computed using DnaSP v. 6 (Rozas et al., 2017). Mutation biases were inferred by Maximum Composite Likelihood Estimation of the nucleotide substitution pattern in Mega 11 (Tamura et al., 2021). The nucleotide differentiation coefficient (Nst) was estimated using DnaSP v. 6.

**Temporal signal evaluation and demographic analysis**

We looked for signs of structuring over time in the populations. At first, we carried out an exploratory analysis and evaluated the quality of the temporal signal through a root-end correlation analysis carried out in TempEst (Rambaut et al., 2016). Although TempEst is widely used to infer temporal signal, other approaches such as Bayesian Evaluation of Temporal Signal (BETS) are more accurate for this purpose (Duchene et al., 2020). We performd simulations in BEAST with and without the dates of the sequences (Barido-Sottani et al., 2017), then estimated the marginal likelihood using nested sampling (Russel et al., 2018), and then computed the Bayes factor (Kass and Raftery, 1995). The molecular clock that best suited the data was determined based on the Bayes factor (Kass and Raftery, 1995). The trajectory of populations

over time was monitored through the construction of Bayesian skyline plots (Drummond et al., 2005) with a rate of 1.0 x$10^{-3}$, which is consistent with the documented rates for begomoviruses (Duffy and Holmes, 2009). The runs were carried out with a chain length equal to 100,000,000, and at the end of the run we evaluated the effective sample sizes (ESS) and checked if they were >200.

**Recombination analysis**

To investigate the occurrence of putative recombination events, multiple alignments of complete DNA-A and DNA-B sequences were scanned separately using the Rdp, Geneconv, Bootscan, Maximum χ2, Chimaera, Siscan and 3Seq methods implemented in the RDP5 (Martin et al., 2021) using default parameters. Statistical significance was inferred by *P* values lower than a Bonferroni-corrected $\alpha = 0.05$ cutoff. As recommended by the authors, only recombination events detected by at least four methods were considered reliable.

Phylogenetic networks were built with the aim of capturing phylogenetic inconsistencies caused by hybridization. The networks were inferred using the Neighbor-Net algorithm implementing in SplitsTree v. 4.19.2 (Huson and Bryant, 2006). Distances were computed using the GTR+G substitution model determinate in jModelTest2, using 1,000 bootstrap replications (Huson and Bryant, 2006).

To investigate recombination events on a fine scale, recombination rates were inferred throughout the genome. We estimated the average scaled recombination rate for the population (ρ) and the average rate across the genome using LDHat (McVean et al., 2002). We applied filtering for minor alleles at frequencies <1%. Analyzes were performed using 1,000,000 interactions, a blocking penalty of 5, sampling every 5,000 interactions and a burnin of 0.01. We used two different likelihood lookup tables, one with theta = 0.01 and the other with theta =0.001. The res-files. command was used to plot graphs of ρ variation across the genome using

the ggplot2 package in R (Wickham, 2009). Watterson's estimator of the mutation rate ($\theta_W$) was also calculated using LDHtat. Furthermore, we estimated the relative contribution of mutation and recombination to the diversification of the populations by calculating the population-scaled ratio between $\rho/\theta_W$. Some adjustments needed to be done to the OxYVV data set, since the likelihood lookup table available with theta =0.001 goes up to only 120 sequences and the OxYVV data set exceeded this value. As the computational cost to generate a likelihood lookup table is high, we adjusted the data set using CD-Hit (Fu et al., 2012), eliminating sequences with >99.96% identity and thus reducing the data set to 99 sequences.

**Selection analysis**

To identify potential sites that could be experiencing positive or negative selection, we performed selection analyzes for each of the coding regions of the genome of each species. Three methods were used to carry out these analyses: Single Likelihood Ancestor Counting (SLAC) (Kosakovsky-Pond and Frost, 2005), Mixed Effects Model of Evolution (MEME) (Murrell et al., 2012) and Fast Unconstrained Bayesian AppRoximation (FUBAR) (Murrell et al., 2013), all implemented in the DataMonkey webserver (Weaver et al., 2018). Relationships between synonymous and non-synonymous substitution rates ($\omega$) were calculated using SLAC. To avoid any artifacts in our analyses, a search for recombination breakpoints was carried out for each data set using the Genetic Algorithm Recombination Detection (GARD) (Pond et al., 2006). We also performed Tajima's D neutrality tests and Fu and Li's D* and F* statistics in DnaSP v. 6 (Rozas et al., 2017).

## Results

### *Sida acuta* is a "mixing vessel" host for begomoviruses

Over the course of 12 years, we collected 360 *Sida acuta* plants with symptoms of begomovirus infection (Figure 1) in the same small area (300 $m^2$) near Viçosa, MG (Figure 2). A total of 371 clones corresponding to full-length begomovirus genomic components were obtained from 242 plants, 262 corresponding to DNA-A and 109 corresponding to DNA-B (Table 1).

Following the 91% identity cut-off for species demarcation determined by the *Geminiviridae* Study Group of the ICTV (Brown et al., 2015; Fiallo-Olive et al., 2021), five species were detected (Table 1; Table 2). The most common virus was Oxalis yellow vein virus (OxYVV), with 162 DNA-A (127 haplotypes) and 52 DNA-B (40 haplotypes) clones, followed by Sida yellow leaf curl virus (SiYLCV) with 77 DNA-A (59 haplotypes) and 44 DNA-B (35 haplotypes) clones, Sida micrantha mosaic virus (SimMV) with 17 DNA-A (10 haplotypes) and 9 DNA-B (6 haplotypes) clones, Sida mottle virus (SiMV) with 5 DNA-A and 4 DNA-B clones, and Macroptilium yellow vein virus (MaYVV) with one DNA-A clone. Furthermore, by applying the 94% identity cut-off for strain demarcation (Brown et al., 2015), we found that the OxYVV population comprises two distinct strains, with isolates from each strain sharing a maximum identity of 93.8% with those from the other strain (Figure 3). Strain OxYVV-S1 is much more abundant, totaling 155 clones, and can be subdivided into five clusters (S1a, S1b, S1c, S1d and S1e), which we named variants since they present percentages of pairwise identity above the strain threshold (95-97% among groups; Figure 3). The other seven clones belong to the OxYVV-S2 strain. Although pairwise comparisons for SiYLCV indicate the formation of four groups, given their high degree of similarity (97.5-98% among groups) we decided to treat

them as a single variant (Figure 4). SimMV harbors two highly divergent variants that are very close to the strain demarcation threshold, with 93.8-94.5% identity between groups (Figure 5).

The phylogenetic tree inferred from the DNA-A showed four well supported clusters and one singleton corresponding to each of the species mentioned above (Figure 6). The cluster corresponding to OxYVV branches into six subclades, but the bootstrap support values of some of the branches that separate the OxYVV variants are low, possibly due to the high similarity between individuals (Figure 6; Suppl. Figure S1). The clade that harbors SiYLCV also presented several subclades but with short genetic distances, consistent with the classification of all the the isolates as a single variant (Figure 6; Suppl. Figure S2).

The phylogenetic tree of the DNA-B also formed four large clades corresponding to the four most prevalent species (Figure 7). The clade corresponding to OxYVV is subdivided into three well-supported subclades. A second clade corresponding to SiYLCV is subdivided into four subclades, all well supported, but with shorter phylogenetic distances when compared to the subclades formed by OxYVV isolates (Figure 7). The tree also has a singleton, but the species was not determined considering that the DNA-B has no taxonomic value (Brown et al., 2015) and no associated DNA-A was cloned from the sample.

Together, these results indicate that the sampled *Sida acuta* plants harbor a complex begomovirus community composed of at least five viruses, some of which can be divided into strains and variants. Taking into consideration the small sampling area, these results demonstrate how non-cultivated hosts may constitute sources of viral diversity.

**Temporal dynamics reveal fluctuations in the frequencies of viruses and their variants in the landscape**

Many changes were observed in the composition of viruses and variants over the years (Figure 8; Table 2). OxYVV was the prevalent virus from 2011 to 2014, with three variants

present (OxYVV-S1a, OxYVV-S1b, OxYVV-S1c). OxYVV-S1a was at a higher frequency since the first year and its frequency increased until 2014. The OxYVV-S1b variant had a lower frequency during this period, not being detected in 2013 or 2014. The OxYVV-S1c variant appeared in second place in terms of frequency, but its incidence was reduced in subsequent years. In 2013 a single plant infected with SiYLCV was detected for the first time. The year 2015 was a gap in our sampling. In 2016 there was a major change in the proportion of species and variants present at the site, with SiYLCV outnumbering OxYVV as the most common virus. Another change was that the OxYVV-S1b variant was detected again and this time at a higher frequency than OxYVV-S1a. In 2017 the frequency of variant OxYVV-S1a increased again, while OxYVV-S1b and SiLCV had a slight reduction in their frequencies. In 2018 we observed the local emergence of SimMV, with OxYVV-S1 and SiYLCV exhibiting balanced frequencies between themselves. In the three subsequent years there were fluctuations in the frequencies of these three viruses, but always with an alternation between OxYVV and SiYLCV in terms of predominance. The variant OxYVV-S1e emerged in 2020. The year 2021 marked the first detection of MaYVV and SiMV, in addition to the OxYVV-S2 strain. In 2022 we detected the two strains of OxYVV and the emergence of OxYVV-S1d (Figure 8).

Hill numbers were calculated with the aim of accessing diversity over time (Figure 9). We adopted this strategy because it translates into a simple and intuitive measure that allows us to compare the diversity of species that make up a community. Here we opted to use species counts to assess diversity; another option would be to use variant diversity, but this could make our interpretation confusing (see below). The years 2011, 2013 and 2014 had only one species detected, in which case all values converged to unity (Figure 9). The years 2012, 2016 and 2017 also had a very low diversity, and the overlap of the three orders of diversity in 2016 and 2017 indicates that two species were represented in similar proportions in those years (Figure 9; Suppl. Figure S3). In the years 2018, 2019, 2020 and 2022 the richness values were equal to 3,

and in 2021 the richness was equal to 5, the highest value observed in our time series. There was no significant difference between diversity orders 1 and 2 in the series from 2018 to 2022 (Figure 9; Suppl. Figure S3; Suppl. Table S1). The effective number of species approached richness in the years 2016, 2017, 2018 e 2020, indicating that in these years the community was dominated by equally abundant species.

To capture variations in diversity on a finer scale, we used an approach which is also based on Hill numbers, but which uses DNA sequences and calculates the degree of entropy. KHILL performs comparisons between unaligned substrings of length = *k*, thus the containers are considered as libraries of *k*-mers. The sets of *k*-mers were determined based on complete sequences, using sliding windows of *k*=19 (the program's default). *betaEnt* is a function of the sum of the contribution of each individual genome to total entropy, which in turn is given by the frequency at which this *k*-mer is represented within the sample. Total entropy is then used to determine KHILL, which is given by exp(betaEnt), providing a measure of diversity (Narechania et al., 2023). We noticed changes in the behavior of the KHILL curve that follow the dynamics of diversity changes over time (Figure 8). The KHILL curve was able to effectively capture changes in the diversity of species present at the site and beyond, being able to detect nuances in the dynamics of variants within the community. This can be observed in the first four years, as the KHILL values decrease together with the reduction in incidence of minor variants of OxYVV (Figure 8). The possible factors responsible for changes in the frequencies of species and variants will be addressed in the next sections.

**Measuring the genetic variability of begomoviruses in *Sida acuta***

The genetic variability of each virus was inferred separately. Due to the size of the data sets, we did these estimates only for three (OxYVV, SiYLCV SimMV) of the five viruses detected in the area. The other two viruses (SiMV and MaYVV) were represented by a very

small number of sequences (5 and 1 respectively). We estimated the variability for each genomic component and also for their genes by calculating the nucleotide diversity index, π (Table 3). In general, the DNA-B showed greater genetic variability compared to the DNA-A, as has already been reported for most bipartite begomoviruses (Briddon et al., 2010; Xavier et al., 2021). For both components, SimMV was the virus that showed the greatest variability, followed by OxYVV and then SiYLCV (Table 3). When we looked at each gene separately, *Rep* and *Ren* were the ones that showed the greatest variability. For the DNA-B, the *MP* gene of SimMV and OxYVV showed greater variability, while for SiYLCV the *NSP* gene had higher variability (Table 3).

Although all viruses were sampled from the same host species, large difference in nucleotide diversity were observed among them. To understand whether there was any mechanism favoring certain types of mutations in the genomes and being responsible for this variation, mutation bias was estimated based on the frequencies of the bases. A trend in the direction of changes was observed, with C->T, G->T and G->A being favoured (Table 4). This pattern was observed for the two components of the three species analyzed. Similar patterns have been reported (Duffy and Holmes, 2008; Duffy and Holmes, 2009; Ge et al., 2007; van der Walt et al., 2008), and have been attributed to base deamination (Caulfield et al., 1998).

**Absence of a temporal signal in OxYVV and SiYCV populations**

To investigate temporal structuring patterns, we estimated Nst values for the OxYVV and SiYLCV data sets. At various times we detected high values (>0.25) for both viruses (Figure 10a, b). The OxYVV 2021 subpopulation showed the highest degree of genetic differentiation in relation to the others, possibly due to the emergence of the OxYVV-S2 strain in this subpopulation (Figure 8; Figure 10a; Suppl. Fig. S1). The 2018 and 2019 subpopulations were made up of a single variant (OxYVV-S1a), while the 2011, 2016, 2020, 2021 and 2022

subpopulations were made up of multiple variants. The 2016 subpopulation is composed of variants S1a and S1b, however it is the only population where S1b is present at higher frequency. *Nst* values indicated a small degree of genetic differentiation between the 2016 and the 2014, 2018, 219 and 2021 subpopulations (Figure 8; Figure 10a). A similar pattern was observed for SiYLCV, in which the 2016 and 2017 subpopulations showed low levels of genetic differentiation from the 2019, 2021 and 2022 subpopulations (Figure 10b). This reflected the phylogenetic grouping pattern, in which the majority of isolates sampled in 2016 and 2017 grouped separately from those of 2019, 2021 and 2022 (Suppl. Figure S2).

We conducted root tip regression analyzes in TempEst for the OxYVV and SiYLCV populations. For the OxYVV data set we obtained a correlation coefficient of 0.4314 ($R^2$ = 0.1709), with a slope of $2.215x10^{-3}$ and 1994 as the Time to Most Recent Common Ancestor (TMRCA). The SiYLCV data set generated a correlation coefficient of 0.502 ($R^2$ = 0.2522), with a slope of $1.409x10^{-3}$ and TMRCA in 2008. The determination coefficients were low, indicating an absence of temporal signal for both data sets (Table 5).

**Recombination analysis**

Since the begomoviruses sampled in this study are part of the same community (with several cases of mixed infections), recombination was analyzed in an inter-specific data set including sequences from the five viruses. Interestingly, we were able to identify recombination events involving the DNA-A of at least one individual from each sampled species (Table 6a). Only one recombination event was detected for OxYVV, in a sequence (BR_VIC1006_1) of the S2 strain. The event involves a major parent of the same strain and an unknown minor parent. Conversely, all 77 SiYLCV sequences were identified as recombinants, in an event involving OxYVV as a minor parent and an unknown major parent (Table 6a). Three recombination events were detected for SimMV, one of which was strictly intraspecific and the

other two involved minor parents of the same species and unknown major parents (Table 6a). Two events were detected for SiMV, the first involving OxYVV and SiYLCV and the second involving SiYLCV and SimMV. We also detected evidence of recombination in MaYVV involving OxYVV as the main parent. Most of the recombination breakpoints were located between the intergenic region and the *Rep* gene, the only exception being event 8 where the breakpoints were located in the *CP* gene (Table 6a).

As for the DNA-B component, no significant recombination events were identified in the OxYVV population (Table 6b). Conversely, three recombination events were detected for SiYLCV (Table 6b). Event 7 was detected in all SiYLCV sequences analyzed and involved OxYVV and an unknown major parent. The second event was observed in 35 SiYLCV sequences, the major parent being unknown and the minor SiYLCV. The third event was an intraspecific recombination event detected in five SiYLCV sequences. A single SimMV DNA-B sequence showed evidence of intraspecific recombination (Table 6b). The breakpoints detected in the DNA-B varied in their location (Table 6b). For four of the seven events (events 2, 4, 5 and 7) the breakpoints were found in the larger intergenic region (LIR). The breakpoints of events 1 and 3 are located within the *MP* gene, while those of event 5 spanned part of the *NSP* gene up to the LIR.

The evolutionary history and the impact of recombination were captured by reconstructing phylogenetic networks. These networks, unlike phylogenetic trees, allow us to visualize the occurrence of lateral transfers of genomic regions between individuals. The DNA-A network formed five large clusters corresponding to each of the five viruses (Figure 11). The OxYVV cluster showed a clear division into six dense clusters with little cross-linking between them. One of these cross-links connects the BR_ViC_1006_1 sequence belonging to the OxYVV-S2 strain to the other individuals affiliated with the same strain, indicating a pattern of genetic exchange. SiYLCV formed a group separated by a long branch with rare

reticulations. Some reticulations connected the SiMV and OxYVV-S2 groups, indicating patterns of recombination between these viruses. Some edges are shared within the SimMV cluster. Also, exchange patterns were found between SimMV and MaYVV.

The DNA-B network also presented some crosslinking patterns. Five clusters were formed corresponding to each of the viruses (including the one for which the species was not identified). Edges connecting SiMV individuals were observed. Some side branches also connected SimMV and the unidentified virus, indicating possible recombination events (Figure 12).

We inferred the relative contribution of recombination and mutation to the diversification of the *S. acuta* begomovirus community by calculating the ratio between these two rates ($\rho/\theta$). In general, recombination rates were quite similar regardless of the mutation rate per site. For both components and most data sets, the $\rho/\theta$ ratio was <1 (Table 7), indicating a greater relative probability of the polymorphism being the result of mutation rather than recombination. The only case where there was a greater relative contribution of recombination was for SiYLCV (Table 7). Even though most of the ratios were <1, they can be considered high, revealing the important role of recombination as a driver of diversification.

Lastly, we mapped the distribution of recombination rates by base pairs per generation (mean $\rho$) across the genomes. In general, the most recombination-prone regions are the intergenic regions of each component (Figure 13). Nevertheless, recombination breakpoints were also detected in coding regions. In the cases of OxYVV and SiYLCV, breakpoint were located in the *CP* gene (Figure 13a, b) and for SimMV several small peaks mapped to the *Rep* gene and to the region that overlaps the *TrAP* and *REn* genes (13c). Due to the small number of sequences for SimMV DNA-B, we did not estimate these rates for this component.

**Evidence of recent population expansion, purifying selection and one gene under diversifying selection**

Neutrality tests were performed to investigate the role of selection in different coding regions. The tests were performed for the OxYVV and SiYLCV data sets but not for SiMVV, due to the small number of sequences in this data set and the detection of several recombination events, which could lead to misinterpretation of the results. We obtained negative and significant values for Tajima's *D*, Fu & Li *D*,* Fu an& Li *F** in some genes of OxYVV and SiYLCV (Table 8), indicating an abundance of rare alleles in the populations and suggesting that these genes underwent a selective sweep or expansion after a recent genetic bottleneck.

To identify the type of selection that is acting at the amino acid level in each region of the genome, we estimated ω (dN/dS) using the SLAC method. Most genes showed values of ω <1, indicating that purifying selection is acting on those genes (Table 8). The only exception was the *AC4* gene, which is under diversifying selection for both OxYVV and SiYLCV (Table 8). Furthermore, we observed that the intensity of selection on each of the genes varied. For example, OxYVV *CP, Rep, MP* and *NSP* genes are under strong negative selection, indicated by very low values of ω. On the other hand, OxYVVs *TrAP* and *REn* seem to experience more relaxed negative selection (Table 8). SiYLCV *CP, MP* and *NSP* are subject to strong restrictions imposed by purifying selection (Table 8).

Using SLAC, we identified several amino acid sites under negative selection and none under positive selection in the data sets. Using FUBAR, we were able to identify a larger number of sites under selection, including those detected by SLAC and several others also under negative selection, in addition to detecting some sites under positive selection (Table 8). We also found several sites on positive selection using MEME. In general, the *CP, Rep* and *MP* genes exhibited a greater number of sites under selection, with OxYVV being the virus that presented the largest number of sites (Table 8). Together, these results indicate that both viruses

experience slightly different selection regimes, evidenced by the number of sites detected in each of the data sets.

## Discussion

Systematic sampling and sequencing of an organism over time provides information that allows the tracking of changes in allele frequencies over generations, the identification of marks of natural selection, the detection of evidence of lateral transfer of genomic segments, and the monitoring of demographic processes, giving us an overview of the action of evolutionary mechanisms and their impacts on populations (Billard et al., 2023; Bondaryuk et al., 2023; Ghafari et al., 2024; Mühlemann et al., 2018; Preska Steinberg et al., 2023). Over more than a decade (2011-2022) we monitored a community of begomoviruses infecting *Sida acuta*, a non-cultivated host, in a small area with little, if any, human intervention. Remarkably, even in such a small are we observed a complex dynamic that involved several changes in terms of species, strain and variant composition within the landscape. Our results suggest the contribution of several mechanisms to the observed patterns. Evolution is a dynamic and complex process and evolutionary mechanisms may act simultaneously.

The importance of plants from the Malvaceae family as begomovirus hosts has been constantly reinforced by several studies describing new species in these hosts (Costa, 1955; Emmanuel et al., 2020; Ferro et al., 2017; Fiallo-Olivé et al., 2012; Fiallo-Olivé et al., 2015; Frischmuth et al., 1997; Jovel et al., 2004; Lima et al., 2021; Macedo et al., 2020; Passos et al., 2017; Pinto et al., 2016; Quadros et al., 2019; Tavares et al., 2012; Zubair et al., 2017), but studies aimed at understanding the evolution of begomoviruses restricted to wild plants are still incipient (Mar et al., 2017). We demonstrat that begomoviruses in *Sida acuta* co-exist in the form of a complex community formed by populations of three viruses (OxYVV, SiYLCV and SimMV) subdivided into strains and variants, plus at least two more viruses (SiMV and

MaYVV) present at a lower frequency. Thus, *Sida acuta* is a "mixing vessel" host, which are important players from an evolutionary and ecological point of view, serving as reservoirs and sources of viral genetic diversity (García-Arenal and Zerbini, 2019).

In terms of genetic variability, SimMV is the virus that presented the greatest variability, followed by OxYVV. SiYLCV has a very low degree of genetic variability when compared to the others. These observations at the species level were true for both genomic components. Moreover, the DNA-B components of all three viruses showed a higher degree of variability than their cognate DNA-A components, as previously reported for other begomoviruses infecting both non-cultivated and cultivated hosts (Xavier et al., 2021). There is direct and indirect evidence pointing to a differential accumulation between the two components, favoring the DNA-B (Pinto et al., 2021; Xiao et al., 2023). The higher the replication rate, the greater the chance of incorrect incorporation of bases (Duffy and Holmes, 2008). In addition, differential accumulation of two components can result in a reduction in the bottleneck effect for DNA-B (Billard et al., 2023; Pinto et al., 2021). Lastly, a large region of the DNA-A contains overlapping genes, which could impose strong selection pressure against mutations in these regions (Chen et al., 2019; Kutnjak et al., 2017; Xiao et al., 2023). Interestingly, even though they infect the same host in the same area, these viruses presented such distinct variability, suggesting distinct evolutionary trajectories. As previously suggested, the genetic variability of begomoviruses is independent of the nature of the host (Mar et al., 2017; Ramos-Sobrinho et al., 2014; Rocha et al., 2013).

Recombination is another important mechanism that generates genetic variability in begomoviruses, contributing to their rapid adaptation to new hosts and environmental conditions (Belabess et al., 2015; Crespo-Bellido et al., 2021; Davino et al., 2009; Lefeuvre and Moriones, 2015; Pita et al., 2001; Ribeiro et al., 2007; Zhou et al., 1997). Indeed, we identified highly reliable recombination events for both the DNA-A and DNA-B in all viruses, albeit at

different proportions. Interestingly, two recombination events were identified in SiYLCV, one in the DNA-A and the other in the DNA-B, both with OxYVV as the minor parent. These events could explain the drastic change in the community's species composition observed in 2016, and may have contributed to the increase in the adaptability of SiYLCV, allowing its co-existence with OxYVV. There is evidence that begomoviruses can co-exist in the same host, but their relative accumulation varies according to their adaptability, with the least adapted virus often being found at levels below the detection limit of conventional PCR amplification (Quadros et al., 2023). Several studies have already demonstrated that recombination may lead to the emergence of well adapted begomoviruses (Belabess et al., 2015; Davino et al., 2009; Monci et al., 2002; Padidam et al., 1999; Pita et al., 2001), so it is not unreasonable to propose that the recombination event between a SiYLCV-like parental and OxYVV generated a better adapted virus (SiYLCV) that became predominant in the community.

Three recombination events were identified in the SimMV DNA-A revealing the highly recombinant nature of this species. SimMV has a wide host range, which increases the probability of mixed infections increasing the chances of recombining with other viruses (Fernandes et al., 2009; Fernandes-Acioli et al., 2011; Fontenele et al., 2018; Jovel et al., 2004; Quadros et al., 2023).

The phylogenetic network constructed for OxYVV showed few cross-linking patterns, and indeed a single recombinant individual was identified in the OxYVV population using RDP and LDHat. To date, OxYVV has been reported only from *Oxalis debilis* (Herrera et al., 2015) and *Sida acuta* (this work), and its true host range is unknown. Nevertheless, *Sida acuta* is a host of several begomoviruses, which favors recombination events due to frequent mixed infections. Added to the high rates of recombination normally detected in begomoviruses (Padidam et al., 1999; Rocha et al., 2013), the absence of detected recombination events in OxYVV is surprising. It is possible that intraspecific recombination occurs between very

genetically similar individuals (>97% identity), which would make detection by the alignment-based methods in RDP very difficult. Alternatively, a virus that is extremely well adapted to its host may not generate recombinants with improved fitness (or do so at an exceedingly low frequency), and thus the recombinants which are generated (with lower fitness) will be purged from the population. Some examples that support this idea have been reported: no intraspecific recombination events were detected in populations of African cassava mosaic virus, bean golden mosaic virus and tomato severe rugose virus, three begomoviruses which are very well adapted to their hosts (cassava, common bean and tomato, respectively) (Lima et al., 2017; Xavier et al., 2021). But whether OxYVV is really well adpated to *Sida acuta* remains to be determined.

The neutrality test deviated from the hypothesis of neutral selection acting on populations, indicating evidence of a selective sweep or rapid expansion after a genetic bottleneck. The common origin of SiYLCV isolates suggests that this virus experienced a founder effect. The ω estimates point to strong evidence of purifying selection in most genes, except for *AC4*, which was shown to be under diversifying selection in most begomoviruses (Deom et al., 2021). *AC4* overlaps in its entirety with *Rep*. Overlapping genes can experience different types of selection, and usually the gene that is involved in accessory functions evolves freely, while the other involved in essential functions experiences more rigorous selective restrictions in order to preserve protein function (Deom et al., 2021; Martín-Hernández and Pagán, 2022; Rancurel et al., 2009). The AC4 protein has distinct functions in the viral infection cycle, which can vary depending on the virus (Medina-Puche et al., 2021). It was shown to be a suppressor of different host defense pathways (Li et al., 2019; Mei et al., 2020; Mei et al., 2021; Vanitharani et al., 2004), but also to confer drought tolerance to some hosts (Corrales-Gutierrez et al., 2020; Medina-Puche et al., 2020). It would be interesting to determine the precise function(s) of AC4 in the infection of *S. acuta* by OxYVV, which could shed some light

on the frequent association of begomoviruses with species of the *Sida* genus. Interestingly, amino acid sites under positive selection were identified in all OxYVV genes using MEME, and some were identified in three SiYLCV genes.

A hypothesis to explain the changes in species composition observed in 2016 would be the occurrence of a random event which resulted in a drastic reduction in the effective size of the OxYVV population. This genetic bottleneck could have altered the adaptive landscape, creating an opportunity for SiYLCV to establish itself in the area (Gallet et al., 2018; Zwart and Elena, 2015). Another hypothesis would be that changes in whitefly populations could have favored the transmission of SiYLCV in relation to OxYVV. It is known that the efficiency of viral transmission can vary among the species of the *Bemisia tabaci* complex (Gautam et al., 2022; Gottlieb et al., 2010). We did not sample whiteflies and therefore do not have information about the temporal dynamics of the vectors present in the area. Finally, we should not disregard the possibility of gene flow, which would be a reasonable explanation for the emergence of SimMV, SiMV and MaYSV. Expanding the sampling area would be of value as it could identify source populations. Another alternative would be to explore the dynamics of the landscape, sampling other hosts present in the location - perhaps these sources are not so far away. Possible differences in fitness among the viruses and variants deserve to be biologically tested. Competition assays between the viruses, strains and variants in different contexts can help answer many of the questions that are still open. Furthermore, construction of infectious clones of SiYLCV containing the reversal of the recombination event could clarify whether this event actually culminated in the displacement of OxYVV. These are the first contributions of a major effort to understand ecological and evolutionary processes of begomovirus communities infecting wild hosts outside the agricultural context.

## References


Alberdi, A., Gilbert, M.T.P., 2019. A guide to the application of Hill numbers to DNA-based diversity analyses. Mol Ecol Resour 19, 804-817.

Altschul, S.F., Gish, W., Miller, W., Myers, E.W., Lipman, D.J., 1990. Basic local alignment search tool. J Mol Biol 215, 403-410.

Barido-Sottani, J., Bošková, V., Plessis, L.D., Kühnert, D., Magnus, C., Mitov, V., Müller, N.F., PečErska, J., Rasmussen, D.A., Zhang, C., Drummond, A.J., Heath, T.A., Pybus, O.G., Vaughan, T.G., Stadler, T., 2017. Taming the BEAST - A community teaching material resource for BEAST 2. Syst Biol 67, 170-174.

Barreto, S.S., Hallwass, M., Aquino, O.M., Inoue-Nagata, A.K., 2013. A study of weeds as potential inoculum sources for a tomato-infecting begomovirus in central Brazil. Phytopathology 103, 436-444.

Belabess, Z., Dallot, S., El-Montaser, S., Granier, M., Majde, M., Tahiri, A., Blenzar, A., Urbino, C., Peterschmitt, M., 2015. Monitoring the dynamics of emergence of a non-canonical recombinant of tomato yellow leaf curl virus and displacement of its parental viruses in tomato. Virology 486, 291-306.

Belabess, Z., Peterschmitt, M., Granier, M., Tahiri, A., Blenzar, A., Urbino, C., 2016. The non-canonical tomato yellow leaf curl virus recombinant that displaced its parental viruses in Southern Morocco exhibits a high selective advantage in experimental conditions. J Gen Virol 97, 3433-3445.

Billard, E., Barro, M., Sérémé, D., Bangratz, M., Wonni, I., Koala, M., Kassankogno, A.I., Hébrard, E., Thébaud, G., Brugidou, C., Poulicard, N., Tollenaere, C., 2023. Dynamics of the rice yellow mottle disease in western Burkina Faso: Epidemic monitoring, spatio-temporal variation of viral diversity, and pathogenicity in a disease hotspot. Virus Evol 9, vead049.

Bondaryuk, A.N., Belykh, O.I., Andaev, E.I., Bukin, Y.S., 2023. Inferring evolutionary timescale of Omsk hemorrhagic fever virus. Viruses 15, 1576.

Briddon, R.W., Patil, B.L., Bagewadi, B., Nawaz-ul-Rehman, M.S., Fauquet, C.M., 2010. Distinct evolutionary histories of the DNA-A and DNA-B components of bipartite begomoviruses. BMC Evol Biol 10, 97.

Brown, J.K., Zerbini, F.M., Navas-Castillo, J., Moriones, E., Ramos-Sobrinho, R., Silva, J.C., Fiallo-Olive, E., Briddon, R.W., Hernandez-Zepeda, C., Idris, A., Malathi, V.G., Martin, D.P., Rivera-Bustamante, R., Ueda, S., Varsani, A., 2015. Revision of *Begomovirus* taxonomy based on pairwise sequence comparisons. Arch Virol 160, 1593-1619.

Campbell, L.I., Nwezeobi, J., van Brunschot, S.L., Kaweesi, T., Seal, S.E., Swamy, R.A.R., Namuddu, A., Maslen, G.L., Mugerwa, H., Armean, I.M., Haggerty, L., Martin, F.J., Malka, O., Santos-Garcia, D., Juravel, K., Morin, S., Stephens, M.E., Muhindira, P.V., Kersey, P.J., Maruthi, M.N., Omongo, C.A., Navas-Castillo, J., Fiallo-Olivé, E., Mohammed, I.U., Wang, H.-L., Onyeka, J., Alicai, T., Colvin, J., 2023. Comparative evolutionary analyses of eight whitefly *Bemisia tabac*i sensu lato genomes: Cryptic species, agricultural pests and plant-virus vectors. BMC Genomics 24, 408.

Castillo-Urquiza, G.P., Beserra Jr., J.E.A., Bruckner, F.P., Lima, A.T.M., Varsani, A., Alfenas-Zerbini, P., Zerbini, F.M., 2008. Six novel begomoviruses infecting tomato and associated weeds in Southeastern Brazil. Arch Virol 153, 1985-1989.

Caulfield, J.L., Wishnok, J.S., Tannenbaum, S.R., 1998. Nitric oxide-induced deamination of cytosine and guanine in deoxynucleosides and oligonucleotides. J Biol Chem 273, 12689-12695.

Chen, K., Khatabi, B., Fondong, V.N., 2019. The AC4 protein of a cassava geminivirus is required for virus infection. Mol Plant Microbe In 32, 865-875.

Corrales-Gutierrez, M., Medina-Puche, L., Yu, Y., Wang, L., Ding, X., Luna, A.P., Bejarano, E.R., Castillo, A.G., Lozano-Duran, R., 2020. The C4 protein from the geminivirus *Tomato yellow leaf curl virus* confers drought tolerance in Arabidopsis through an ABA-independent mechanism. Plant Biotechnol J 18, 1121-1123.

Costa, A.S., 1955. Studies on *Abutilon* mosaic in Brazil. J Phytopath 24, 97-112.

Costa, A.S., Carvalho, A.M.B., 1960. Comparative studies between *Abutilon* and *Euphorbia* mosaic viruses. J Phytopathol, 129-152.

Crespo-Bellido, A., Hoyer, J.S., Dubey, D., Jeannot, R.B., Duffy, S., 2021. Interspecies recombination has driven the macroevolution of cassava mosaic begomoviruses. J Virol 95, e00541-00521.

Darriba, D., Posada, D., Kozlov, A.M., Stamatakis, A., Morel, B., Flouri, T., 2020. ModelTest-NG: A new and scalable tool for the selection of DNA and protein evolutionary models. Mol Biol Evol 37, 291-294.

Davino, S., Napoli, C., Dellacroce, C., Miozzi, L., Noris, E., Davino, M., Accotto, G.P., 2009. Two new natural begomovirus recombinants associated with the tomato yellow leaf curl disease co-exist with parental viruses in tomato epidemics in Italy. Virus Res 143, 15-23.

De Barro, P.J., Liu, S.S., Boykin, L.M., Dinsdale, A.B., 2011. *Bemisia tabaci*: A statement of species status. Annu Rev Entomol 56, 1-19.

Deom, C.M., Brewer, M.T., Severns, P.M., 2021. Positive selection and intrinsic disorder are associated with multifunctional C4(AC4) proteins and geminivirus diversification. Sci Rep 11, 11150.

Dinsdale, A., Cook, L., Riginos, C., Buckley, Y.M., De Barro, P., 2010. Refined global analysis of *Bemisia tabaci* (Hemiptera: Sternorrhyncha: Aleyrodoidea: Aleyrodidae) mitochondrial cytochrome oxidase 1 to identify species level genetic boundaries. Ann Entomol Soc Am 103, 196-208.

Dolan, P.T., Whitfield, Z.J., Andino, R., 2018. Mechanisms and concepts in RNA virus population dynamics and evolution. Annu Rev Virol 5, 69-92.

Doyle, J.J., Doyle, J.L., 1987. A rapid DNA isolation procedure for small amounts of fresh leaf tissue. Phytochem Bull 19, 11-15.

Drummond, A.J., Rambaut, A., Shapiro, B., Pybus, O.G., 2005. Bayesian coalescent inference of past population dynamics from molecular sequences. Mol Biol Evol 22, 1185-1192.

Duchene, S., Lemey, P., Stadler, T., Ho, S.Y.W., Duchene, D.A., Dhanasekaran, V., Baele, G., 2020. Bayesian Evaluation of Temporal Signal in Measurably Evolving Populations. Mol Biol Evol 37, 3363-3379.

Duffy, S., Holmes, E.C., 2008. Phylogenetic evidence for rapid rates of molecular evolution in the single-stranded DNA begomovirus *Tomato yellow leaf curl virus*. J Virol 82, 957-965.

Duffy, S., Holmes, E.C., 2009. Validation of high rates of nucleotide substitution in geminiviruses: Phylogenetic evidence from East African cassava mosaic viruses. J Gen Virol 90, 1539-1547.

Elena, S.F., Fraile, A., Garcia-Arenal, F., 2014. Evolution and emergence of plant viruses. Adv Virus Res 88, 161-191.

Emmanuel, C.J., Manohara, S., Shaw, M.W., 2020. Molecular characterization of begomovirus-betasatellite-alphasatellite complex associated with okra enation leaf curl disease in Northern Sri Lanka. 3 Biotech 10, 506.

Fernandes, F.R., Albuquerque, L.C., Giordano, L.B., Boiteux, L.S., Ávila, A.C., Inoue-Nagata, A.K., 2008. Diversity and prevalence of Brazilian bipartite begomovirus species associated to tomatoes. Virus Genes 36, 251-258.

Fernandes, F.R., Cruz, A.R.R., Faria, J.C., Zerbini, F.M., Aragão, F.J.L., 2009. Three distinct begomoviruses associated with soybean in central Brazil. Arch Virol 154, 1567-1570.

Fernandes-Acioli, N.A.N., Pereira-Carvalho, R.C., Fontenele, R.S., Lacorte, C., Ribeiro, S.G., Fonseca, M.E.N., Boiteux, L.S., 2011. First report of *Sida micrantha mosaic virus* in *Phaseolus vulgaris* in Brazil. Plant Dis 95, 1196.

Ferro, C.G., Silva, J.P., Xavier, C.A.D., Godinho, M.T., Lima, A.T.M., Mar, T.B., Lau, D., Zerbini, F.M., 2017. The ever increasing diversity of begomoviruses infecting non-cultivated hosts: new species from *Sida* spp. and *Leonurus sibiricus*, plus two New World alphasatellites. Ann Appl Biol 170, 204-218.

Fiallo-Olivé, E., Chirinos, D.T., Geraud-Pouey, F., Moriones, E., Navas-Castillo, J., 2013. Complete genome sequences of two begomoviruses infecting weeds in Venezuela. Arch Virol 158, 277-280.

Fiallo-Olive, E., Lett, J.M., Martin, D.P., Roumagnac, P., Varsani, A., Zerbini, F.M., Navas-Castillo, J., 2021. ICTV Virus Taxonomy Profile: *Geminiviridae* 2021. J Gen Virol 102, 001696.

Fiallo-Olivé, E., Navas-Castillo, J., Moriones, E., Martinez-Zubiaur, Y., 2010. Two novel begomoviruses belonging to different lineages infecting *Rhynchosia minima*. Arch Virol 155, 2053-2058.

Fiallo-Olivé, E., Navas-Castillo, J., Moriones, E., Martinez-Zubiaur, Y., 2012. Begomoviruses infecting weeds in Cuba: Increased host range and a novel virus infecting *Sida rhombifolia*. Arch Virol 157, 141-146.

Fiallo-Olivé, E., Trenado, H.P., Louro, D., Navas-Castillo, J., 2019. Recurrent speciation of a tomato yellow leaf curl geminivirus in Portugal by recombination. Sci Rep 9, 1-8.

Fiallo-Olivé, E., Zerbini, F.M., Navas-Castillo, J., 2015. Complete nucleotide sequences of two new begomoviruses infecting the wild malvaceous plant *Melochia* sp. in Brazil. Arch Virol 160, 3161-3164.

Fontenele, R.S., Ribeiro, G.C., Lamas, N.S., Ribeiro, S.G., Costa, A.F., Boiteux, L.S., Fonseca, M.E.N., 2018. First report of *Sida micrantha mosaic virus* Infecting *Oxalis* species in Brazil. Plant Dis 102, 1862.

Frischmuth, T., Engel, M., Lauster, S., Jeske, H., 1997. Nucleotide sequence evidence for the occurrence of three distinct whitefly-transmitted, *Sida*-infecting bipartite geminiviruses in Central America. J Gen Virol 78, 2675-2682.

Fu, L., Niu, B., Zhu, Z., Wu, S., Li, W., 2012. CD-HIT: accelerated for clustering the next-generation sequencing data. Bioinformatics 28, 3150-3152.

Gallet, R., Fabre, F., Thebaud, G., Sofonea, M.T., Sicard, A., Blanc, S., Michalakis, Y., 2018. Small bottleneck size in a highly multipartite virus during a complete infection cycle. J Virol 92, e00139-00118.

García-Arenal, F., Zerbini, F.M., 2019. Life on the edge: geminiviruses at the interface between crops and wild plant hosts. Annu Rev Virol 6, 411-433.

Gautam, S., Mugerwa, H., Buck, J.W., Dutta, B., Coolong, T., Adkins, S., Srinivasan, R., 2022. Differential transmission of Old and New World begomoviruses by Middle East-Asia Minor 1 (MEAM1) and Mediterranean (MED) cryptic species of *Bemisia tabaci*. Viruses 14, 1104.

Ge, L.M., Zhang, J.T., Zhou, X.P., Li, H.Y., 2007. Genetic structure and population variability of tomato yellow leaf curl China virus. J Virol 81, 5902-5907.

Ghafari, M., Sõmera, M., Sarmiento, C., Niehl, A., Hébrard, E., Tsoleridis, T., Ball, J., Moury, B., Lemey, P., Katzourakis, A., Fargette, D., 2024. Revisiting the origins of the *Sobemovirus* genus: A case for ancient origins of plant viruses. PLOS Pathog 20, e1011911.

Gottlieb, Y., Zchori-Fein, E., Mozes-Daube, N., Kontsedalov, S., Skaljac, M., Brumin, M., Sobol, I., Czosnek, H., Vavre, F., Fleury, F., Ghanim, M., 2010. The transmission efficiency of tomato yellow leaf curl virus by the whitefly *Bemisia tabaci* is correlated with the presence of a specific symbiotic bacterium species. J Virol 84, 9310-9317.

Hanley-Bowdoin, L., Bejarano, E.R., Robertson, D., Mansoor, S., 2013. Geminiviruses: Masters at redirecting and reprogramming plant processes. Nat Rev Microbiol 11, 777-788.

Herrera, F., Aboughanem-Sabanadzovic, N., Valverde, R.A., 2015. A begomovirus associated with yellow vein symptoms of *Oxalis debilis*. Eur J Plant Pathol 142, 203-208.

Hesketh, E.L., Saunders, K., Fisher, C., Potze, J., Stanley, J., Lomonossoff, G.P., Ranson, N.A., 2018. The 3.3 Å structure of a plant geminivirus using cryo-EM. Nature Comm 9, 2369.

Hill, M.O., 1973. Diversity and evenness: A unifying notation and its consequences. Ecology 54, 427-432.

Hsieh, T.C., Ma, K.H., Chao, A., 2016. iNEXT: An R package for rarefaction and extrapolation of species diversity (Hill numbers). Met Ecol Evol 7, 1451-1456.

Huson, D.H., Bryant, D., 2006. Application of phylogenetic networks in evolutionary studies. Mol Biol Evol 23, 254-267.

Inoue-Nagata, A.K., Albuquerque, L.C., Rocha, W.B., Nagata, T., 2004. A simple method for cloning the complete begomovirus genome using the bacteriophage phi29 DNA polymerase. J Virol Met 116, 209-211.

Jost, L., 2006. Entropy and diversity. Oikos 113, 363-375.

Jovel, J., Reski, G., Rothenstein, D., Ringel, M., Frischmuth, T., Jeske, H., 2004. *Sida micrantha* mosaic is associated with a complex infection of begomoviruses different from *Abutilon mosaic virus*. Arch Virol 149, 829-841.

Kass, R.E., Raftery, A.E., 1995. Bayes Factors. J Am Stat Assoc 90, 773-795.

Katoh, K., Standley, D.M., 2013. MAFFT Multiple Sequence Alignment Software Version 7: Improvements in Performance and Usability. Mol Biol Evol 30, 772-780.

Kearse, M., Moir, R., Wilson, A., Stones-Havas, S., Cheung, M., Sturrock, S., Buxton, S., Cooper, A., Markowitz, S., Duran, C., Thierer, T., Ashton, B., Meintjes, P., Drummond, A., 2012. Geneious Basic: an integrated and extendable desktop software platform for the organization and analysis of sequence data. Bioinformatics 28, 1647-1649.

Kilpatrick, A.M., Randolph, S.E., 2012. Drivers, dynamics, and control of emerging vector-borne zoonotic diseases. Lancet 380, 1946-1955.

Kosakovsky-Pond, S.L., Frost, S.D.W., 2005. Not so different after all: A comparison of methods for detecting amino acid sites under selection. Mol Biol Evol 22, 1208-1222.

Kozlov, A.M., Darriba, D., Flouri, T., Morel, B., Stamatakis, A., 2019. RAxML-NG: a fast, scalable and user-friendly tool for maximum likelihood phylogenetic inference. Bioinformatics 35, 4453-4455.

Kutnjak, D., Elena, S.F., Ravnikar, M., 2017. Time-sampled population sequencing reveals the interplay of selection and genetic drift in experimental evolution of Potato virus Y. J Virol 91, e00690-00617.

Lee, W., Park, J., Lee, G.S., Lee, S., Akimoto, S.I., 2013. Taxonomic status of the *Bemisia tabaci* complex (Hemiptera: Aleyrodidae) and reassessment of the number of its constituent species. PLOS ONE 8, e63817.

Lefeuvre, P., Moriones, E., 2015. Recombination as a motor of host switches and virus emergence: Geminiviruses as case studies. Curr Opin Virol 10, 14-19.

Li, T., Huang, Y., Xu, Z.S., Wang, F., Xiong, A.S., 2019. Salicylic acid-induced differential resistance to the Tomato yellow leaf curl virus among resistant and susceptible tomato cultivars. BMC Plant Biol 19, 173.

Lima, A.T.M., Orílio, A.F., Almeida, M.M.S., Rocha, C.S., Barros, D.R., Castillo-Urquiza, G.P., Silva, F.N., Xavier, C.A.D., Bruckner, F.P., Alfenas-Zerbini, P., Barbosa, J.C., Albuquerque, L.C., Inoue-Nagata, A.K., Kitajima, E.W., Zerbini, F.M., 2021. Malvaviscus yellow mosaic virus, a divergent begomovirus carrying a nanovirus-like nonanucleotide and a modified stem-loop structure. Ann Appl Biol 179, 96-107.

Lima, A.T.M., Silva, J.C.F., Silva, F.N., Castillo-Urquiza, G.P., Silva, F.F., Seah, Y.M., Mizubuti, E.S.G., Duffy, S., Zerbini, F.M., 2017. The diversification of begomovirus populations is predominantly driven by mutational dynamics. Virus Evol 3, vex005.

Lima, A.T.M., Sobrinho, R.R., Gonzalez-Aguilera, J., Rocha, C.S., Silva, S.J.C., Xavier, C.A.D., Silva, F.N., Duffy, S., Zerbini, F.M., 2013. Synonymous site variation due to recombination explains higher genetic variability in begomovirus populations infecting non-cultivated hosts. J Gen Virol 94, 418-431.

Macedo, M.A., Rego-Machado, C.M., Maliano, M.L., Rojas, M.R., Inoue-Nagata, A.K., Gilbertson, R.L., 2020. Complete sequence of a new bipartite begomovirus infecting Sida sp. in Northeastern Brazil. Arch Virol 165, 253-256.

Mar, T.B., Xavier, C.A.D., Lima, A.T.M., Nogueira, A.M., Silva, J.C.F., Ramos-Sobrinho, R., Lau, D., Zerbini, F.M., 2017. Genetic variability and population structure of the New World begomovirus *Euphorbia yellow mosaic virus*. J Gen Virol 98, 1537-1551.

Martin, D.P., Varsani, A., Roumagnac, P., Botha, G., Maslamoney, S., Schwab, T., Kelz, Z., Kumar, V., Murrell, B., 2021. RDP5: A computer program for analyzing recombination in, and removing signals of recombination from, nucleotide sequence datasets. Virus Evol 7, veaa087.

Martín-Hernández, I., Pagán, I., 2022. Gene overlapping as a modulator of begomovirus evolution. Microorganisms 10.

McLeish, M.J., Fraile, A., García-Arenal, F., 2021. Population genomics of plant viruses: The ecology and evolution of virus emergence. Phytopathology 111, 32-39.

McVean, G., Awadalla, P., Fearnhead, P., 2002. A coalescent-based method for detecting and estimating recombination from gene sequences. Genetics 160, 1231-1241.

Medina-Puche, L., Orilio, A.F., Zerbini, F.M., Lozano-Duran, R., 2021. Small but mighty: Functional landscape of the versatile geminivirus-encoded C4 protein. PLOS Pathog 17, e1009915.

Medina-Puche, L., Tan, H., Dogra, V., Wu, M., Rosas-Diaz, T., Wang, L., Ding, X., Zhang, D., Fu, X., Kim, C., Lozano-Duran, R., 2020. A defense pathway linking plasma membrane and chloroplasts and co-opted by pathogens. Cell 182, 1109-1124.e1125.

Mei, Y., Ma, Z., Wang, Y., Zhou, X., 2020. Geminivirus C4 antagonizes the HIR1-mediated hypersensitive response by inhibiting the HIR1 self-interaction and promoting degradation of the protein. New Phytol 225, 1311-1326.

Mei, Y., Wang, Y., Hu, T., He, Z., Zhou, X., 2021. The C4 protein encoded by *Tomato leaf curl Yunnan virus* interferes with mitogen-activated protein kinase cascade-related defense responses through inhibiting the dissociation of the ERECTA/BKI1 complex. New Phytol 231, 747-762.

Monci, F., Sanchez-Campos, S., Navas-Castillo, J., Moriones, E., 2002. A natural recombinant between the geminiviruses tomato yellow leaf curl Sardinia virus and tomato yellow leaf curl virus exhibits a novel pathogenic phenotype and is becoming prevalent in Spanish populations. Virology 303, 317-326.

Mühlemann, B., Jones, T.C., Damgaard, P.d.B., Allentoft, M.E., Shevnina, I., Logvin, A., Usmanova, E., Panyushkina, I.P., Boldgiv, B., Bazartseren, T., Tashbaeva, K., Merz, V., Lau, N., Smrčka, V., Voyakin, D., Kitov, E., Epimakhov, A., Pokutta, D., Vicze, M., Price, T.D., Moiseyev, V., Hansen, A.J., Orlando, L., Rasmussen, S., Sikora, M., Vinner, L., Osterhaus, A.D.M.E., Smith, D.J., Glebe, D., Fouchier, R.A.M., Drosten, C., Sjögren, K.-G., Kristiansen, K., Willerslev, E., 2018. Ancient hepatitis B viruses from the Bronze Age to the Medieval period. Nature 557, 418-423.

Murrell, B., Moola, S., Mabona, A., Weighill, T., Sheward, D., Kosakovsky Pond, S.L., Scheffler, K., 2013. FUBAR: A fast, unconstrained bayesian approximation for inferring selection. Mol Biol Evol 30, 1196-1205.

Murrell, B., Wertheim, J.O., Moola, S., Weighill, T., Scheffler, K., Kosakovsky Pond, S.L., 2012. Detecting individual sites subject to episodic diversifying selection. PLOS Genet 8, e1002764.

Narechania, A., Bobo, D., Deitz, K., Desalle, R., Planet, P., Mathema, B., 2023. Hill numbers at the edge of a pandemic: Rapid SARS-COV2 surveillance using clinical, pooled, or wastewater sequence as a sensor for population change. medRxiv, 2022.2006.2023.22276807.

Nei, M., 1987. Molecular Evolutionary Genetics. Columbia University Press, New York.

Padidam, M., Sawyer, S., Fauquet, C.M., 1999. Possible emergence of new geminiviruses by frequent recombination. Virology 265, 218-224.

Passos, L.S., Teixeira, J.W.M., Teixeira, K.J.M.L., Xavier, C.A.D., Zerbini, F.M., Araújo, A.S.F., Beserra, J.E.A., 2017. Two new begomoviruses that infect non-cultivated malvaceae in Brazil. Arch Virol 162, 1795-1797.

Pinto, V.B., Quadros, A.F.F., Godinho, M.T., Silva, J.C., Alfenas-Zerbini, P., Zerbini, F.M., 2021. Intra-host evolution of the ssDNA virus tomato severe rugose virus (ToSRV). Virus Res 292, 198234.

Pinto, V.B., Silva, J.P., Fiallo-Olivé, E., Navas-Castillo, J., Zerbini, F.M., 2016. Novel begomoviruses recovered from *Pavonia* sp. in Brazil. Arch Virol 161, 735-739.

Pita, J.S., Fondong, V.N., Sangare, A., Otim-Nape, G.W., Ogwal, S., Fauquet, C.M., 2001. Recombination, pseudorecombination and synergism of geminiviruses are determinant keys to the epidemic of severe cassava mosaic disease in Uganda. J Gen Virol 82, 655-665.

Pond, S.L.K., Posada, D., Gravenor, M.B., Woelk, C.H., Frost, S.D.W., 2006. GARD: a genetic algorithm for recombination detection. Bioinformatics 22, 3096-3098.

Preska Steinberg, A., Silander, O.K., Kussell, E., 2023. Correlated substitutions reveal SARS-like coronaviruses recombine frequently with a diverse set of structured gene pools. Proc Natl Acad Sci U S A 120, e2206945119.

Pybus, O.G., Tatem, A.J., Lemey, P., 2015. Virus evolution and transmission in an ever more connected world. Proc Royal Soc B - Biol Sci 282, 20142878.

Quadros, A.F.F., Ferro, C.G., de Rezende, R.R., Godinho, M.T., Xavier, C.A.D., Nogueira, A.M., Alfenas-Zerbini, P., Zerbini, F.M., 2023. Begomovirus populations in single plants are complex and may include both well-adapted and poorly-adapted viruses. Virus Res 323, 198969.

Quadros, A.F.F., Silva, J.P., Xavier, C.A.D., Zerbini, F.M., Boari, A.J., 2019. Two new begomoviruses infecting tomato and Hibiscus sp. in the Amazon region of Brazil. Arch Virol 164, 1897-1901.

Rambaut, A., Lam, T.T., Max Carvalho, L., Pybus, O.G., 2016. Exploring the temporal structure of heterochronous sequences using TempEst (formerly Path-O-Gen). Virus Evol 2, vew007.

Ramos-Sobrinho, R., Xavier, C.A.D., Pereira, H.M.B., Lima, G.S.A., Assunção, I.P., Mizubuti, E.S.G., Duffy, S., Zerbini, F.M., 2014. Contrasting genetic structure between two begomoviruses infecting the same leguminous hosts. J Gen Virol 95, 2540-2552.

Rancurel, C., Khosravi, M., Dunker, A.K., Romero, P.R., Karlin, D., 2009. Overlapping genes produce proteins with unusual sequence properties and offer insight into de novo protein creation. J Virol 83, 10719-10736.

Ribeiro, S.G., Ávila, A.C., Bezerra, I.C., Fernandes, J.J., Faria, J.C., Lima, M.F., Gilbertson, R.L., Zambolim, E.M., Zerbini, F.M., 1998. Widespread occurrence of tomato geminiviruses in Brazil, associated with the new biotype of the whitefly vector. Plant Dis 82, 830.

Ribeiro, S.G., Martin, D.P., Lacorte, C., Simões, I.C., Orlandini, D.R.S., Inoue-Nagata, A.K., 2007. Molecular and biological characterization of *Tomato chlorotic mottle virus* suggests that recombination underlies the evolution and diversity of Brazilian tomato begomoviruses. Phytopathology 97, 702-711.

Rocha, C.S., Castillo-Urquiza, G.P., Lima, A.T.M., Silva, F.N., Xavier, C.A.D., Hora-Junior, B.T., Beserra-Junior, J.E.A., Malta, A.W.O., Martin, D.P., Varsani, A., Alfenas-Zerbini, P., Mizubuti, E.S.G., Zerbini, F.M., 2013. Brazilian begomovirus populations are highly

recombinant, rapidly evolving, and segregated based on geographical location. J Virol 87, 5784-5799.

Rodelo-Urrego, M., Pagán, I., González-Jara, P., Betancourt, M., Moreno-Letelier, A., Ayllón, M.A., Fraile, A., Piñero, D., García-Arenal, F., 2013. Landscape heterogeneity shapes host-parasite interactions and results in apparent plant-virus codivergence. Mol Ecol 22, 2325-2340.

Rojas, M.R., Macedo, M.A., Maliano, M.R., Soto-Aguilar, M., Souza, J.O., Briddon, R.W., Kenyon, L.A., Rivera-Bustamante, R.F., Zerbini, F.M., Adkins, S., Legg, J.P., Kvarnheden, A., Wintermantel, W.M., Sudarshana, M.R., Peterschmitt, M., Lapidot, M., Martin, D.P., Moriones, E., Inoue-Nagata, A.K., Gilbertson, R.L., 2018. World management of geminiviruses. Annu Rev Phytopathol 56, 637-677.

Roossinck, M.J., Garcia-Arenal, F., 2015. Ecosystem simplification, biodiversity loss and plant virus emergence. Curr Opin Virol 10, 56-62.

Roye, M.E., McLaughlin, W.A., Nakhla, M.K., Maxwell, D.P., 1997. Genetic diversity among geminiviruses associated with the weed species *Sida* spp., *Macroptilium lathyroides*, and *Wissadula amplissima* from Jamaica. Plant Dis 81, 1251-1258.

Rozas, J., Ferrer-Mata, A., Sánchez-DelBarrio, J.C., Guirao-Rico, S., Librado, P., Ramos-Onsins, S.E., Sánchez-Gracia, A., 2017. DnaSP 6: DNA sequence polymorphism analysis of large data sets. Mol Biol Evol 34, 3299-3302.

Russel, P.M., Brewer, B.J., Klaere, S., Bouckaert, R.R., 2018. Model Selection and Parameter Inference in Phylogenetics Using Nested Sampling. Syst Biol 68, 219-233.

Sánchez-Campos, S., Diaz, J.A., Monci, F., Bejarano, E.R., Reina, J., Navas-Castillo, J., Aranda, M.A., Moriones, E., 2002. High genetic stability of the begomovirus tomato yellow leaf curl Sardinia virus in southern Spain over an 8-year period. Phytopathology 92, 842-849.

Sayers, E.W., Bolton, E.E., Brister, J.R., Canese, K., Chan, J., Comeau, D.C., Connor, R., Funk, K., Kelly, C., Kim, S., Madej, T., Marchler-Bauer, A., Lanczycki, C., Lathrop, S., Lu, Z., Thibaud-Nissen, F., Murphy, T., Phan, L., Skripchenko, Y., Tse, T., Wang, J., Williams, R., Trawick, B.W., Pruitt, K.D., Sherry, S.T., 2022. Database resources of the National Center for Biotechnology Information. Nucleic Acids Res 50, D20-d26.

Silva, S.J.C., Castillo-Urquiza, G.P., Hora-Junior, B.T., Assunção, I.P., Lima, G.S.A., Pio-Ribeiro, G., Mizubuti, E.S.G., Zerbini, F.M., 2012. Species diversity, phylogeny and genetic variability of begomovirus populations infecting leguminous weeds in northeastern Brazil. Plant Pathol 61, 457-467.

Souza, J.O., Melgarejo, T.A., Vu, S., Nakasu, E.Y.T., Chen, L.F., Rojas, M.R., Zerbini, F.M., Inoue-Nagata, A.K., Gilbertson, R.L., 2022. How to be a successful monopartite begomovirus in a bipartite-dominated world: Emergence and spread of tomato mottle leaf curl virus in Brazil. J Virol 96, e0072522.

Tamura, K., Stecher, G., Kumar, S., 2021. MEGA11: Molecular Evolutionary Genetics Analysis Version 11. Mol Biol Evol 38, 3022-3027.

Tavares, S.S., Ramos-Sobrinho, R., Gonzalez-Aguilera, J., Lima, G.S.A., Assunção, I.P., Zerbini, F.M., 2012. Further molecular characterization of weed-associated begomoviruses in Brazil with an emphasis on *Sida* spp. Planta Dan 30, 305-315.

van der Walt, E., Martin, D.P., Varsani, A., Polston, J.E., Rybicki, E.P., 2008. Experimental observations of rapid Maize streak virus evolution reveal a strand-specific nucleotide substitution bias. Virol J 5, 104.

Vanitharani, R., Chellappan, P., Pita, J.S., Fauquet, C.M., 2004. Differential roles of AC2 and AC4 of cassava geminiviruses in mediating synergism and suppression of posttranscriptional gene silencing. J Virol 78, 9487-9498.

Weaver, S., Shank, S.D., Spielman, S.J., Li, M., Muse, S.V., Kosakovsky Pond, S.L., 2018. Datamonkey 2.0: A modern web application for characterizing selective and other evolutionary processes. Mol Biol Evol 35, 773-777.

Wickham, H., 2009. ggplot2: Elegant Graphics for Data Analysis. Springer New York, New York, NY.

Wyant, P.S., Gotthardt, D., Schafer, B., Krenz, B., Jeske, H., 2011. The genomes of four novel begomoviruses and a new *Sida micrantha mosaic virus* strain from Bolivian weeds. Arch Virol 156, 347-352.

Xavier, C.A.D., Godinho, M.T., Mar, T.B., Ferro, C.G., Sande, O.F.L., Silva, J.C., Ramos-Sobrinho, R., Nascimento, R.N., Assuncao, I., Lima, G.S.A., Lima, A.T.M., Zerbini, F.M., 2021. Evolutionary dynamics of bipartite begomoviruses revealed by complete genome analysis. Mol Ecol 15, 3747-3767.

Xiao, Y.X., Li, D., Wu, Y.J., Liu, S.S., Pan, L.L., 2023. Constant ratio between the genomic components of bipartite begomoviruses during infection and transmission. Virol J 20, 186.

Yan, Z., Wolters, A.A., Navas-Castillo, J., Bai, Y., 2021. The global dimension of Tomato Yellow Leaf Curl Disease: current status and breeding perspectives. Microorganisms 9.

Yang, X.L., Zhou, M.N., Qian, Y.J., Xie, Y., Zhou, X.P., 2014. Molecular variability and evolution of a natural population of *Tomato yellow leaf curl virus* in Shanghai, China. J Zhejiang Univ-Sc B 15, 133-142.

Zamfir, A.D., Babalola, B.M., Fraile, A., McLeish, M.J., Garcia-Arenal, F., 2023. Tobamoviruses show broad host ranges and little genetic diversity among four habitat types of a heterogeneous ecosystem. Phytopathology 113, 1697-1707.

Zhou, X., Liu, Y., Calvert, L., Munoz, C., Otim-Nape, G.W., Robinson, D.J., Harrison, B.D., 1997. Evidence that DNA-A of a geminivirus associated with severe cassava mosaic disease in Uganda has arisen by interspecific recombination. J Gen Virol 78, 2101-2111.

Zubair, M., Zaidi, S.S., Shakir, S., Farooq, M., Amin, I., Scheffler, J.A., Scheffler, B.E., Mansoor, S., 2017. Multiple begomoviruses found associated with cotton leaf curl disease in Pakistan in early 1990 are back in cultivated cotton. Sci Rep 7, 680.

Zwart, M.P., Elena, S.F., 2015. Matters of size: genetic bottlenecks in virus infection and their potential impact on evolution. Annu Rev Virol 2, 161-179.

**Table 1.** *Sida acuta* samples collected in Viçosa, MG, from 2011 to 2022, and the corresponding begomovirus clones obtained from each sample.

| Sample | Year | Isolate | Component | Enzyme | Species-variant |
|---|---|---|---|---|---|
| 01 | 2011 | BR-Vic01D5C | DNA-A | ClaI | OxYVV-S1a |
| | | BR-Vic01D1B | DNA-B | BamHI | OxYVV |
| 03 | 2011 | BR-Vic03D1C | DNA-A | ClaI | OxYVV-S1b |
| | | BR-Vic03D3C | DNA-A | ClaI | OxYVV-S1b |
| | | BR-Vic03D1B | DNA-B | BamHI | OxYVV |
| | | BR-Vic03D1B1 | DNA-B | BamHI | OxYVV |
| | | BR-Vic03D2B | DNA-B | BamHI | OxYVV |
| 04 | 2011 | BR-Vic04D1C | DNA-A | ClaI | OxYVV-S1c |
| | | BR-Vic04D1EV | DNA-A | EcoRV | OxYVV-S1c |
| | | BR-Vic04D3C | DNA-A | ClaI | OxYVV-S1a |
| 05 | 2011 | BR-Vic05D1C | DNA-A | ClaI | OxYVV-S1a |
| | | BR-Vic05D3B | DNA-B | BamHI | OxYVV |
| 06 | 2011 | BR-Vic06D1C | DNA-A | ClaI | OxYVV-S1a |
| | | BR-Vic06D2EV | DNA-A | EcoRV | OxYVV-S1a |
| | | BR-Vic06D1B | DNA-B | BamHI | OxYVV |
| 07 | 2011 | BR-Vic07D1C1 | DNA-A | ClaI | OxYVV-S1a |
| | | BR-Vic07D2C | DNA-A | ClaI | OxYVV-S1a |
| | | BR-Vic07D1B | DNA-B | BamHI | OxYVV |
| | | BR-Vic07D2B | DNA-B | BamHI | OxYVV |
| 09 | 2011 | BR-Vic09D1C | DNA-A | ClaI | OxYVV-S1a |
| | | BR-Vic09D3EV | DNA-A | EcoRV | OxYVV-S1a |
| | | BR-Vic09D1B | DNA-B | BamHI | OxYVV |
| 10 | 2011 | BR-Vic10D3C | DNA-A | ClaI | OxYVV-S1a |
| | | BR-Vic10D1B | DNA-B | BamHI | OxYVV |
| 12 | 2011 | BR-Vic12D1C | DNA-A | ClaI | OxYVV-S1a |
| | | BR-Vic12D2C | DNA-A | ClaI | OxYVV-S1a |
| | | BR-Vic12D1B | DNA-B | BamHI | OxYVV |
| 13 | 2011 | BR-Vic13D1B | DNA-B | BamHI | OxYVV |
| | | BR-Vic13D1B1 | DNA-B | BamHI | OxYVV |
| 14 | 2011 | BR-Vic14D1C | DNA-A | ClaI | OxYVV-S1a |
| | | BR-Vic14D2B | DNA-B | BamHI | OxYVV |
| 15 | 2011 | BR-Vic15D2C | DNA-A | ClaI | OxYVV-S1a |
| | | BR-Vic15D2C1 | DNA-A | ClaI | OxYVV-S1a |
| | | BR-Vic15D5C | DNA-A | ClaI | OxYVV-S1a |
| | | BR-Vic15D1B | DNA-B | BamHI | OxYVV |

| | | | | | |
|---|---|---|---|---|---|
| | | BR-Vic15D1C | DNA-B | ClaI | OxYVV |
| 16 | 2011 | BR-Vic16D2C | DNA-A | ClaI | OxYVV-S1a |
| | | BR-Vic16D2C1 | DNA-B | ClaI | OxYVV-S1a |
| | | BR-Vic16D3C | DNA-B | ClaI | OxYVV-S1a |
| 18 | 2011 | BR-Vic18D1EV | DNA-A | EcoRV | OxYVV-S1c |
| | | BR-Vic18D1C | DNA-B | ClaI | OxYVV-S1c |
| 19 | 2011 | BR-Vic19D1C | DNA-A | ClaI | OxYVV-S1c |
| | | BR-Vic19D2C | DNA-A | ClaI | OxYVV-S1c |
| | | BR-Vic19D1B | DNA-B | BamHI | OxYVV-S1c |
| 20 | 2011 | BR-Vic20D1C | DNA-B | ClaI | OxYVV |
| 23 | 2011 | BR-Vic23D4C | DNA-A | ClaI | OxYVV-S1a |
| | | BR-Vic23D1B | DNA-B | BamHI | OxYVV |
| 24 | 2011 | BR-Vic24D1C | DNA-A | ClaI | OxYVV-S1c |
| 27 | 2011 | BR-Vic27D1C | DNA-B | ClaI | OxYVV |
| 32 | 2011 | BR-Vic32D2B | DNA-B | BamHI | OxYVV |
| 36 | 2011 | BR-Vic36D1C | DNA-A | ClaI | OxYVV-S1c |
| 40 | 2011 | BR-Vic40D2C | DNA-A | ClaI | OxYVV-S1a |
| | | BR-Vic40D1C | DNA-B | ClaI | OxYVV-S1a |
| 41 | 2011 | BR-Vic41D3C | DNA-A | ClaI | OxYVV-S1c |
| | | BR-Vic41D3C1 | DNA-B | ClaI | OxYVV-S1c |
| 42 | 2011 | BR-Vic42D1C | DNA-B | ClaI | OxYVV |
| | | BR-Vic42D2C | DNA-B | ClaI | OxYVV |
| 44 | 2011 | BR-Vic44D1B | DNA-B | BamHI | OxYVV |
| | | BR-Vic44D3B | DNA-B | BamHI | OxYVV |
| 45 | 2011 | BR-Vic45D1EV | DNA-A | EcoRV | OxYVV-S1a |
| 46 | 2011 | BR-Vic46D1B | DNA-B | BamHI | OxYVV |
| | | BR-Vic46D2C | DNA-B | ClaI | OxYVV |
| 47 | 2011 | BR-Vic47D1C | DNA-A | ClaI | OxYVV-S1c |
| | | BR-Vic47D2C | DNA-A | ClaI | OxYVV-S1c |
| 104 | 2012 | BR-Vic104-4EV | DNA-A | EcoRV | OxYVV-S1a |
| 105 | 2012 | BR-Vic105-3EV | DNA-A | EcoRV | OxYVV-S1a |
| 106 | 2012 | BR-Vic106-1EV | DNA-A | EcoRV | OxYVV-S1a |
| | | BR-Vic106-5EV | DNA-A | EcoRV | OxYVV-S1a |
| 111 | 2012 | BR-Vic111-1EV | DNA-A | EcoRV | OxYVV-S1a |
| | | BR-Vic111-2EV | DNA-A | EcoRV | OxYVV-S1a |
| 112 | 2012 | BR-Vic112-1EV | DNA-A | EcoRV | OxYVV-S1c |
| 114 | 2012 | BR-Vic114-1C | DNA-A | ClaI | OxYVV-S1b |
| 116 | 2012 | BR-Vic116-5EV | DNA-A | EcoRV | OxYVV-S1c |
| 117 | 2012 | BR-Vic117-3EV | DNA-A | EcoRV | OxYVV-S1c |

| | | | | | |
|---|---|---|---|---|---|
| 119 | 2012 | BR-Vic119-1EV | DNA-A | EcoRV | OxYVV-S1a |
| 120 | 2012 | BR-Vic120-3EV | DNA-A | EcoRV | OxYVV-S1a |
| 123 | 2012 | BR-Vic123-2EV | DNA-A | EcoRV | OxYVV-S1a |
| 125 | 2012 | BR-Vic125-2EV | DNA-A | EcoRV | SiYLCV |
| 126 | 2012 | BR-Vic126-1EV | DNA-A | EcoRV | OxYVV-S1a |
| | | BR-Vic126-2EV | DNA-B | EcoRV | OxYVV |
| 128 | 2012 | BR-Vic128-4EV | DNA-A | EcoRV | OxYVV-S1a |
| 131 | 2012 | BR-Vic131-1EV | DNA-A | EcoRV | OxYVV-S1a |
| 132 | 2012 | BR-Vic132-2EV | DNA-A | EcoRV | OxYVV-S1a |
| 133 | 2012 | BR-Vic133-6C | DNA-A | ClaI | OxYVV-S1a |
| 136 | 2012 | BR-Vic136-1-C | DNA-A | ClaI | OxYVV-S1c |
| 201 | 2013 | BR-Vic201-1C | DNA-A | ClaI | OxYVV-S1c |
| 206 | 2013 | BR-Vic206-PT | DNA-A | PteI | OxYVV-S1a |
| 211 | 2013 | BR-Vic211-2C | DNA-A | ClaI | OxYVV-S1a |
| 212 | 2013 | BR-Vic212-1BS | DNA-A | BssHII | OxYVV-S1a |
| 215 | 2013 | BR-Vic215-1BS | DNA-A | BssHII | OxYVV-S1a |
| 218 | 2013 | BR-Vic218-1C | DNA-A | ClaI | OxYVV-S1a |
| 220 | 2013 | BR-Vic220-1BS | DNA-A | BssHII | OxYVV-S1a |
| 224 | 2013 | BR-Vic224-4bs | DNA-B | BssHII | SiYLCV |
| 225 | 2013 | BR-Vic225-4BS | DNA-A | BssHII | OxYVV-S1a |
| 226 | 2013 | BR-Vic226-1C | DNA-A | ClaI | OxYVV-S1a |
| 227 | 2013 | BR-Vic227-4BS | DNA-A | BssHII | OxYVV-S1a |
| 228 | 2013 | BR-Vic228-1C | DNA-A | ClaI | OxYVV-S1a |
| 229 | 2013 | BR-Vic229-2C | DNA-A | ClaI | OxYVV-S1a |
| 231 | 2013 | BR-Vic231-2BS | DNA-A | BssHII | OxYVV-S1c |
| 232 | 2013 | BR-Vic232-2BS | DNA-A | BssHII | OxYVV-S1a |
| 233 | 2013 | BR-Vic233-1C | DNA-A | ClaI | OxYVV-S1a |
| 237 | 2013 | BR-Vic237-1BS | DAN-A | BssHII | OxYVV-S1a |
| 253 | 2013 | BR-Vic253-2BS | DNA-A | BssHII | OxYVV-S1a |
| 256 | 2013 | BR-Vic256-1BS | DNA-A | BssHII | OxYVV-S1a |
| 301 | 2014 | BR-Vic301-1PT | DNA-B | PteI | SiYLCV |
| 303 | 2014 | BR-Vic303-1BS | DNA-A | BssHII | OxYVV-S1a |
| | | BR-Vic303-2-BS | DNA-A | BssHII | OxYVV-S1a |
| 304 | 2014 | BR-Vic304-6C | DNA-B | ClaI | SiYLCV |
| 307 | 2014 | BR-Vic307-1BS | DNA-A | BssHII | OxYVV-S1a |
| 309 | 2014 | BR-Vic309-1PT | DNA-A | PteI | OxYVV-S1c |
| 310 | 2014 | BR-Vic310-1C | DNA-A | ClaI | OxYVV-S1a |
| | | BR-Vic310-2C | DNA-B | ClaI | OxYVV-S1a |

| | | | | | |
|---|---|---|---|---|---|
| 311 | 2014 | BR-Vic311-2-BS | DNA-A | BssHII | OxYVV-S1a |
| | | BR-Vic311-6-BS | DNA-A | BssHII | OxYVV-S1a |
| 312 | 2014 | BR-Vic312-2BS | DNA-A | BssHII | OxYVV-S1a |
| 313 | 2014 | BR-Vic313-2BS | DNA-A | BssHII | OxYVV-S1a |
| 315 | 2014 | BR-Vic315-1C | DNA-A | ClaI | OxYVV-S1a |
| 317 | 2014 | BR-Vic317-2BS | DNA-A | BssHII | OxYVV-S1a |
| 318 | 2014 | BR-Vic318-1BS | DNA-A | BssHII | OxYVV-S1a |
| 319 | 2014 | BR-Vic319-2BS | DNA-A | BssHII | OxYVV-S1a |
| 320 | 2014 | BR-Vic320-2BS | DNA-A | BssHII | OxYVV-S1a |
| 321 | 2014 | BR-Vic321-10BS | DNA-A | BssHII | OxYVV-S1a |
| 323 | 2014 | BR-Vic323-3C | DNA-B | ClaI | OxYVV-S1a |
| | | BR-Vic323-6C | DNA-A | ClaI | OxYVV-S1a |
| 325 | 2014 | BR-Vic325-6PT | DNA-A | PteI | OxYVV-S1a |
| 326 | 2014 | BR-Vic326-1BS | DNA-A | BssHII | OxYVV-S1a |
| | | BR-Vic326-6BS | DNA-A | BssHII | OxYVV-S1a |
| 327 | 2014 | BR-Vic327-1BS | DNA-A | BssHII | OxYVV-S1a |
| 329 | 2014 | BR-Vic329-4BS | DNA-A | BssHII | OxYVV-S1a |
| 331 | 2014 | BR-Vic331-6PT | DNA-A | PteI | OxYVV-S1a |
| 334 | 2014 | BR-Vic334-19EV | DNA-A | EcoRV | OxYVV-S1a |
| 335 | 2014 | BR-Vic335-3PT | DNA-A | PteI | OxYVV-S1a |
| 337 | 2014 | BR-Vic337-5PT | DNA-A | PteI | OxYVV-S1a |
| 338 | 2014 | BR-Vic338-1PT | DNA-A | PteI | OxYVV-S1a |
| 401 | 2016 | BR-Vic401-1BS | DNA-A | BssHII | OxYVV-S1b |
| 403 | 2016 | BR-Vic403-5BS | DNA-A | BssHII | SIYLCV |
| 404 | 2016 | BR-Vic404-1BS | DNA-B | BssHII | SiYLCV |
| | | BR-Vic404-3PT | DNA-B | BssHII | SiYLCV |
| | | BR-Vic404-9BS | DNA-B | BssHII | SiYLCV |
| 405 | 2016 | BR-Vic405-1PT | DNA-A | PteI | OxYVV-S1b |
| 406 | 2016 | BR-Vic406-2BS | DNA-A | BssHII | OxYVV-S1b |
| 407 | 2016 | BR-Vic407-18C | DNA-A | ClaI | OxYVV-S1b |
| 408 | 2016 | BR-Vic408-1PT | DNA-A | PteI | OxYVV-S1b |
| 409 | 2016 | BR-Vic409-2PT | DNA-A | PteI | OxYVV-S1a |
| | | BR-Vic409-3PT | DNA-A | PteI | OxYVV-S1a |
| | | BR-Vic409-6PT | DNA-A | PteI | OxYVV-S1a |
| 410 | 2019 | BR-Vic410-13PT | DNA-A | PteI | OxYVV-S1a |
| 411 | 2016 | BR-Vic411-3PT | DNA-B | PteI | SiYLCV |
| 412 | 2016 | BR-Vic412-12EV | DNA-A | EcoRV | SiYLCV |
| 414 | 2016 | BR-Vic414-1PT | DNA-A | PteI | SiYLCV |
| | 2016 | BR-Vic414-16PT | DNA-B | PteI | n.d. |

| | | | | | |
|---|---|---|---|---|---|
| 415 | 2016 | BR-Vic415-5BS | DNA-A | BssHII | SiYLCV |
| | | BR-Vic415-7BS | DNA-B | BssHII | SiYLCV |
| 416 | 2016 | BR-Vic416-2BS | DNA-A | BssHII | SiYLCV |
| | | BR-Vic416-PT | DNA-A | PteI | SiYLCV |
| 418 | 2016 | BR-Vic418-2BS | DNA-B | BssHII | SiYLCV |
| 419 | 2016 | BR-Vic419-5PT | DNA-B | PteI | SiYLCV |
| | | BR-Vic419-7PT | DNA-B | PteI | SiYLCV |
| 421 | 2016 | BR-Vic421-3EV | DNA-A | EcoRV | SiYLCV |
| 423 | 2016 | BR-Vic423-1PT | DNA-A | PteI | SiYLCV |
| | | BR-Vic423-4PT | DNA-B | PteI | SiYLCV |
| 426 | 2016 | BR-Vic426-1EV | DNA-A | EcoRV | SiYLCV |
| 428 | 2016 | BR-Vic428-1PT | DNA-A | PteI | SiYLCV |
| | | BR-Vic428-6PT | DNA-A | PteI | SiYLCV |
| 429 | 2016 | BR-Vic429-6BS | DNA-A | BssHII | SiYLCV |
| | | BR-Vic429-6BS | DNA-A | BssHII | SiYLCV |
| 501 | 2017 | BR-Vic501-18PT | DNA-A | PteI | SiYLCV |
| | | BR-Vic501-9PT | DNA-A | PteI | SiYLCV |
| 502 | 2017 | BR-Vic502-9PT | DNA-A | PteI | SiYLCV |
| 504 | 2017 | BR-Vic504-19PT | DNA-A | PteI | SiYLCV |
| 505 | 2017 | BR-Vic505-7PT | DNA-A | PteI | SiYLCV |
| | | BR-Vic505-2PT | DNA-B | PteI | SiYLCV |
| 506 | 2017 | BR-Vic506-18BS | DNA-A | BssHII | SiYLCV |
| | | BR-Vic506-1BS | DNA-B | BssHII | SiYLCV |
| 507 | 2017 | BR-Vic507-1PT | DNA-A | PteI | SiYLCV |
| 508 | 2017 | BR-Vic508-8EV | DNA-A | EcoRV | OxYVV-S1a |
| 510 | 2017 | BR-Vic510-2PT | DNA-B | PteI | SiYLCV |
| 511 | 2017 | BR-Vic511-19PT | DNA-A | PteI | SiYLCV |
| 512 | 2017 | BR-Vic512-5PT | DNA-A | PteI | SiYLCV |
| 513 | 2017 | BR-Vic513-4EV | DNA-A | EcoRV | OxYVV-S1a |
| 514 | 2017 | BR-Vic514-3PT | DNA-A | PteI | OxYVV-S1b |
| 515 | 2017 | BR-Vic515-1PT | DNA-A | PteI | OxYVV-S1a |
| 516 | 2017 | BR-Vic516-6EV | DNA-A | EcoRV | SiYLCV |
| 517 | 2017 | BR-Vic517-9PT | DNA-A | PteI | OxYVV-S1a |
| 518 | 2017 | BR-Vic518-1PT | DNA-A | PteI | OxYVV-S1a |
| | | BR-Vic518-2PT | DNA-A | PteI | SiYLCV |
| 520 | 2017 | BR-Vic520-4PT | DNA-A | PteI | OxYVV-S1a |
| 522 | 2017 | BR-Vic522-3PT | DNA-A | PteI | OxYVV-S1a |
| | | BR-Vic522-15PT | DNA-A | PteI | OxYVV-S1a |
| 524 | 2017 | BR-Vic524-2PT | DNA-A | PteI | OxYVV-S1a |

| | | | | | |
|---|---|---|---|---|---|
| 525 | 2017 | BR-Vic525-1PT | DNA-B | PteI | n.d. |
| 527 | 2017 | BR-Vic527-1PT | DNA-A | PteI | SiYLCV |
| | | BR-Vic527-5PT | DNA-A | PteI | OxYVV-S1a |
| | | BR-Vic527-15PT | DNA-A | PteI | OxYVV-S1a |
| 529 | 2017 | BR-Vic529-1PT | DNA-A | PteI | OxYVV-S1a |
| 530 | | BR-Vic530-1PT | DNA-A | PteI | SiYLCV |
| | | BR-Vic530-8PT | DNA-A | PteI | SiYLCV |
| 531 | 2017 | BR-Vic531-1EV | DNA-A | EcoRV | SiYLCV |
| 603 | 2018 | BR-Vic603-5PT | DNA-B | PteI | SiYLCV |
| 604 | 2018 | BR-Vic603-28PT | DNA-A | PteI | SiYLCV |
| 607 | 2018 | BR-Vic607-7PT | DNA-B | PteI | SimMV |
| 608 | 2018 | BR-Vic608-22PT | DNA-A | PteI | SimMV-a |
| 610 | 2018 | BR-Vic-610-2PT | DNA-A | PteI | SiYLCV |
| | | BR-Vic-610-1PT | DNA-B | PteI | SiYLCV |
| 612 | 2018 | BR-Vic612-7PT | DNA-B | PteI | SiYLCV |
| 615 | 2018 | BR-Vic615-8PT | DNA-A | PteI | SiYLCV |
| 618 | 2018 | BR-Vic618-4PT | DNA-A | PteI | SimMV-a |
| | | BR-Vic618-6PT | DNA-A | PteI | SimMV-a |
| 619 | 2018 | BR-Vic619-1PT | DNA-A | PteI | OxYVV-S1a |
| 620 | 2018 | BR-Vic620-7PT | DNA-A | PteI | OxYVV-S1a |
| 622 | 2018 | BR-Vic622-2PT | DNA-B | PteI | SiYLCV |
| | | BR-Vic622-17PT | DNA-B | PteI | SiYLCV |
| | | BR-Vic622-24PT | DNA-B | PteI | SiYLCV |
| 623 | 2018 | BR-Vic623-5PT | DNA-A | PteI | OxYVV-S1a |
| 624 | 2018 | BR-Vic624-8PT | DNA-A | PteI | OxYVV-S1a |
| 625 | 2018 | BR-Vic625-15PT | DNA-A | PteI | OxYVV-S1a |
| 626 | 2018 | BR-Vic626-6PT | DNA-A | PteI | SiYLCV |
| | | BR-Vic626-7PT | DNA-A | PteI | SiYLCV |
| | | BR-Vic626-8PT | DNA-A | PteI | SiYLCV |
| 627 | 2018 | BR-Vic627-15PT | DNA-A | PteI | SimMV-b |
| 628 | 2018 | BR-Vic628-8PT | DNA-A | PteI | SimMV-b |
| 630 | 2018 | BR-Vic630-4PT | DNA-A | PteI | OxYVV-S1a |
| 631 | 2018 | BR-Vic631-13PT | DNA-A | PteI | OxYVV-S1a |
| 632 | 2018 | BR-Vic632-27PT | DNA-B | PteI | SiMV |
| 634 | 2018 | BR-Vic634-3PT | DNA-A | PteI | OxYVV-S1a |
| 636 | 2018 | BR-Vic636-9PT | DNA-A | PteI | OxYVV-S1a |
| 637 | 2018 | BR-Vic637-36PT | DNA-A | PteI | SiYLCV |
| | | BR-Vic637-2PT | DNA-B | PteI | SiYLCV |
| 639 | 2018 | BR-Vic639-10PT | DNA-A | PteI | SimMV-a |

| | | | | | |
|---|---|---|---|---|---|
| 701 | 2019 | BR-Vic701-4BS | DNA-B | BssHII | SiYLCV |
| 702 | 2019 | BR-Vic702-5Xh | DNA-A | XhoI | SiYLCV |
| | | BR-Vic702-8Xh | DNA-A | XhoI | SiYLCV |
| 703 | 2019 | BR-Vic703-10BS | DNA-B | BssHII | SiYLCV |
| 704 | 2019 | BR-Vic704-5EV | DNA-A | EcoRV | SiYLVC |
| | | BR-Vic704-13BS | DNA-B | BssHII | SiYLVC |
| 705 | 2019 | BR-Vic705-1B | DNA-B | BamHI | SiYLCV |
| | | BR-Vic705-2B | DNA-B | BamHI | SiYLCV |
| | | BR-Vic705-11BS | DNA-B | BssHII | SiYLCV |
| 706 | 2019 | BR-Vic706-4PT | DNA-A | PteI | SiYLCV |
| 707 | 2019 | BR-Vic707-1BS | DNA-B | BssHII | SiYLCV |
| | | BR-Vic707-4BS | DNA-B | BssHII | SiYLCV |
| | | BR-Vic707-7BS | DNA-B | BssHII | SiYLCV |
| 708 | 2019 | BR-Vic708-2BS | DNA-B | BssHII | SiYLCV |
| | | BR-Vic708-5BS | DNA-B | BssHII | SiYLCV |
| | | BR-Vic708-10BS | DNA-B | BssHII | SiYLCV |
| 710 | 2019 | BR-Vic710-3BS | DNA-A | BssHII | OxYVV-S1a |
| | | BR-Vic710-9BS | DNA-A | BssHII | OxYVV-S1a |
| | | BR-Vic710-10BS | DNA-A | BssHII | SimMV-a |
| 712 | 2019 | BR-Vic712-1BS | DNA-A | BssHII | SimMV-a |
| | | BR-Vic712-4C | DNA-B | ClaI | SimMV |
| 713 | 2019 | BR-Vic713-9BS | DNA-A | BssHII | SiYLCV |
| 714 | 2019 | BR-Vic714-1BS | DNA-A | BssHII | SiYLCV |
| | | BR-Vic714-8BS | DNA-A | BssHII | SiYLVC |
| 715 | 2019 | BR-Vic715-12BS | DNA-A | BssHII | SiYLCV |
| 716 | 2019 | BR-Vic716-15BS | DNA-A | BssHII | SiYLCV |
| 718 | 2019 | BR-Vic718-2BS | DNA-A | BssHII | OxYVV-S1a |
| | | BR-Vic718-8BS | DNA-A | BssHII | OxYVV-S1a |
| 719 | 2019 | BR-Vic719-8BS | DNA-A | BssHII | OxYVV-S1a |
| | | BR-Vic719-2BS | DNA-B | BssHII | OxYVV |
| 720 | 2019 | BR-Vic720-BS | DNA-A | BssHII | SimMV-b |
| 723 | 2019 | BR-Vic723-8BS | DNA-A | BssHII | SIYLCV |
| 724 | 2019 | BR-Vic724-6BS | DNA-A | BssHII | OxYVV-S1a |
| 725 | 2019 | BR-Vic725-6BS | DNA-A | BssHII | OxYVV-S1a |
| | | BR-Vic725-3BS | DNA-B | BssHII | SiYLCV |
| 726 | 2019 | BR-Vic726-6BS | DNA-B | BssHII | SimM |
| 736 | 2019 | BR-Vic736-2EV | DNA-A | EcoRV | SimMV-a |
| | | BR-Vic736-1BS | DNA-B | BssHII | SimM |
| | | BR-Vic736-2BS | DNA-B | BssHII | SimM |

| | | | | | |
|---|---|---|---|---|---|
| 741 | 2019 | BR-Vic741-4BS | DNA-A | BssHII | OxYVV-S1a |
| 742 | 2019 | BR-Vic742-4BS | DNA-A | BssHII | SiYLCV |
| 801 | 2020 | BR-Vic801-1C | DNA-A | ClaI | OxYVV-S1a |
| | | BR-Vic801-3C | DNA-B | ClaI | OxYVV |
| 802 | 2020 | BR-Vic802-9BS | DNA-A | BssHII | SiYLCV |
| 803 | 2020 | BR-Vic803-3EV | DNA-A | EcoRV | SimMV-a |
| | | BR-Vic803_4EV | DNA-A | EcoRV | SimMV-a |
| | | BR-Vic803-1BS | DNA-B | BssHII | SiYLCV |
| | | BR-Vic803-5BS | DNA-B | BssHII | SimMV |
| | | BR-Vic803-2EV | DNA-B | EcoRV | SimMV |
| | | BR-Vic803-8EV | DNA-B | EcoRV | SimMV |
| 804 | 2020 | BR-Vic804-1BS | DNA-A | BssHII | SiYLCV |
| | | BR-Vic804-5BS | DNA-A | BssHII | SiYLCV |
| | | BR-Vic804-8BS | DNA-A | BssHII | SiYLCV |
| | | BR-Vic804-2C | DNA-B | ClaI | SiYLCV |
| 805 | 2020 | BR-Vic805-3C | DNA-B | ClaI | OxYVV |
| 807 | 2020 | BR-Vic807-1-PT | DNA-A | BssHII | SiYLCV |
| 808 | 2020 | BR-Vic808-1BS | DNA-A | BssHII | OxYVV-S1b |
| 809 | 2020 | BR-Vic809-1BS | DNA-A | BssHII | OxYVV-S1e |
| 810 | 2020 | BR-Vic810-1BS | DNA-A | BssHII | SimMV-b |
| | | BR-Vic810-2BS | DNA-A | BssHII | SimMV-b |
| 812 | 2020 | BR-Vic812-10BS | DNA-A | BssHII | SiYLCV |
| | | BR-Vic812-2C | DNA-B | ClaI | SiYLCV |
| 814 | 2020 | BR-Vic814-BS | DNA-A | BssHII | SimMV-b |
| 815 | 2020 | BR-Vic815-C | DNA-B | ClaI | SiMV |
| 816 | 2020 | BR-Vic816-3C | DNA-A | ClaI | OxYVV-S1a |
| | | BR-Vic816-1EV | DNA-A | EcoRV | OxYVV-S1a |
| | | BR-Vic816-3EV | DNA-B | EcoRV | OxYVV |
| 818 | 2020 | BR-Vic818-1EV | DNA-A | EcoRV | SiYLCV |
| | | BR-Vic818-8EV | DNA-A | EcoRV | SiYLCV |
| | | BR-Vic818-1BS | DNA-A | BssHII | SiYLCV |
| | | BR-Vic818-3BS | DNA-A | BssHII | SiYLCV |
| 819 | 2020 | BR-Vic819-9BS | DNA-A | BssHII | SiYLCV |
| 831 | 2020 | BR-Vic831-2EV | DNA-A | BssHII | SiYLCV |
| | | BR-Vic831-1C | DNA-B | ClaI | SiYLCV |
| 832 | 2020 | BR-Vic832-1EV | DNA-A | EcoRV | OxYVV-S1b |
| | | BR-Vic832-2EV | DNA-A | EcoRV | OxYVV-S1b |
| | | BR-Vic832-4C | DNA-A | ClaI | OxYVV-S1b |
| | | BR-Vic832-1C | DNA-B | ClaI | OxYVV |

| | | | | | |
|---|---|---|---|---|---|
| | | BR-Vic832-2C | DNA-B | ClaI | OxYVV |
| 836 | 2020 | BR-Vic836-7BS | DNA-B | BssHII | SimMV |
| 837 | 2020 | BR-Vic837-5EV | DNA-A | EcoRV | SimMV-a |
| | | BR-Vic837-1BS | DNA-B | BssHII | SimMV |
| | | BR-Vic837-13BS | DNA-B | BssHII | SimMV |
| 839 | 2020 | BR-Vic839-1EV | DNA-A | EcoRV | SiYLCV |
| | | BR-Vic839-3EV | DNA-A | EcoRV | SiYLCV |
| | | BR-Vic839-10BS | DNA-A | BssHII | SiYLCV |
| 901 | 2021 | BR-Vic901-1BS | DNA-A | BssHII | OxYVV-S2 |
| | | BR-Vic901-1B | DNA-B | BamHI | OxYVV |
| | | BR-Vic901-2B | DNA-B | BamHI | OxYVV |
| 902 | 2021 | BR-Vic902-6BS | DNA-A | BssHII | OxYVV-S2 |
| | | BR-Vic902-10BS | DNA-B | BssHII | SiYLCV |
| 903 | 2021 | BR-Vic903-1BS | DNA-A | BssHII | OxYVV-S1a |
| 904 | 2021 | BR-Vic904-10C | DNA-A | ClaI | OxYVV-S1a |
| 905 | 2021 | BR-Vic905-1EV | DNA-A | EcoRV | OxYVV-S1a |
| | | BR-Vic905-8EV | DNA-A | EcoRV | SiYLCV |
| | | BR-Vic905-2C | DNA-B | ClaI | SiYLCV |
| 907 | 2021 | BR-Vic907-6BS | DNA-A | BssHII | SiYLCV |
| | | BR-Vic907-8BS | DNA-A | BssHII | SiYLCV |
| 908 | 2021 | BR-Vic908-2BS | DNA-A | BssHII | OxYVV-S2 |
| 909 | 2021 | BR-Vic909-8EV | DNA-A | EcoRV | OxYVV-S2 |
| 910 | 2021 | BR-Vic910-7BS | DNA-A | BssHII | OxYVV-S2 |
| 911 | 2021 | BR-Vic911-4EV | DNA-A | EcoRV | MaYVV |
| 912 | 2021 | BR-Vic912-9C | DNA-A | ClaI | SiMV |
| | | BR-Vic912-10C | DNA-B | ClaI | SiMV |
| 913 | 2021 | BR-Vic913-4C | DNA-A | ClaI | SimMV |
| 916 | 2021 | 916_7_PT | DNA-A | BssHII | OxYVV-S1a |
| | | 916_8_PT | DNA-A | BssHII | OxYVV-S1a |
| 917 | 2021 | BR-Vic917-2BS | DNA-A | BssHII | OxYVV-S1a |
| | | BR-Vic917-1C | DNA-B | ClaI | OxYVV |
| 918 | 2021 | BR-Vic918-5BS | DNA-A | BssHII | SiYLCV |
| 919 | 2021 | BR-Vic919-1BS | DNA-A | BssHII | SiYLCV |
| 921 | 2021 | BR-Vic921-1EV | DNA-A | BssHII | SiMV |
| 923 | 2021 | BR-Vic923-8BS | DNA-A | BssHII | SiYLCV |
| | | BR-Vic923-7-BS | DNA-B | BssHII | SiYLCV |
| 924 | 2021 | BR-Vic924-1EV | DNA-A | EcoRV | SiMV |
| | | BR-Vic924-6EV | DNA-A | EcoRV | SiMV |

| | | | | | |
|---|---|---|---|---|---|
| 925 | 2021 | BR-Vic925-1BS | DNA-B | BssHII | SiYLCV |
| 926 | 2021 | BR-Vic926-6BS | DNA-A | BssHII | SiYLCV |
| | | BR-Vic926-2BS | DNA_B | BssHII | SiYLCV |
| | | BR-Vic926-5BS | DNA-B | BssHII | SiYLCV |
| | | BR-Vic926-10BS | DNA-B | BssHII | SiYLCV |
| 928 | 2021 | BR-Vic928-2BS | DNA-B | BssHII | SiYLCV |
| 1001 | 2022 | BR-Vic1001-1EV | DNA-A | EcoRV | SiYLCV |
| 1002 | 2022 | BR-Vic1002-2EV | DNA-B | EcoRV | SiYLCV |
| 1003 | 2022 | BR-Vic1003-2EV | DNA-A | EcoRV | SiYLCV |
| 1004 | 2022 | BR-Vic1004-3EV | DNA-A | EcoRV | SiYLCV |
| | | BR-Vic1004-1EV | DNA-B | EcoRV | SiYLCV |
| 1006 | 2022 | BR-Vic1006-1EV | DNA-A | EcoRV | OxYVV-S1a |
| 1008 | 2022 | BR-Vic1008-3EV | DNA-A | EcoRV | SiYLCV |
| 1009 | 2022 | BR-Vic1009-2EV | DNA-A | EcoRV | SiYLCV |
| | | BR-Vic1009-3EV | DNA-A | EcoRV | OxYVV-S1a |
| | | BR-Vic1009-5EV | DNA-A | EcoRV | OxYVV-S1a |
| | | BR-Vic1009-1EV | DNA-B | EcoRV | SiYLCV |
| 1010 | 2022 | BR-Vic1010-1EV | DNA-A | EcoRV | SiYLCV |
| 1012 | 2022 | BR-Vic1012-1EV | DNA-A | EcoRV | OxYVV-S1d |
| | | BR-Vic1012-2EV | DNA-B | EcoRV | OxYVV |
| 1013 | 2022 | BR-Vic1013-1EV | DNA-A | EcoRV | OxYVV-S1d |
| 1014 | 2022 | BR-Vic1014-5EV | DNA-A | EcoRV | OxYVV-S1d |
| | | BR-Vic1014-6EV | DNA-B | EcoRV | OxYVV |
| 1015 | 2022 | BR-Vic1015-6EV | DNA-A | EcoRV | SiYLCV |
| 1016 | 2022 | BR-Vic1016-2EV | DNA-A | EcoRV | OxYVV-S1d |
| 1018 | 2022 | BR-Vic1018-8EV | DNA-A | EcoRV | OxYVV-S1a |
| 1020 | 2022 | BR-Vic1020-2EV | DNA-A | EcoRV | OxYVV-S1a |
| | | BR-Vic1020-3EV | DNA-B | EcoRV | OxYVV |
| | | BR-Vic1020-8EV | DNA-B | EcoRV | OxYVV |
| 1021 | 2022 | BR-Vic1021-8EV | DNA-A | EcoRV | SiMV |
| | | BR-Vic1021-10EV | DNA-B | EcoRV | OxYVV |

**Table 2.** Number of DNA-A clones of each begomovirus and their respective variants obtained from *Sida acuta* samples collected in Viçosa, MG, from 2011 to 2022.

| Species-variant | 2011 | 2012 | 2013 | 2014 | 2016 | 2017 | 2018 | 2019 | 2020 | 2021 | 2022 | Total |
|---|---|---|---|---|---|---|---|---|---|---|---|---|
| OxYVV-S1a | 19 | 15 | 17 | 25 | 4 | 11 | 9 | 8 | 3 | 3 | 4 | 118 |
| OxYVV-S1b | 2 | 1 | 0 | 0 | 6 | 1 | 0 | 0 | 4 | 0 | 0 | 14 |
| OxYVV-S1c | 10 | 4 | 3 | 1 | 0 | 0 | 0 | 0 | 0 | 0 | 0 | 18 |
| OxYVV-S1d | 0 | 0 | 0 | 0 | 0 | 0 | 0 | 0 | 0 | 0 | 4 | 4 |
| OxYVV-S1e | 0 | 0 | 0 | 0 | 0 | 0 | 0 | 0 | 1 | 0 | 0 | 1 |
| OxYVV-S2 | 0 | 0 | 0 | 0 | 0 | 0 | 0 | 0 | 0 | 6 | 1 | 7 |
| SiYLCV | 0 | 1 | 0 | 0 | 14 | 15 | 9 | 12 | 13 | 7 | 6 | 77 |
| SiMMV-a | 0 | 0 | 0 | 0 | 0 | 0 | 4 | 3 | 3 | 1 | 0 | 11 |
| SiMMV-b | 0 | 0 | 0 | 0 | 0 | 0 | 2 | 1 | 3 | 0 | 0 | 6 |
| SiMV | 0 | 0 | 0 | 0 | 0 | 0 | 0 | 0 | 0 | 4 | 1 | 5 |
| MaYSV | 0 | 0 | 0 | 0 | 0 | 0 | 0 | 0 | 0 | 1 | 0 | 1 |
| Total | 31 | 21 | 20 | 26 | 24 | 27 | 24 | 24 | 26 | 22 | 16 | 262 |

**Table 3.** Genetic variability indices of the begomoviruses infecting *Sida acuta* in Viçosa, MG.

| Species | Number of sequences | Number of haplotypes (h) | Haplotype diversity (Hd) | Nucleotide diversity (π) |
|---|---|---|---|---|
| **OxYVV** | | | | |
| DNA-A | 162 | 127 | 0.993 | 0.0197 +/-0.0003 |
| DNA-B | 52 | 40 | 0.986 | 0.0479 +/- 0.0023 |
| *CP* | 162 | 59 | 0.784 | 0.0176+/- 0.0003 |
| *Rep* | 162 | 77 | 0.952 | 0.0219 +/-0.0004 |
| *Trap* | 162 | 29 | 0.692 | 0.0157 +/- 0.0003 |
| *Ren* | 162 | 45 | 0.804 | 0.0253 |
| *AC4* | 162 | 25 | 0.771 | 0.0178 +/- 0.0005 |
| *MP* | 52 | 22 | 0.917 | 0.0337 +/- 0.0016 |
| *NSP* | 52 | 25 | 0.920 | 0.0407 +/- 0.0018 |
| **SiYLCV** | | | | |
| DNA-A | 77 | 59 | 0.995 | 0.0135 +/- 0.0004 |
| DNA-B | 43 | 35 | 0.990 | 0.0216 +/- 0.0011 |
| *CP* | 75 | 26 | 0.925 | 0.0198 +/- 0.0006 |
| *Rep* | 75 | 37 | 0.963 | 0.0074 +/- 0.0002 |
| *Trap* | 75 | 24 | 0.883 | 0.0068 +/- 0.0001 |
| *Ren* | 75 | 27 | 0.918 | 0.0117 +/- 0.0003 |
| *AC4* | 75 | 20 | 0.822 | 0.0037 +/- 0.0001 |
| *MP* | 43 | 25 | 0.971 | 0.0336 +/- 0.002 |
| *NSP* | 43 | 23 | 0.966 | 0.0111 +/- 0.0004 |
| **SimMV** | | | | |
| DNA-A | 17 | 16 | 0.993 | 0.0432 +/- 0.0034 |
| DNA-B | 9 | 7 | 0.994 | 0.0563 +/- 0.0081 |
| *CP* | 17 | 11 | 0.956 | 0.0267 +/- 0.003 |
| *Rep* | 17 | 13 | 0.963 | 0.0574 +/- 0.0054 |
| *Trap* | 17 | 10 | 0.926 | 0.0174 +/- 0.0013 |
| *Ren* | 17 | 10 | 0.926 | 0.0185 +/- 0.0011 |
| *AC4* | 17 | 10 | 0.926 | 0.0710 +/- 0.0086 |
| *MP* | 9 | 6 | 0.889 | 0.0342 +/- 0.0046 |
| *NSP* | 9 | 5 | 0.833 | 0.0544 +/- 0.0077 |

**Table 4.** Mutational bias matrix of the begomoviruses infecting *Sida acuta* in Viçosa, MG. The values express the probability of changing each base to another.

| **OxYVV- DNA-A** | | | | |
|---|---|---|---|---|
| | Resulting base | | | |
| Original base | A | T | C | G |
| A | - | 5.61 | 4.69 | 10.86 |
| T | 4.82 | - | 17.5 | 5.14 |
| C | 4.82 | 20.94 | - | 5.14 |
| G | 10.18 | 5.61 | 4.69 | - |
| **OxYVV- DNA-B** | | | | |
| | Resulting base | | | |
| Original base | A | T | C | G |
| A | - | 7.06 | 5.38 | 10.09 |
| T | 6.13 | - | 13.1 | 6.41 |
| C | 6.13 | 17.19 | - | 6.41 |
| G | 9.65 | 7.06 | 5.38 | - |
| **SiYLCV-DNA-A** | | | | |
| | Resulting base | | | |
| Original base | A | T | C | G |
| A | - | 5.48 | 4.37 | 11.43 |
| T | 4.7 | - | 17.15 | 4.82 |
| C | 4.7 | 21.53 | - | 4.82 |
| G | 11.14 | 5.48 | 4.37 | - |
| **SiYLCV-DNA-B** | | | | |
| | Resulting base | | | |
| Original base | A | T | C | G |
| A | - | 6 | 4.63 | 10.68 |
| T | 5.28 | - | 15.8 | 5.21 |
| C | 5.28 | 20.45 | - | 5.21 |
| G | 10.83 | 6 | 4.63 | - |
| **SimMV- DNA-A** | | | | |
| | Resulting base | | | |
| Original base | A | T | C | G |
| A | - | 6.02 | 4.98 | 10.2 |
| T | 5.27 | - | 16.55 | 5.21 |
| C | 5.27 | 20.01 | - | 5.21 |
| G | 10.31 | 6.02 | 4.98 | - |
| **SimMV- DNA-B** | | | | |
| | Resulting base | | | |
| Original base | A | T | C | G |
| A | - | 3.77 | 2.76 | 10.12 |
| T | 3.15 | - | 22.91 | 3.19 |
| C | 3.15 | 31.24 | - | 3.19 |
| G | 9.99 | 3.77 | 2.76 | - |

**Table 5.** Determination coefficients of the root-to-tip regression and substitution rate values for the Oxalis yellow vein virus (OxYVV) and Sida yellow leaf curl virus (SiYLCV) populations infecting *Sida acuta* in Viçosa, MG. TMRCA, Time from the Most Recent Common Ancestor.

| Virus | Correlation coefficient | $R^2$ | Slope (rate) | TMRCA |
|---|---|---|---|---|
| OxYVV | 0.4314 | 0.1709 | $2.215x10^{-3}$ | 1994 |
| SiYLCV | 0.502 | 0.2522 | $1.409x10^{-3}$ | 2008 |

**Table 6.** Summary of recombination events detected in the begomovirus community infecting *Sida acuta* in Viçosa, MG. The analysis was performed using complete DNA-A and DNA-B sequences.

| Event # | # seq | Breakpoints | | Recombinant sequence | Parents | | Detection method | | | | | | |
|---|---|---|---|---|---|---|---|---|---|---|---|---|---|
| | | End | Begin | | Minor | Major | RDP | Geneconv | Bootscan | Maxchi | Chimaera | SiSscan | 3Seq |
| **DNA-A** | | | | | | | | | | | | | |
| 1 | 1 | 303 | 31 | OxYVV BR_Vic1006_1 | OxYVV BR_Vic_917_2 | Unknown | $1.316e^{-18}$ | $1.799e^{-18}$ | $1.932e^{-13}$ | $9.167e^{-11}$ | $4.331e^{-12}$ | $9.380e^{-09}$ | $1.027e^{-28}$ |
| 2 | 5 | 91 | 2245 | SiMV BR_Vic_924_1 | SiYLCV BR_Vic_907_8 | OxYVV BR_Vic_917_2 | $1.961e^{-20}$ | $2.684e^{-23}$ | $1.532e^{15}$ | $4.167e^{-17}$ | $1.486e^{-13}$ | $1.778e^{-27}$ | $1.573e^{-10}$ |
| 3 | 1 | 1893 | 2596 | MaYVV BR_Vic_911_4 | OxYVV BR_Vic_1012_1 | Unknown | $5.355e^{-9}$ | NS | $8.853e^{-11}$ | $1.118e^{-18}$ | $4.841e^{-8}$ | $1.101e^{-22}$ | $8.163e^{-22}$ |
| 4 | 3 | 2227 | 133 | SiMMV BR_Vic_837_5 | SiMMV BR_Vic_736_2 | Unknown | $2.818e^{-7}$ | $3.445e^{-3}$ | $6.757e^{-7}$ | $2.420e^{-14}$ | $2.863e^{-5}$ | $5.337e^{-8}$ | $3.629e^{-10}$ |
| 5 | 77 | 194 | 2042 | SiYLCV BR_Vicv_907_8 | OxYVV BR_Vic_1020_2 | Unknown | $5.747e^{-9}$ | $2.858e^{-5}$ | $3.392e^{-4}$ | $3.132e^{-10}$ | $1381e^{-11}$ | $3.536e^{-24}$ | NS |
| 6 | 1 | 1832 | 31 | SiMMV BR_Vic_913_4 | SiMMV BR_Vic_608_1 | SiMMV BR_Vic_810_2 | $8.396e^{-6}$ | NS | $9.318e^{-5}$ | $2.318e^{-13}$ | $1.902e^{-8}$ | NS | $3.436e^{-3}$ |
| 7 | 6 | 31 | 2241 | SiMMV BR_Vic_810_2 | SiMMV BR_Vic_618_2 | Unknown | $3.321e^{-6}$ | $8.206e^{-6}$ | $1.278e^{-5}$ | $4.944e^{-7}$ | $1.482e^{-5}$ | $8.290e^{-19}$ | $3.172e^{-4}$ |
| 8 | 4 | 893 | 673 | SiMV BR_Vic_924_1 | SiYLCV BR_Vic626_1 | SiMMV BR_Vic_618_2 | $8.641e^{-4}$ | $4.256e^{-5}$ | $1.369e^{-3}$ | NS | $2.582e^{-2}$ | $5.368e^{-3}$ | $2.871e^{-3}$ |
| **DNA-B** | | | | | | | | | | | | | |
| 1 | 35 | 1884 | 1546 | BR_Vic_411_3 SiYLCV | Unknown | BR_Vic_1009_1 SiYLCV | $1.837e^{-21}$ | $4.342e^{-19}$ | $2.637e^{-18}$ | $1.982e^{-7}$ | $9.626e^{-8}$ | $1.287e^{-7}$ | $5.387e^{-12}$ |
| 2 | 1 | 2616 | 2514 | BR_Vic_0912_10 SiMV | BR_Vic_1014_06 OxYVV | BR_Vic_0632_27 SiMV | $4.75e^{-12}$ | $1.02e^{-13}$ | $3.22e^{-3}$ | $6.48e^{-07}$ | $6.57e^{-7}$ | $2.14e^{-10}$ | $1.37e^{-12}$ |
| 3 | 1 | 1770 | 1436 | BR_Vic_0525_1 | BR_Vic_1009_1 SiYLCV | Unknown | $4.18e^{-6}$ | $8.37e^{-10}$ | $1.81e^{-7}$ | $6.41e^{-05}$ | $2.74e^{-3}$ | $1.95e^{-09}$ | NS |
| 4 | 2 | 2598 | 2486 | BR_Vic_0632_27 SiMV | Unknown | BR_Vic_0816_3 OxYVV | $2.36e^{-9}$ | $2.71e^{-7}$ | $1.15e^{-6}$ | 1.24e-2 | $4.79e^{-5}$ | $4.27e^{-11}$ | $1.97e^{-7}$ |
| 5 | 1 | 2624 | 2503 | BR_Vic_0726_06 SiMMV | BR_Vic_0607_07 SiMMV | BR_Vic_0712_4 SiMMV | $1.95e^{-4}$ | $5.32e^{-8}$ | $6.18e^{-7}$ | 1.35e-3 | $3.15e^{-3}$ | 1.62e-8 | NS |
| 6 | 5 | 2544 | 1145 | BR_Vic_1009_1 SiYLCV | BR_Vic_0622_24 SiYLCV | BR_Vic_0905_2 SiYLCV | $1.82e^{-3}$ | $2.49e^{-3}$ | NS | 2.30e-7 | $1.64e^{-3}$ | $4.29e^{-10}$ | $3.27e^{-7}$ |
| 7 | 44 | 2485 | 2608 | BR_Vic_0804_2 SiYLCV | BR_Vic_0816_3 OxYVV | Unknown | NS | NS | NS | 2.70e-9 | $1.77e^{-5}$ | $2.78e^{-38}$ | $9.95e^{-6}$ |

**Table 7.** Population-scaled rates of recombination and mutation of the begomoviruses infecting *Sida acuta* in Viçosa, MG. S, number of segregating sites. ρ, population-scaled recombination rate. θw, Watterson's estimator of population-scaled mutation rate (θ). ρ/θ, recombination/mutation ratio.

| **Species/segment** | **S** | **ρ** | **$\theta_W$** | **$\rho/\theta_W$** |
|---|---|---|---|---|
| OxYVV DNA-A | 470 | 45.67 | 90.96 | 0.502 |
| OxYVV DNA-B | 393 | 29.04 | 86.97 | 0.333 |
| SiYLCV DNA-A | 202 | 69.81 | 41.33 | 1.689 |
| SiYLCV DNA-B | 269 | 40.50 | 61.83 | 0.655 |
| SimMV DNA-A | 303 | 30.61 | 89.63 | 0.341 |

**Table 8.** Proportion of non-synonymous to synonymous substitutions for DNA-A genes of the begomoviruses infecting *Sida acuta* in Viçosa, MG, and sites under positive or negative selection according to three maximum likelihood-based methods

| Gene | Tajima's D | Fu & Li's | | dN/dS | SLAC | | MEME | | FUBAR | |
|---|---|---|---|---|---|---|---|---|---|---|
| | | *F** | *D** | | Positive | Negative | Positive | Negative | Positive | Negative |
| **OxYVV** | | | | | | | | | | |
| *CP* | -1,351 | -1.609 | -1.387 | 0.129 | - | 18, 25, 34, 37, 71, 72 86, 94, 137, 149 154, 156, 177, 209, 217, 225 245, 249 | 31 | - | - | 18, 20, 25, 32, 34, 37, 47, 49, 50, 53, 71, 72, 73, 83, 86, 94, 113, 137, 149, 154, 156, 158, 173, 177, 182, 191, 209, 217, 218, 223, 224, 225, 237, 245, 249 |
| *Rep* | -1.356 | -2,45849* | -2,673* | 0.259 | | 40, 70, 72, 78, 116, 144, 151, 157, 186, 187, 220, 251, 274, 321, 324 | 60, 98, 123, 214 | | - | 17, 39, 40, 62, 70, 72, 78, 110, 115, 116, 126, 143, 144, 151, 157, 166, 178, 184, 186, 187, 194, 220, 223, 235, 251, 260, 274, 314, 321, 324, 332, 347 |
| *TrAP* | -1.396 | -2.904* | -3.201* | 0.534 | - | 2, 15, 121 | 92, 94 | - | 92, 119 | 2, 15, 33, 64, 121 |
| *Ren* | -.1264 | -2.216 | -2.324 | 0.379 | | 35, 47, 73, 74, 103 | 126 | | | 27, 31, 35, 42, 47, 73, 74 102, 103, 122, |
| *AC4* | -1.7233 | -1.048 | -1.611 | 1.35 | - | 58 | 6, 19 | - | 9, 17, 75 | 58, 81 |
| *MP* | 1.1025 | 0,8427 | 0,4650 | 0.113 | | 20, 159, 182 | 233 | | - | 159, 182, 20, 179, 71, 215, 123, 66, 120, 124, 220, 62, 129, 260, 10, 151, 35, 14, 63, 84, 85, 112, 161, 203, 97, 171, 206, 278, 291, 277, 140, 2, 180, 82, 148, 139, 193 |
| *NSP* | 0,5616 | 0,0510 | -0,2724 | 0.275 | - | 48, 115 | 120, 160 | | 120 | 48, 63, 95, 110, 115, 129, 133, 145, 215 |
| **SiYLCV** | | | | | | | | | | |
| *CP* | 0,3621 | -0,56344 | -1,0069 | 0.151 | | 80, 94, 155,136 | 81 | | 10 | 49, 80, 83, 90, 94, 127, 136, 155, 182, 190, 222, 239 |
| *Rep* | -1,1275 | -1,6539 | -1,5428 | 0.468 | | 52, 125 | 172 | | 44, 172, 181 | 12, 23, 43, 52, 53, 57, 125, 187, 259, 332 |
| *TrAP* | -1,9271* | -2,4176 | -2,0817 | 0.573 | - | - | - | - | 14, 129 | 34, 42, 99, 103 |

| | | | | | | | | | | |
|---|---|---|---|---|---|---|---|---|---|---|
| *Ren* | -1,6125* | -1,3532 | -0,8311 | 0.319 | - | - | - | - | - | 122, 130 |
| *AC4* | -1,8756* | -1,7871 | -1,2895 | 1.13 | - | - | - | - | - | - |
| *MP* | 0,5227 | 0,8965 | 0,9076 | 0.154 | - | 41, 43, 66, 149, 162 | 32 | - | | 7, 14, 20, 41, 43, 58, 66, 75, 82, 94, 113, 126, 127, 137, 149, 162, 170, 172, 184, 202, 211, 217 |
| *NSP* | -1,0070 | -0,7648 | -0,4408 | 0.319 | - | 201 | - | - | - | 160, 174, 186, 199, 201, 211 |

**Figure legends**

**Figure 1.** *Sida acuta* plants collected in a 300 $m^2$ area near the city of Viçosa, MG, displaying yellow mosaic and yellow vein symptoms due to begomovirus infection.

**Figure 2.** Aspects of the sampling area located near the city of Viçosa, MG. Left: satellite images taken from Google Maps. Right: images of the collection site.

**Figure 3.** Pairwise nucleotide sequence identity matrix of the *Oxalis yellow vein virus* (OxYVV) isolates obtained in this work (DNA-A). The vertical bar at the left indicates the strains and variants identified based on the demarcation criteria established by the *Geminiviridae* Study Group of the ICTV.

**Figure 4.** Pairwise nucleotide sequence identity matrix of the *Sida yellow leaf curl virus* (SiYLCV) isolates obtained in this work (DNA-A).

**Figure 5.** Pairwise nucleotide sequence identity matrix of the *Sida micrantha mosaic virus* (SimMV) isolates obtained in this work (DNA-A). The vertical bar at the left indicates the variants identified based on the demarcation criteria established by the *Geminiviridae* Study Group of the ICTV.

**Figure 6.** Phylogenetic tree based on the DNA-A nucleotide sequence of the begomovirus isolates obtained in this work. The colored circles at the nodes represent bootstrap support values: red, 95-100%; purple, 90-94%; blue, 84-89%; green, 63-83%. Viral isolates classified as members of the species *Oxalis yellow vein virus* (OxYVV) are represented in different shades of blue, *Sida yellow leaf curl virus* (SiYLCV) in green, *Sida micrantha mosaic virus* (SimMV)

in yellow, *Sida motlle virus* (SiMV) in orange, and *Macroptilium yellow vein virus* (MaYVV) in black. The colored bar on the right indicates the species, strains and variants identified based on the demarcation criteria established by the *Geminiviridae* Study Group of the ICTV. The scale bar represents nucleotide substitutions per site.

**Figure 7.** Phylogenetic tree based on the DNA-B nucleotide sequence of the begomovirus isolates obtained in this work. The numbers at the nodes represent the bootstrap support values. Viral isolates classified as members of the species *Oxalis yellow vein virus* (OxYVV) are represented in blue, *Sida yellow leaf curl virus* (SiYLCV) in green, *Sida micrantha mosaic virus* (SimMV) in yellow, and *Sida motlle virus* (SiMV) in orange. An isolate for which species assignment was not possible is represented in grey. The colored bar on the right indicates the species, strains and variants identified based on the demarcation criteria established by the *Geminiviridae* Study Group of the ICTV. The scale bar represents nucleotide substitutions per site.

**Figure 8. A.** Proportion of individuals of each begomovirus sampled in each year. The color scale on the right indicates which species each individual belongs to: MaYVV, *Macroptilium yellow vein virus*; OxYVV, *Oxalis yellow vein virus*; SiYLCV, *Sida yellow leaf curl virus*; SimMV, *Sida micrantha mosaic virus*; SiMV, *Sida motlle virus*. The numbers at the top of the bars indicate the number of plants analyzed (red), the number of DNA-A sequences obtained (blue), and the number of DNA-B sequences obtained (orange). **B.** Relative proportion of each species and their respective variants isolated in each year. **C.** Values of total entropy (the sum of the entropy of each sequence), which represents the dynamics of the landscape over the years. **D.** KHILL values, which are estimated based on the entropy.

**Figure 9.** Diversity accumulation curves for different sample sizes. The shaded background represents 95% confidence intervals of Hill numbers calculated for the three diversity orders (0, 1 and 2) estimated for each year of collection.

**Figure 10.** Results of the subdivision test carried out for the **(A)** OxYVV and **(B)** SiYLCV populations infecting *Sida acuta* in Viçosa, MG. Each year was considered to represent a subpopulation.

**Figure 11.** Phylogenetic evidence of recombination between the DNA-A sequences of the begomovirus community infecting *Sida acuta* in Viçosa, MG. Neighbor-Net network analysis was performed using SplitsTree4. The formation of a reticular network rather than a single bifurcated tree suggests recombination. MaYVV, *Macroptilium yellow vein virus*; OxYVV, *Oxalis yellow vein virus*; SiYLCV, *Sida yellow leaf curl virus*; SimMV, *Sida micrantha mosaic virus*; SiMV, *Sida motlle virus*.

**Figure 12.** Phylogenetic evidence of recombination between the DNA-B sequences of begomovirus community infecting *Sida acuta* in Viçosa, MG. Neighbor-Net network analysis was performed using SplitsTree4. The formation of a reticular network rather than a single bifurcated tree suggests recombination. OxYVV, *Oxalis yellow vein virus*; SiYLCV, *Sida yellow leaf curl virus*; SimMV, *Sida micrantha mosaic virus*; SiMV, *Sida motlle virus*.

**Figure 13.** Recombination maps showing the distribution of recombination hot spots throughout the genomes of **(A)** *Oxalis yellow vein virus* (OxYVV), **(B)** *Sida yellow leaf curl virus* (SiYLCV), and **(C)** *Sida micrantha mosaic virus* (SimMV). The red lines indicate the average recombination rate (rho) per position, and the shaded background represents the 95% confidence interval. The genomic organization is represented at the bottom, with the coding

regions of each segment (DNA-A and DNA-B). For OxYVV and SiYLCV, recombination maps at the left are for the DNA-A and at the right are for the DNA-B, and the maps at the top are for theta=0.001 and at the bottom for theta=0.01. For SimMV, both maps are for the DNA-A, with the one at the left for theta=0.001 and the one at the right for theta=0.01.

**Supplementary Figure S1.** Phylogenetic tree based on the nucleotide sequence of *Oxalis yellow vein virus* (OxYVV) DNA-A. The numbers at the nodes represent bootstrap support values. The colored bar on the right indicates the strains and variants identified based on the demarcation criteria established by the *Geminiviridae* Study Group of the ICTV. The scale bar represents nucleotide substitutions per site.

**Supplementary Figure S2.** Phylogenetic tree based on the nucleotide sequence of *Sida yellow leaf curl virus* (SiYLCV) DNA-A. The numbers at the nodes represent bootstrap support values. The scale bar represents nucleotide substitutions per site.

**Supplementary Figure S3.** Phylogenetic tree based on the nucleotide sequence of *Sida micrantha mosaic virus* (SimMV) DNA-A. The numbers at the nodes represent bootstrap support values. The colored bar on the right indicates the variants identified based on the demarcation criteria established by the *Geminiviridae* Study Group of the ICTV. The scale bar represents nucleotide substitutions per site.

**Supplementary Figure S4.** Diversity accumulation curves for different sample sizes. The shaded background indicates 95% confidence intervals of Hill numbers calculated for the three diversity orders (0, 1 and 2). Each color represents a year of collection.

**Figure 1**

**Figure 2**


Chácara Quintal da Lua
R. Nova
R. Nova
Fantasias Viçosa
Loja de Roupa
Bar do Biro
Estr. Nova Viçosa
R. Apolinário
R. Apolinário
Ac. Romão dos Réis
Ac. Romão dos Réis
Google

**Figure 3**

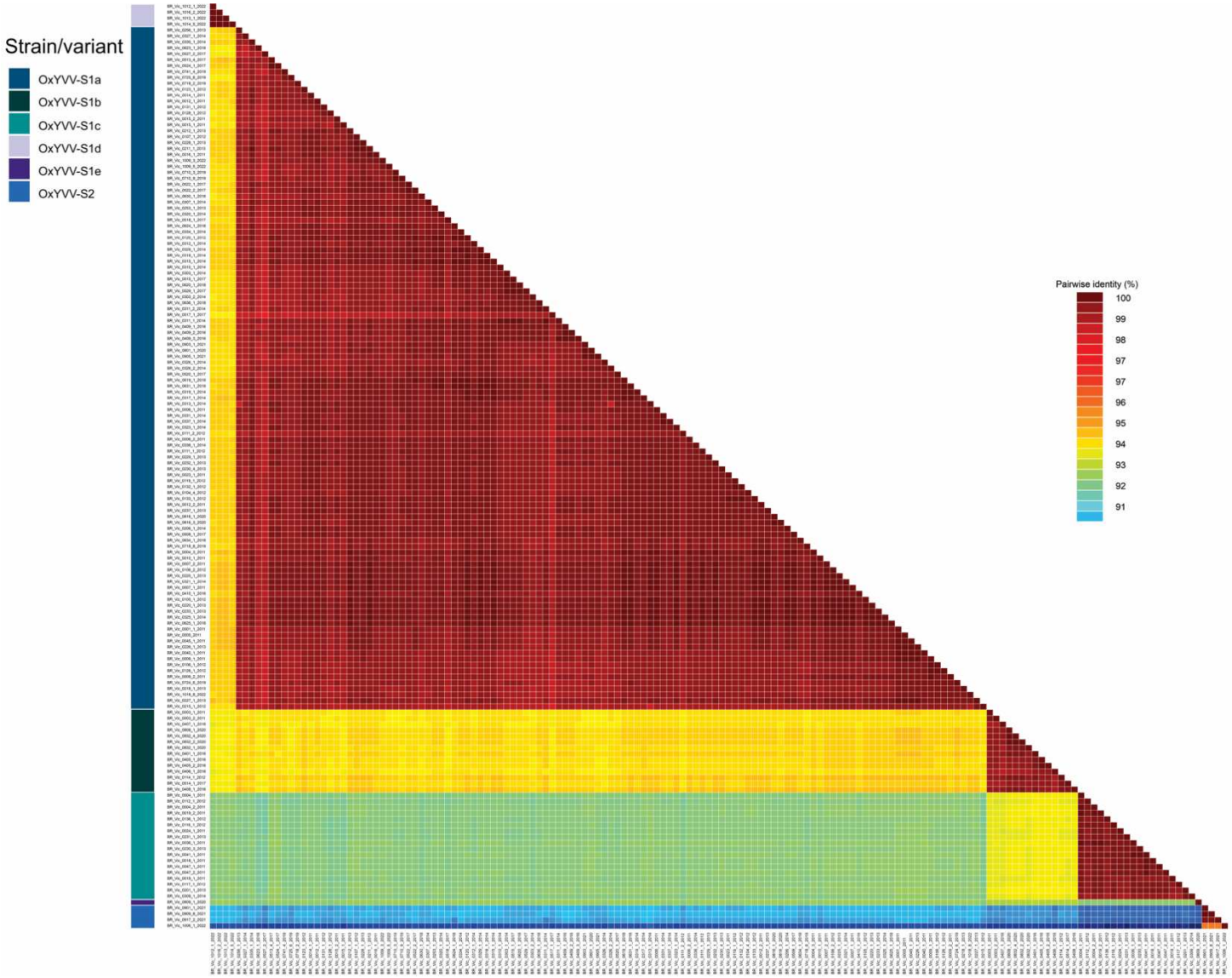
Strain/variant
OxYVV-S1a
OxYVV-S1b
OxYVV-S1c
OxYVV-S1d
OxYVV-S1e
OxYVV-S2
Pairwise identity (%)
100
99
98
97
97
96
95
94
93
92
91

**Figure 4**

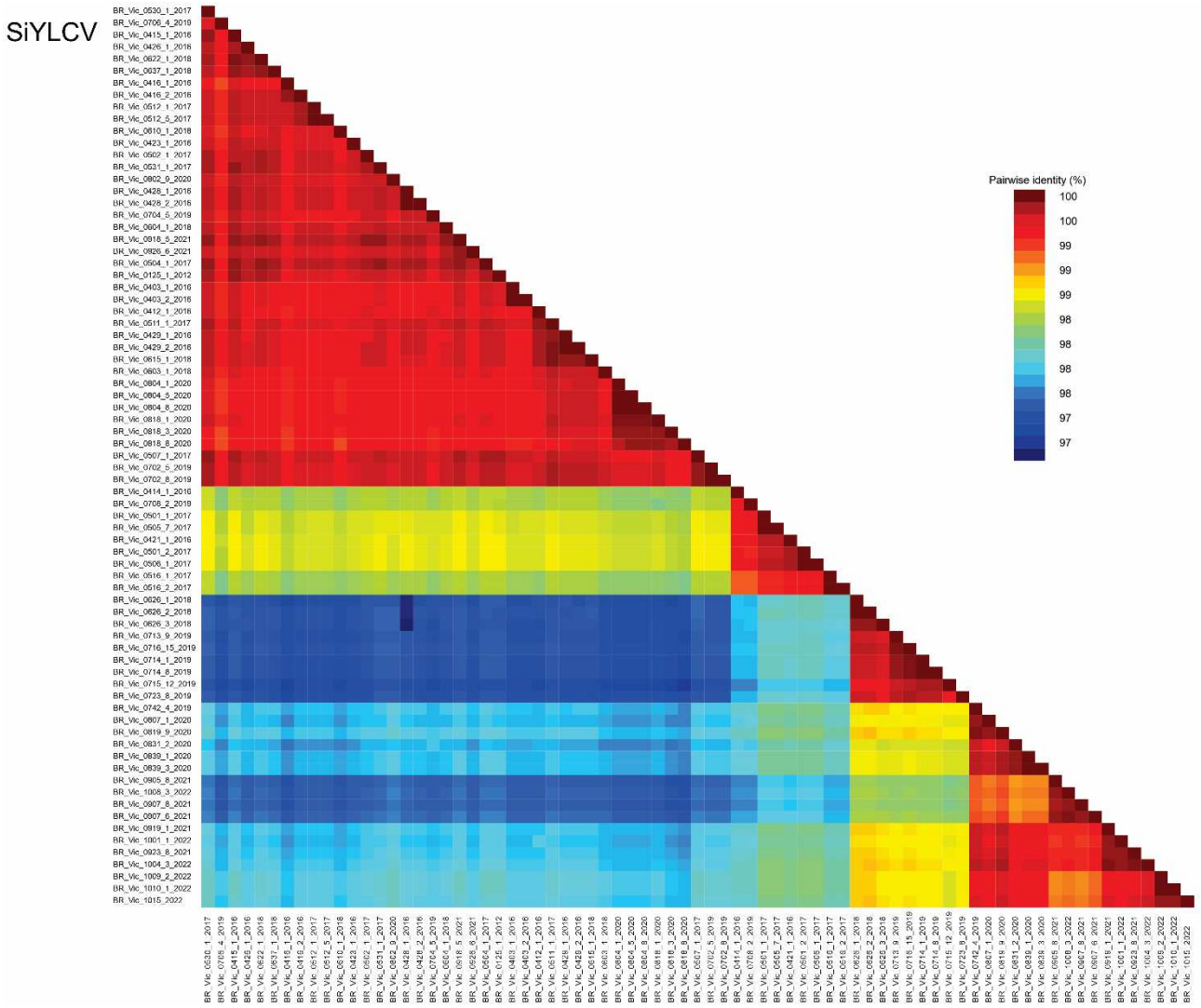

**Figure 5**

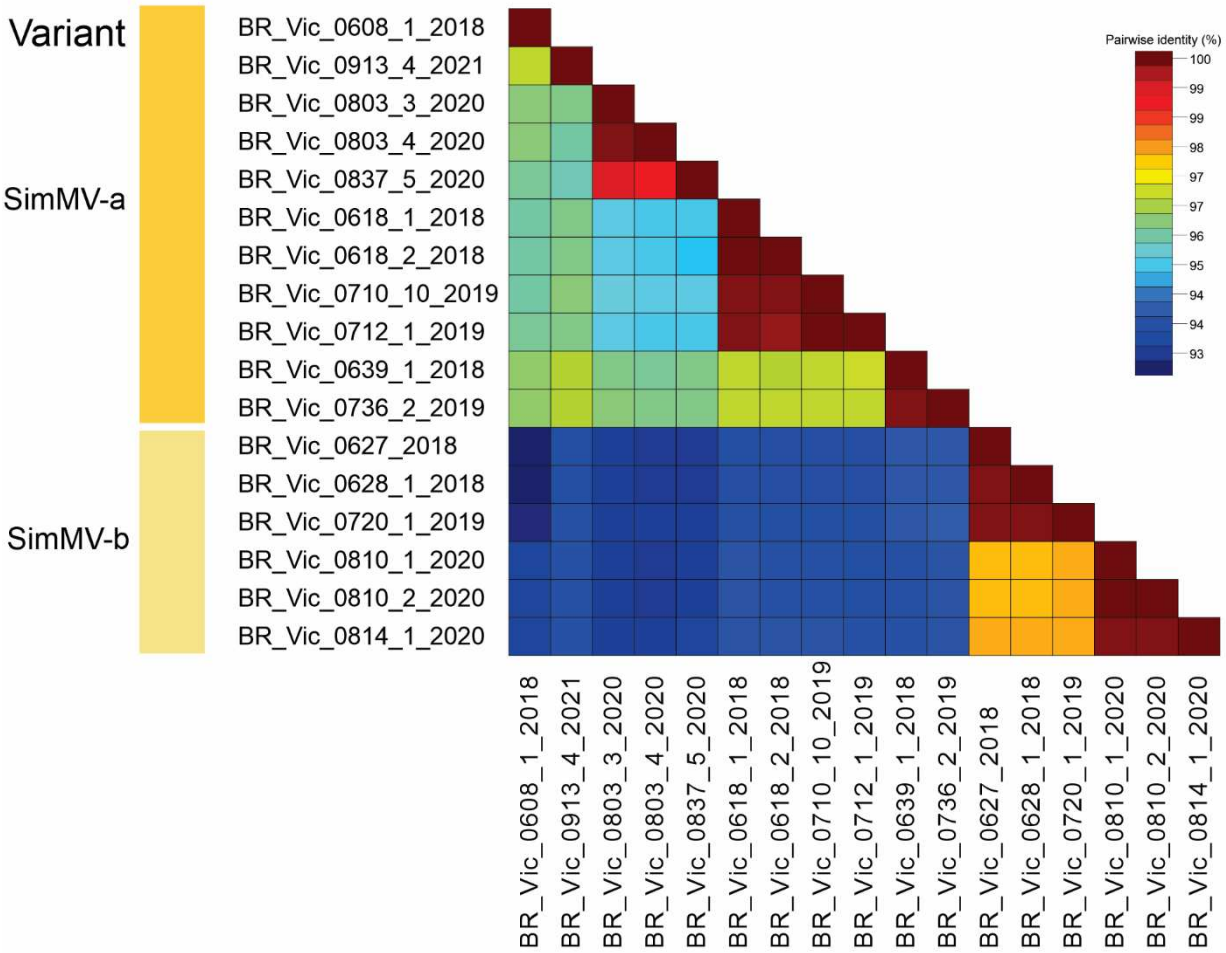
Variant
SimMV-a
SimMV-b
BR_Vic_0608_1_2018
BR_Vic_0913_4_2021
BR_Vic_0803_3_2020
BR_Vic_0803_4_2020
BR_Vic_0837_5_2020
BR_Vic_0618_1_2018
BR_Vic_0618_2_2018
BR_Vic_0710_10_2019
BR_Vic_0712_1_2019
BR_Vic_0639_1_2018
BR_Vic_0736_2_2019
BR_Vic_0627_2018
BR_Vic_0628_1_2018
BR_Vic_0720_1_2019
BR_Vic_0810_1_2020
BR_Vic_0810_2_2020
BR_Vic_0814_1_2020
Pairwise identity (%)
100
99
99
98
97
97
96
95
94
94
93

**Figure 6**

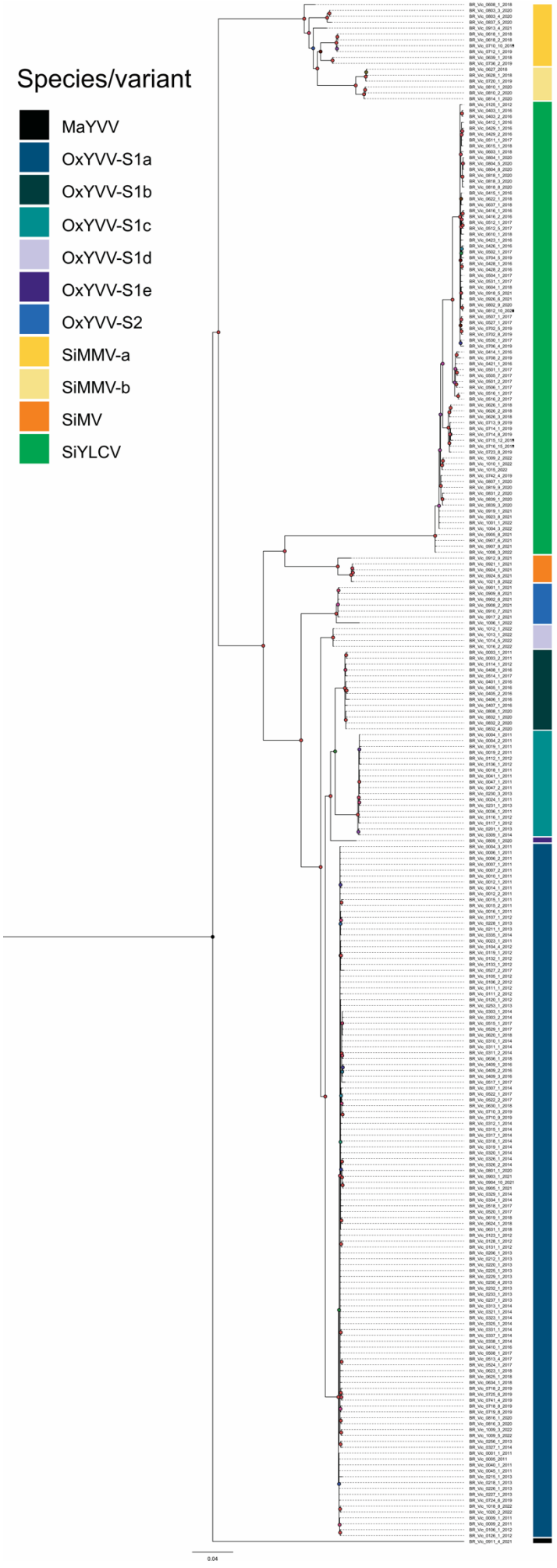
Species/variant
MaYVV
OxYVV-S1a
OxYVV-S1b
OxYVV-S1c
OxYVV-S1d
OxYVV-S1e
OxYVV-S2
SiMMV-a
SiMMV-b
SiMV
SiYLCV
0.04

**Figure 7**

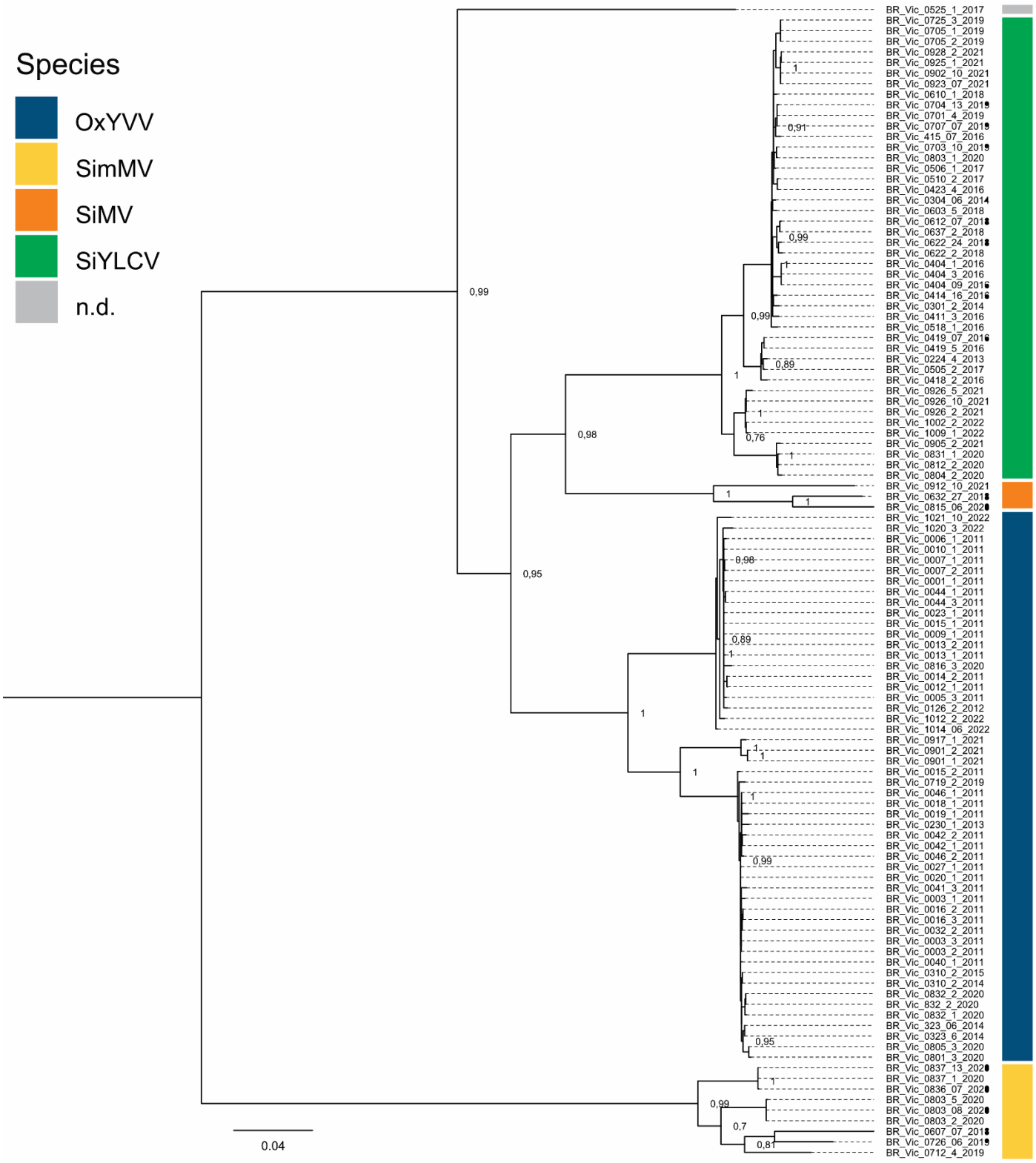

**Figure 8**

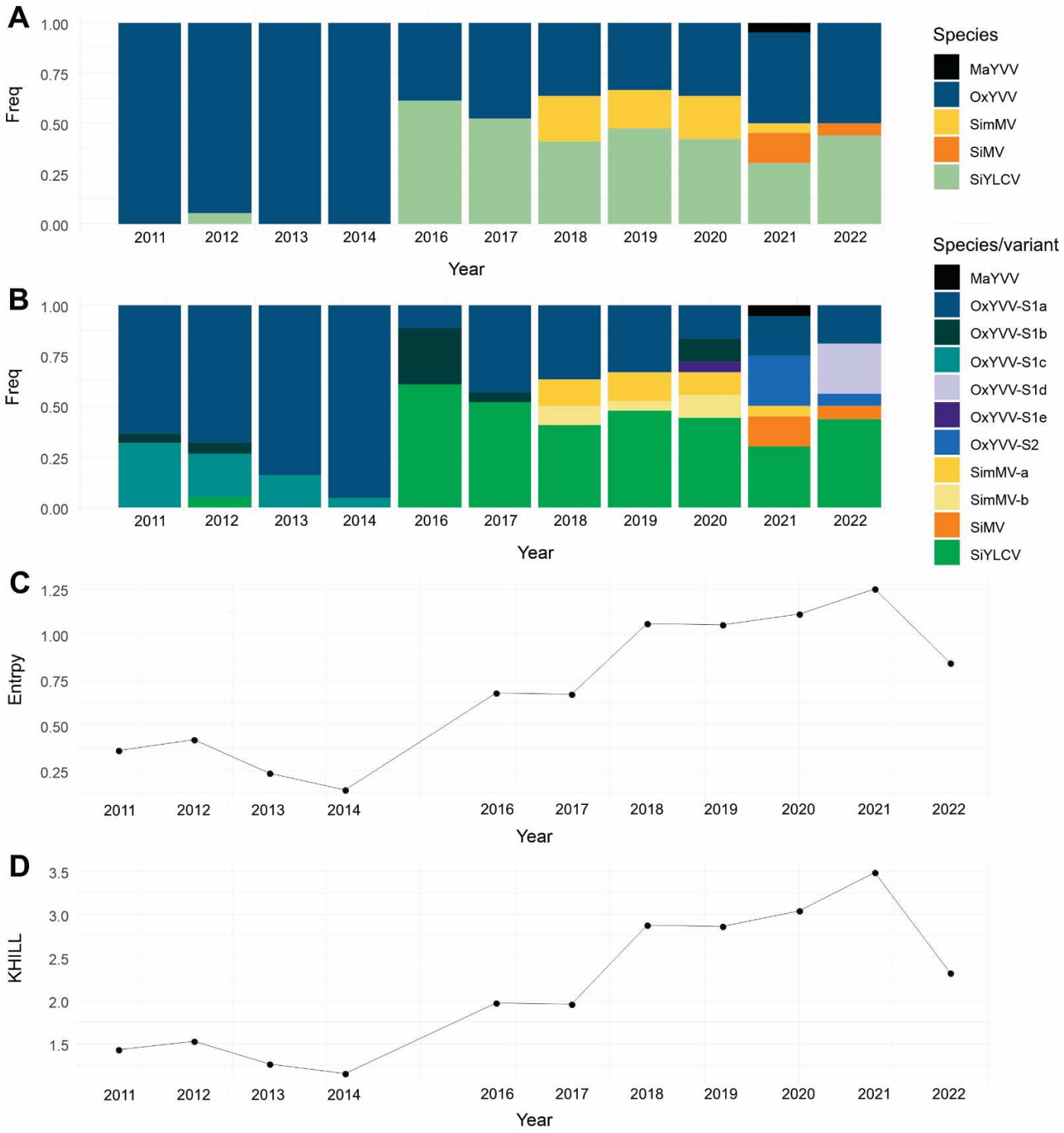
A
Freq
1.00
0.75
0.50
0.25
0.00
2011
2012
2013
2014
2016
2017
2018
2019
2020
2021
2022
Year
Species
MaYVV
OxYVV
SimMV
SiMV
SiYLCV
B
Freq
Year
Species/variant
MaYVV
OxYVV-S1a
OxYVV-S1b
OxYVV-S1c
OxYVV-S1d
OxYVV-S1e
OxYVV-S2
SimMV-a
SimMV-b
SiMV
SiYLCV
C
Entrpy
1.25
1.00
0.75
0.50
0.25
Year
D
KHILL
3.5
3.0
2.5
2.0
1.5
Year

**Figure 9**

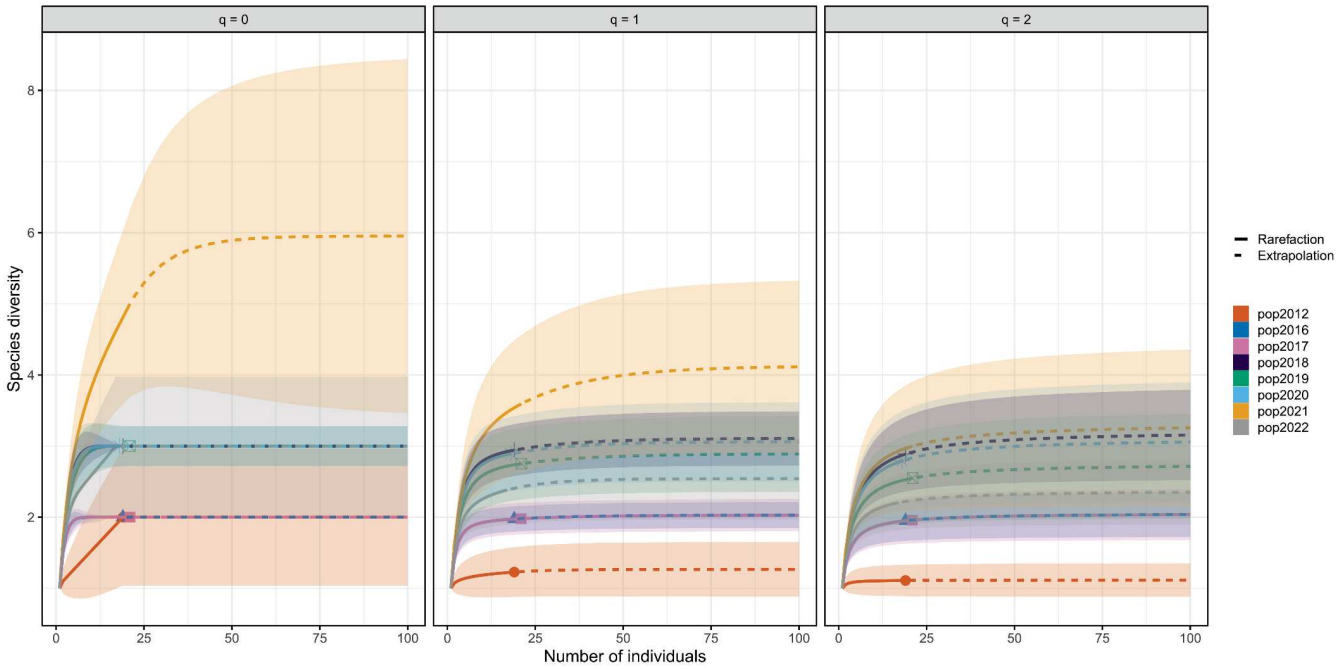
q = 0
q = 1
q = 2
Species diversity
Number of individuals
Rarefaction
Extrapolation
pop2012
pop2016
pop2017
pop2018
pop2019
pop2020
pop2021
pop2022

**Figure 10**

**A**

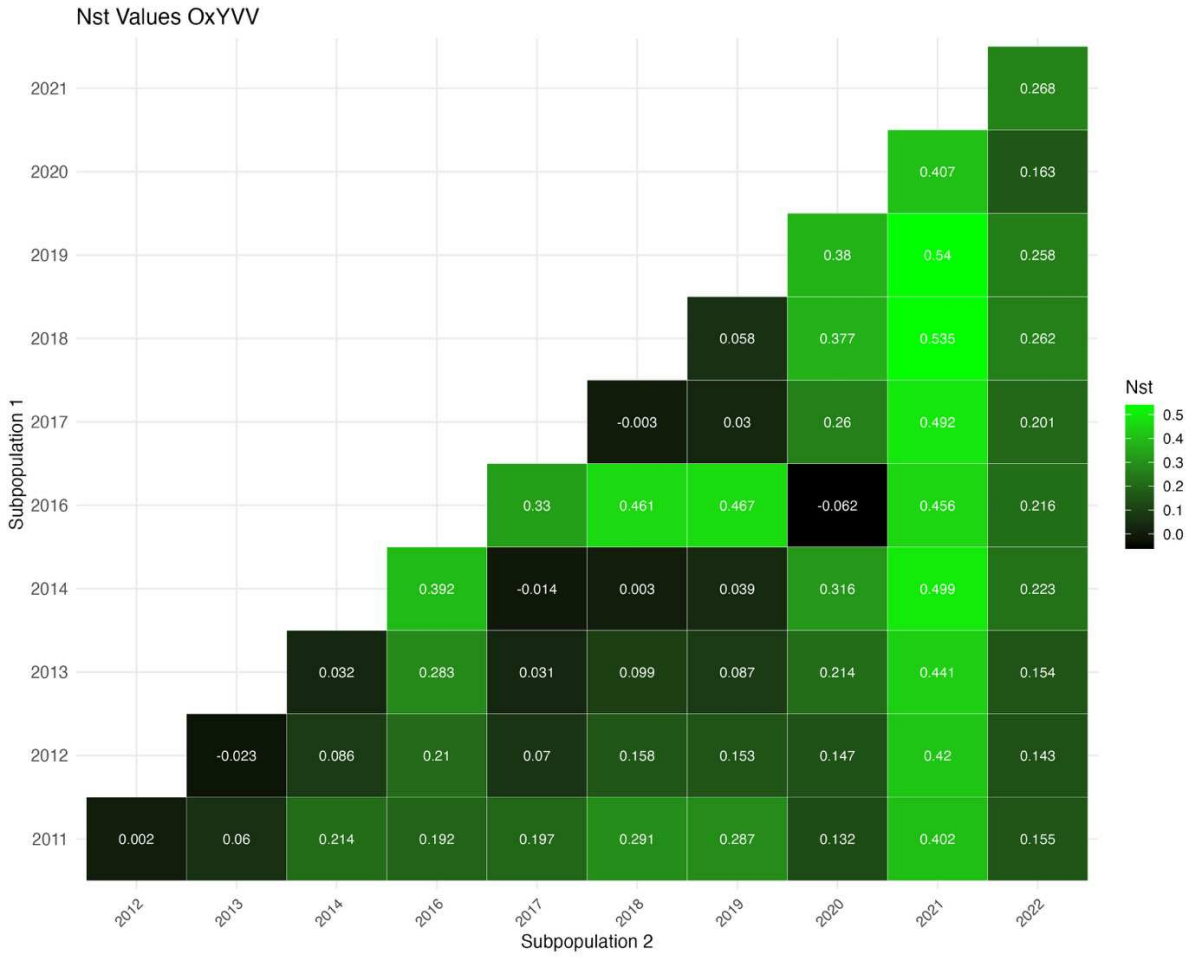
Nst Values OxYVV
Subpopulation 1
2021
2020
2019
2018
2017
2016
2014
2013
2012
2011
0.268
0.407 0.163
0.38 0.54 0.258
0.058 0.377 0.535 0.262
-0.003 0.03 0.26 0.492 0.201
0.33 0.461 0.467 -0.062 0.456 0.216
0.392 -0.014 0.003 0.039 0.316 0.499 0.223
0.032 0.283 0.031 0.099 0.087 0.214 0.441 0.154
-0.023 0.086 0.21 0.07 0.158 0.153 0.147 0.42 0.143
0.002 0.06 0.214 0.192 0.197 0.291 0.287 0.132 0.402 0.155
2012 2013 2014 2016 2017 2018 2019 2020 2021 2022
Subpopulation 2
Nst
0.5
0.4
0.3
0.2
0.1
0.0

**B**

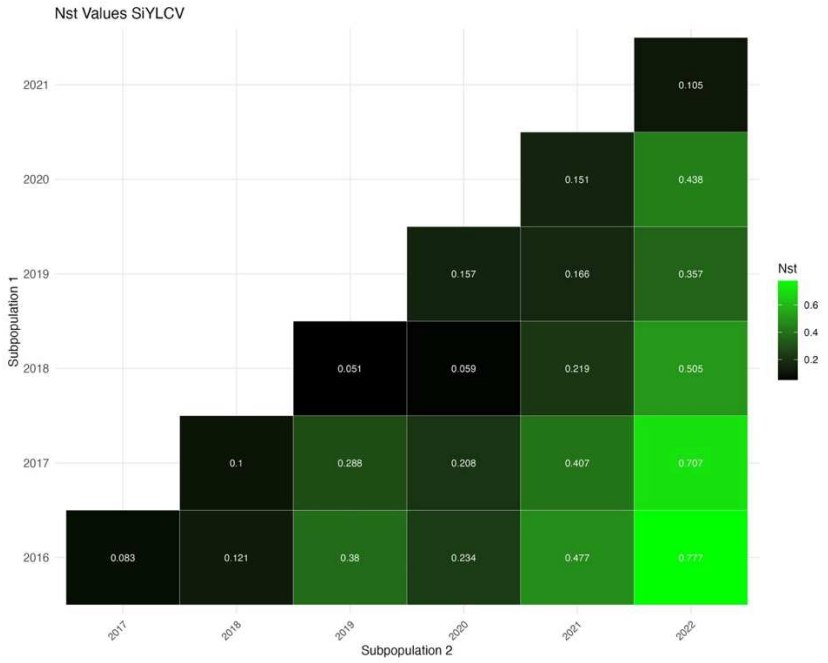
Nst Values SiYLCV
Subpopulation 1
2021
2020
2019
2018
2017
2016
0.105
0.151 0.438
0.157 0.166 0.357
0.051 0.059 0.219 0.505
0.1 0.288 0.208 0.407 0.707
0.083 0.121 0.38 0.234 0.477 0.777
2017 2018 2019 2020 2021 2022
Subpopulation 2
Nst
0.6
0.4
0.2

**Figure 11**

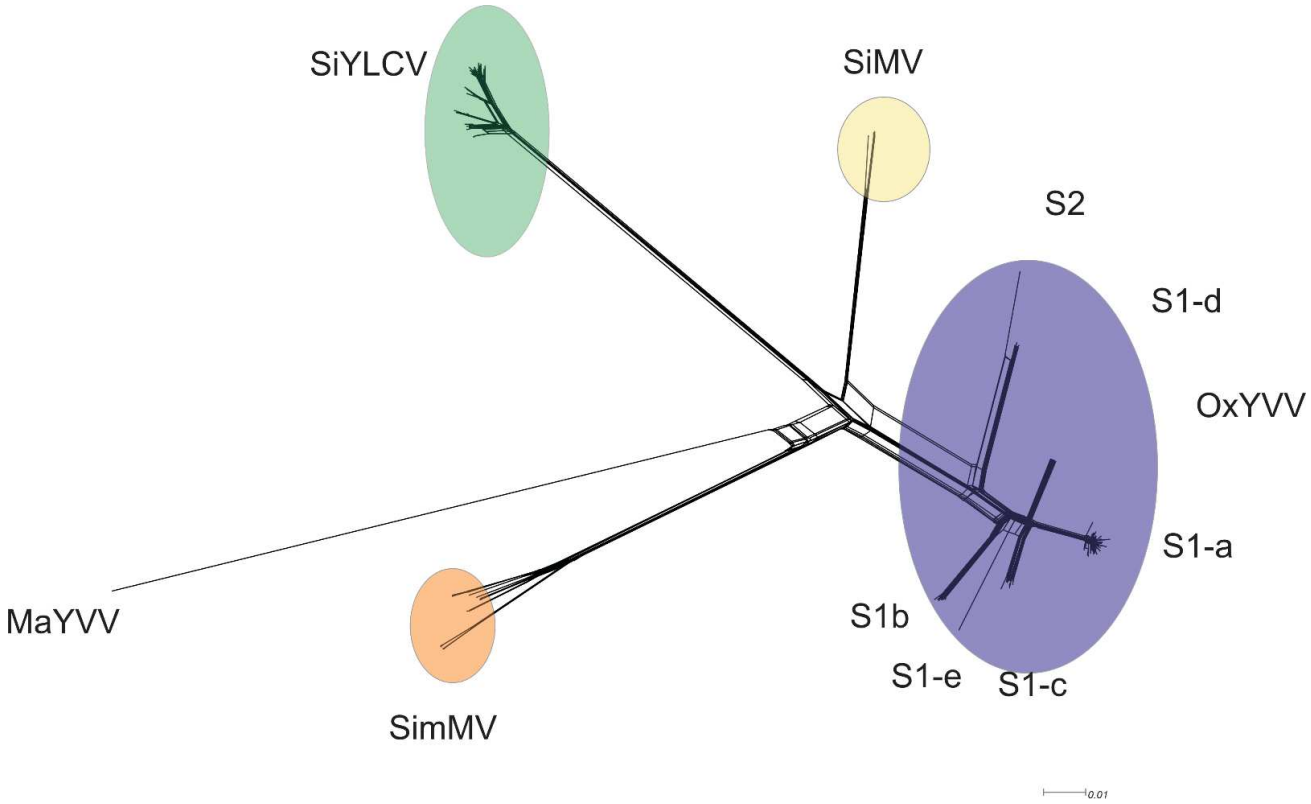

**Figure 12**

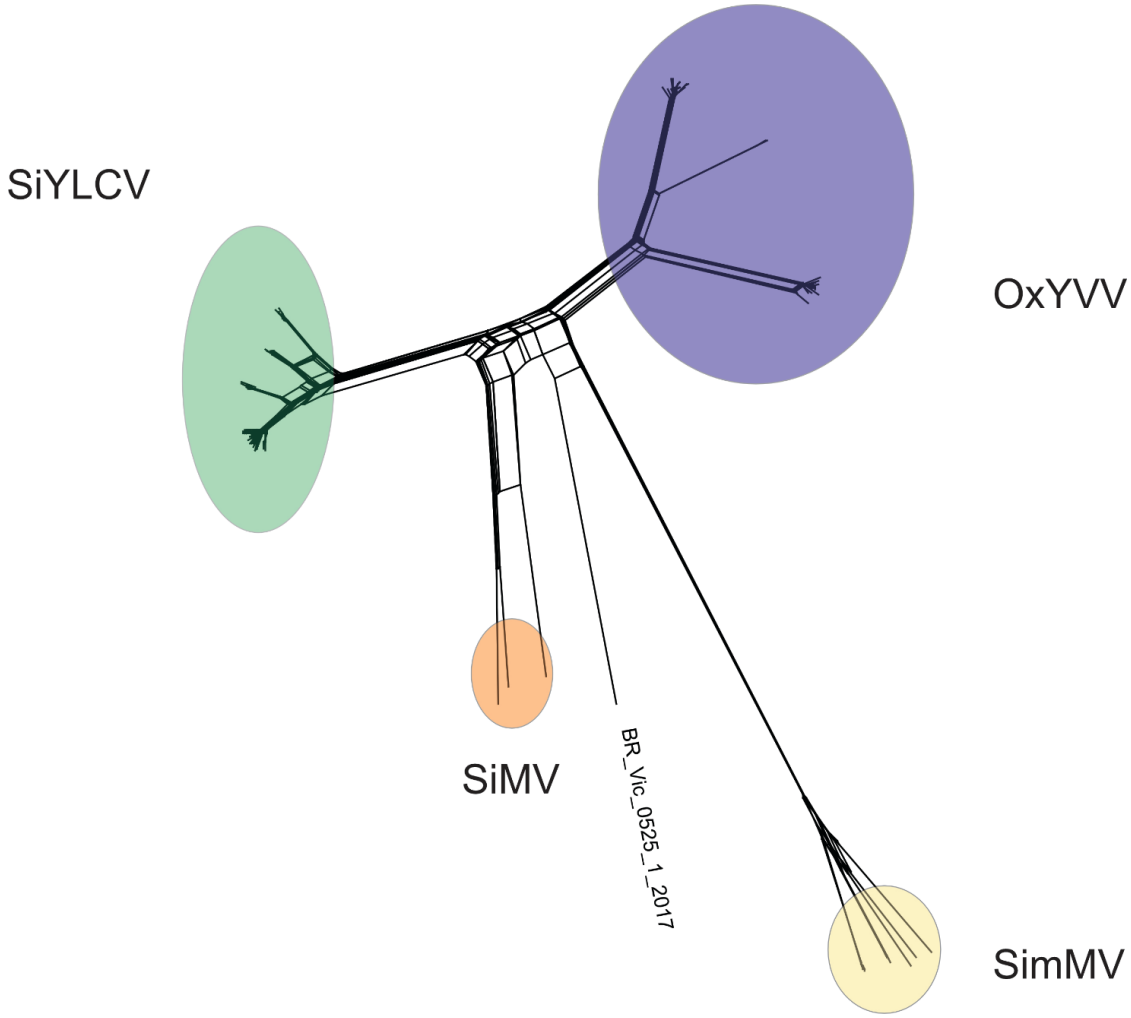

**Figure 13**

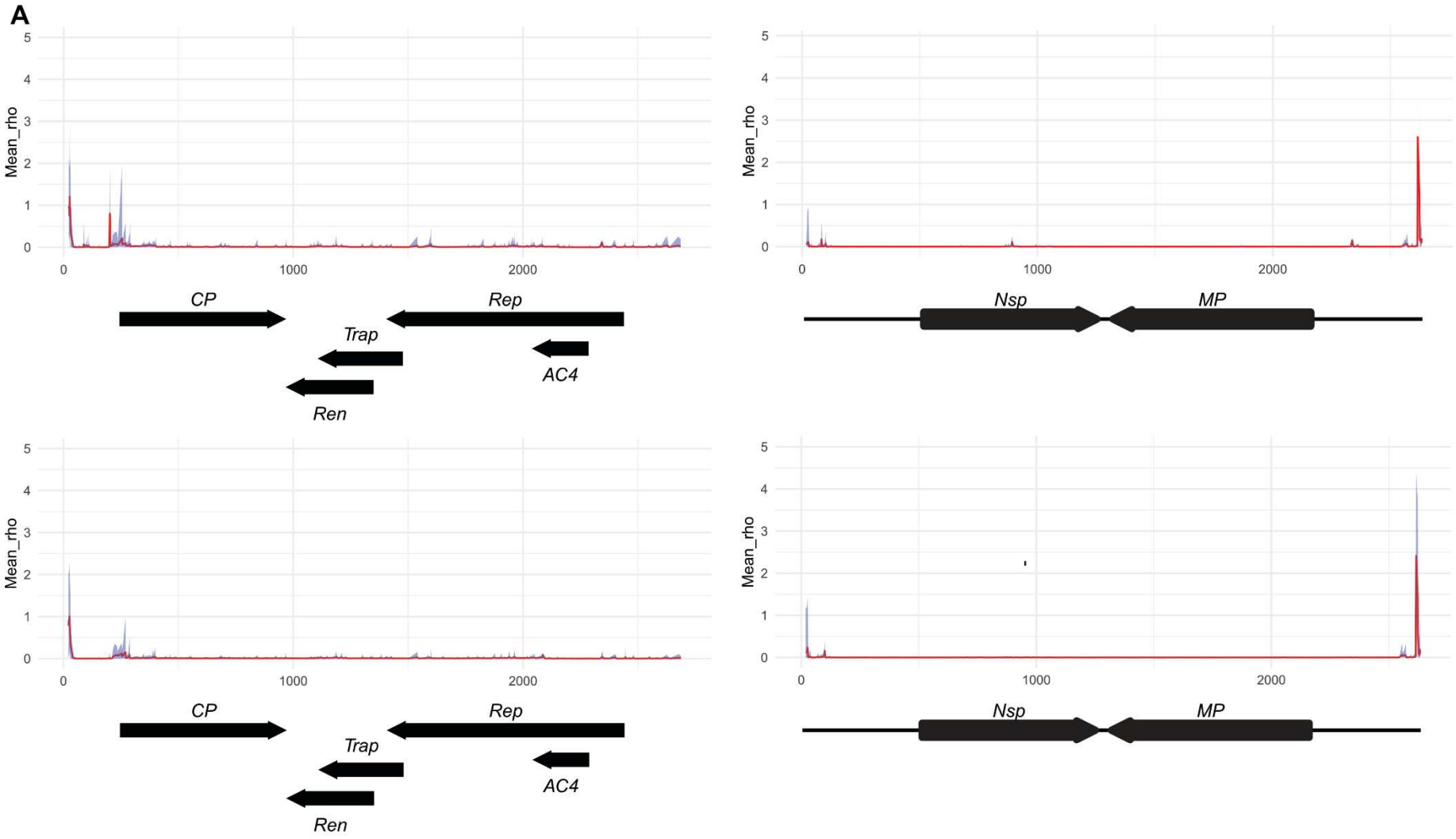

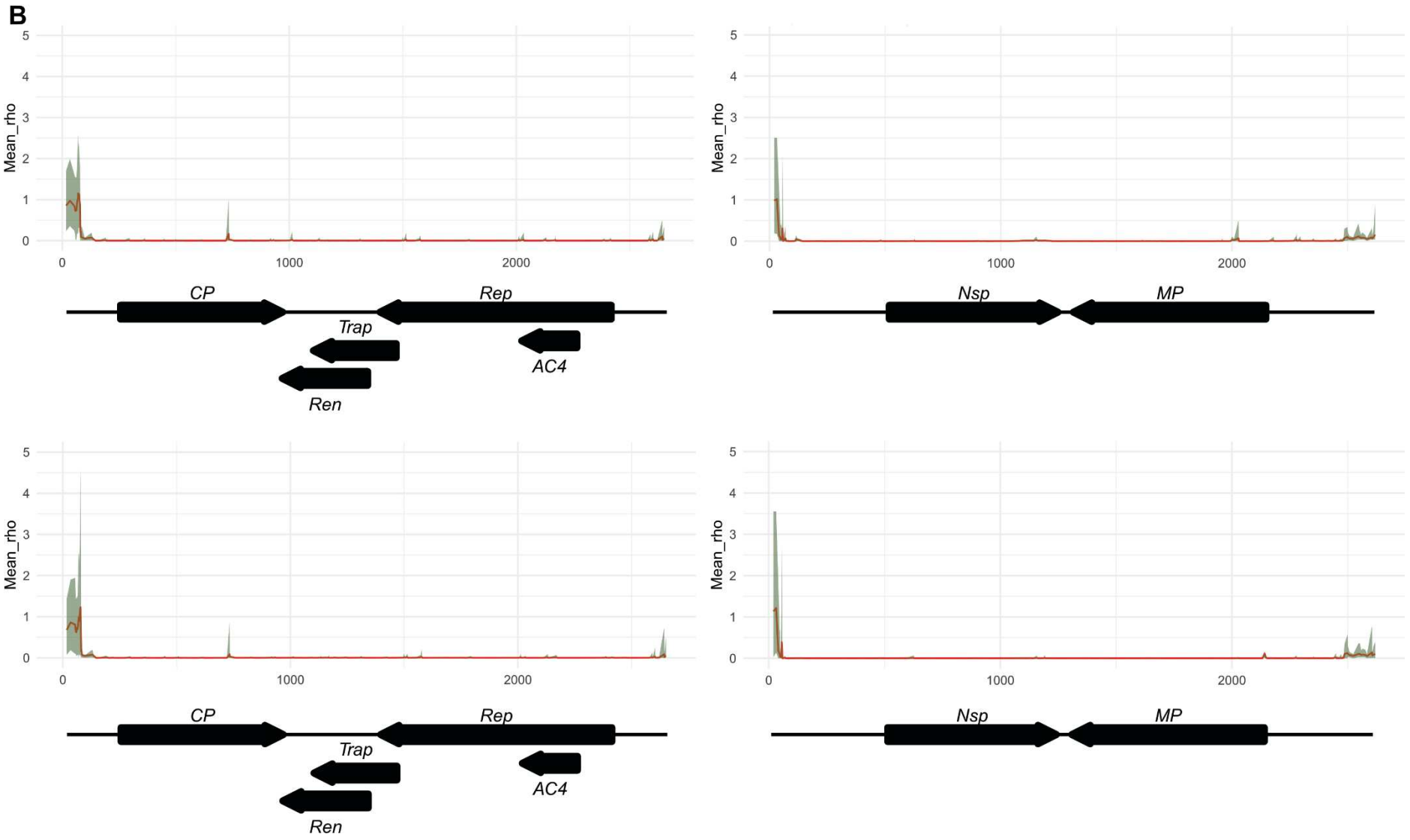
B
Mean_rho
0
1
2
3
4
5
0
1000
2000
CP
Rep
Trap
AC4
Ren
Nsp
MP

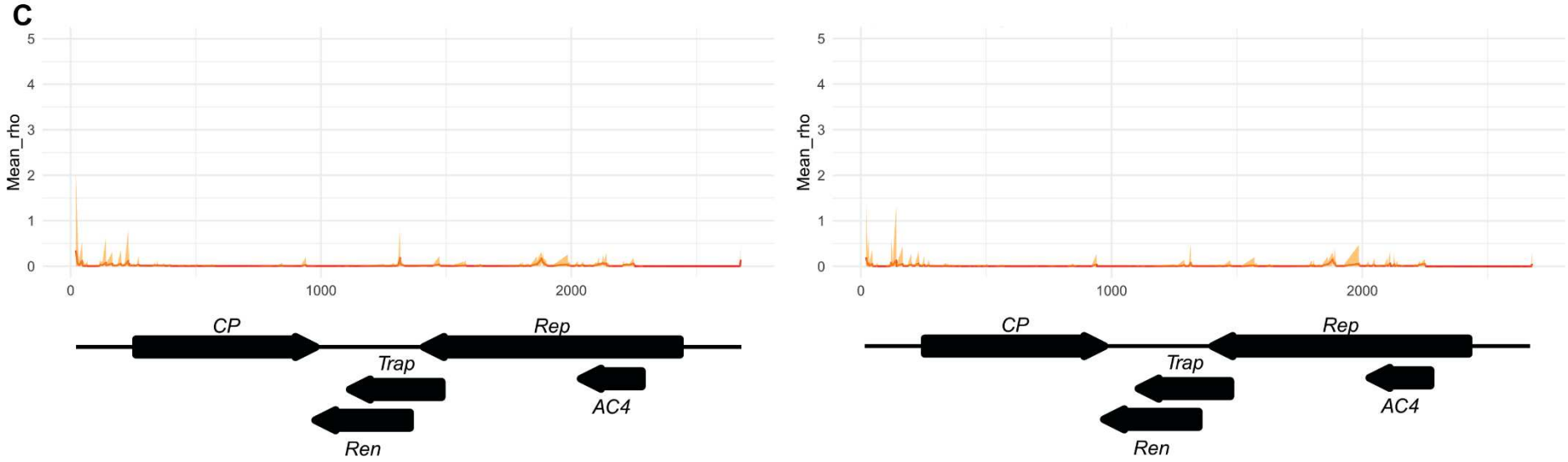
C
Mean_rho
5
4
3
2
1
0
0
1000
2000
CP
Rep
Trap
AC4
Ren
Mean_rho
5
4
3
2
1
0
0
1000
2000
CP
Rep
Trap
AC4
Ren

**Suppl. Table S1.** Summary statistics of Hill numbers. Diversity: species richness for $q = 0$, Shannon diversity for $q = 1$ and Simpson diversity for $q = 2$; Observed: observed diversity; Estimator: asymptotic diversity estimate; s.e.: standard error of the asymptotic estimator (s.e.): LCL, UCL: associated 95% lower and upper confidence limits, respectively.

| Assemblage | Diversity | Observed | Estimator | s.e. | LCL | UCL |
|---|---|---|---|---|---|---|
| pop2012 | Species richness | 2 | 2 | 0,49604496 | 2 | 2,97223 |
| pop2012 | Shannon diversity | 1,228989 | 1,266915 | 0,19849651 | 0,8778688 | 1,655961 |
| pop2012 | Simpson diversity | 1,110769 | 1,117647 | 0,12026413 | 0,8819337 | 1,35336 |
| pop2016 | Species richness | 2 | 2 | 0 | 2 | 2 |
| pop2016 | Shannon diversity | 1,975121 | 2,029238 | 0,08549092 | 1,8616788 | 2,196797 |
| pop2016 | Simpson diversity | 1,951351 | 2,060241 | 0,15558997 | 1,7552902 | 2,365192 |
| pop2017 | Species richness | 2 | 2 | 0 | 2 | 2 |
| pop2017 | Shannon diversity | 1,99811 | 2,042989 | 0,04676065 | 1,9513403 | 2,134639 |
| pop2017 | Simpson diversity | 1,996226 | 2,090909 | 0,09103408 | 1,9124856 | 2,269333 |
| pop2018 | Species richness | 3 | 3 | 0,1 | 3 | 3,195996 |
| pop2018 | Shannon diversity | 2,91835 | 3,065606 | 0,22633373 | 2,6220002 | 3,509212 |
| pop2018 | Simpson diversity | 2,845161 | 3,134328 | 0,35983922 | 2,4290564 | 3,8396 |
| pop2019 | Species richness | 3 | 3 | 0,1 | 3 | 3,195996 |
| pop2019 | Shannon diversity | 2,816121 | 2,958667 | 0,25096289 | 2,466789 | 3,450545 |
| pop2019 | Simpson diversity | 2,672727 | 2,916667 | 0,38843876 | 2,1553407 | 3,677993 |
| pop2020 | Species richness | 3 | 3 | 0,1 | 3 | 3,195996 |
| pop2020 | Shannon diversity | 2,846181 | 3,006223 | 0,25607511 | 2,5043251 | 3,508121 |
| pop2020 | Simpson diversity | 2,714286 | 3 | 0,41040311 | 2,1956247 | 3,804375 |
| pop2021 | Species richness | 5 | 5,95 | 1,48489446 | 5 | 8,86034 |
| pop2021 | Shannon diversity | 3,686441 | 4,261806 | 0,71655652 | 2,8573814 | 5,666231 |
| pop2021 | Simpson diversity | 3,125 | 3,518519 | 0,71913027 | 2,1090491 | 4,927988 |
| pop2022 | Species richness | 3 | 3 | 0,46140176 | 3 | 3,904331 |
| pop2022 | Shannon diversity | 2,416478 | 2,599637 | 0,38303066 | 1,8489108 | 3,350363 |
| pop2022 | Simpson diversity | 2,227723 | 2,44186 | 0,41088504 | 1,6365406 | 3,24718 |

**Suppl. Figure S1**

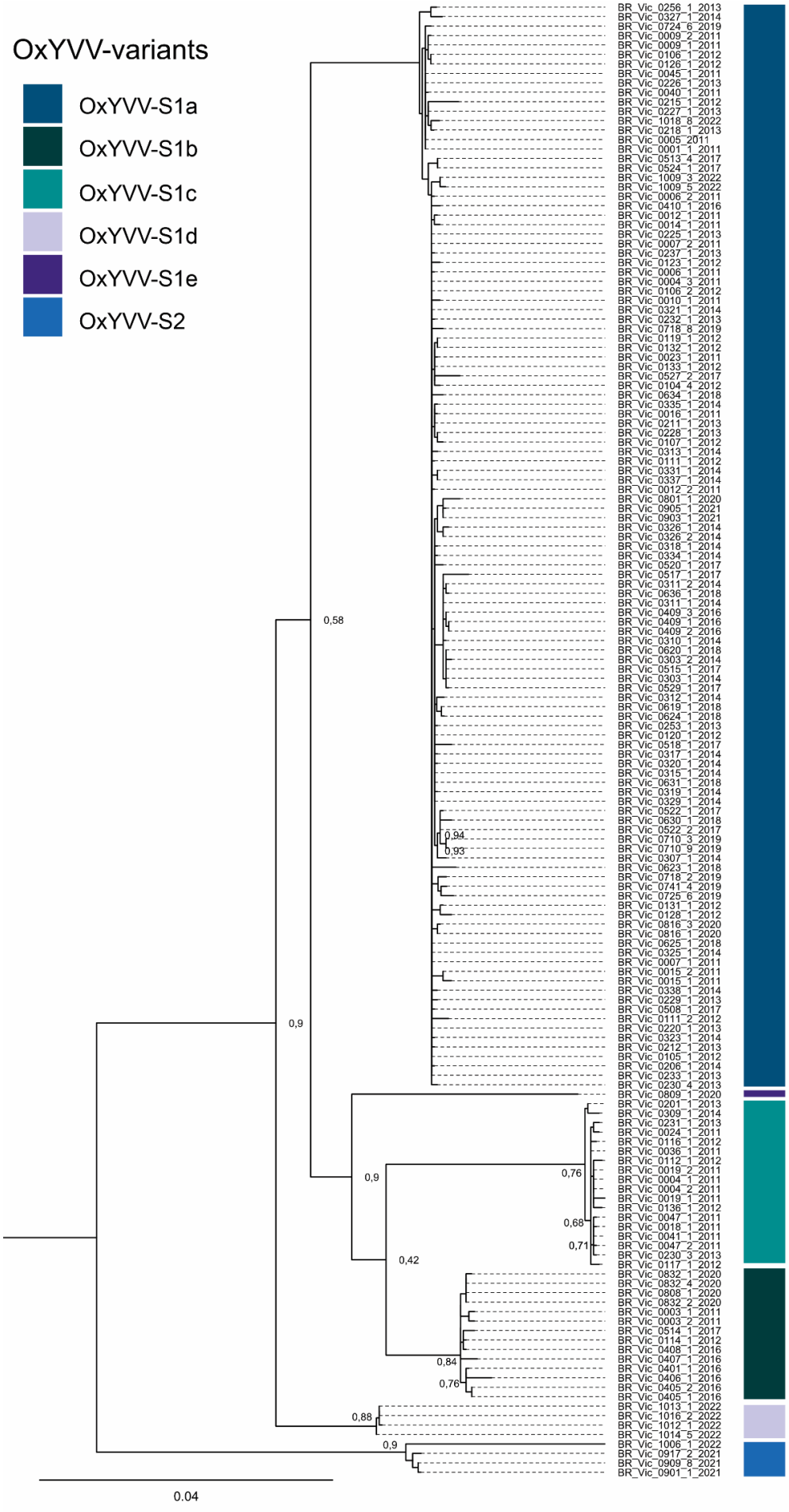

**Suppl. Figure S2**

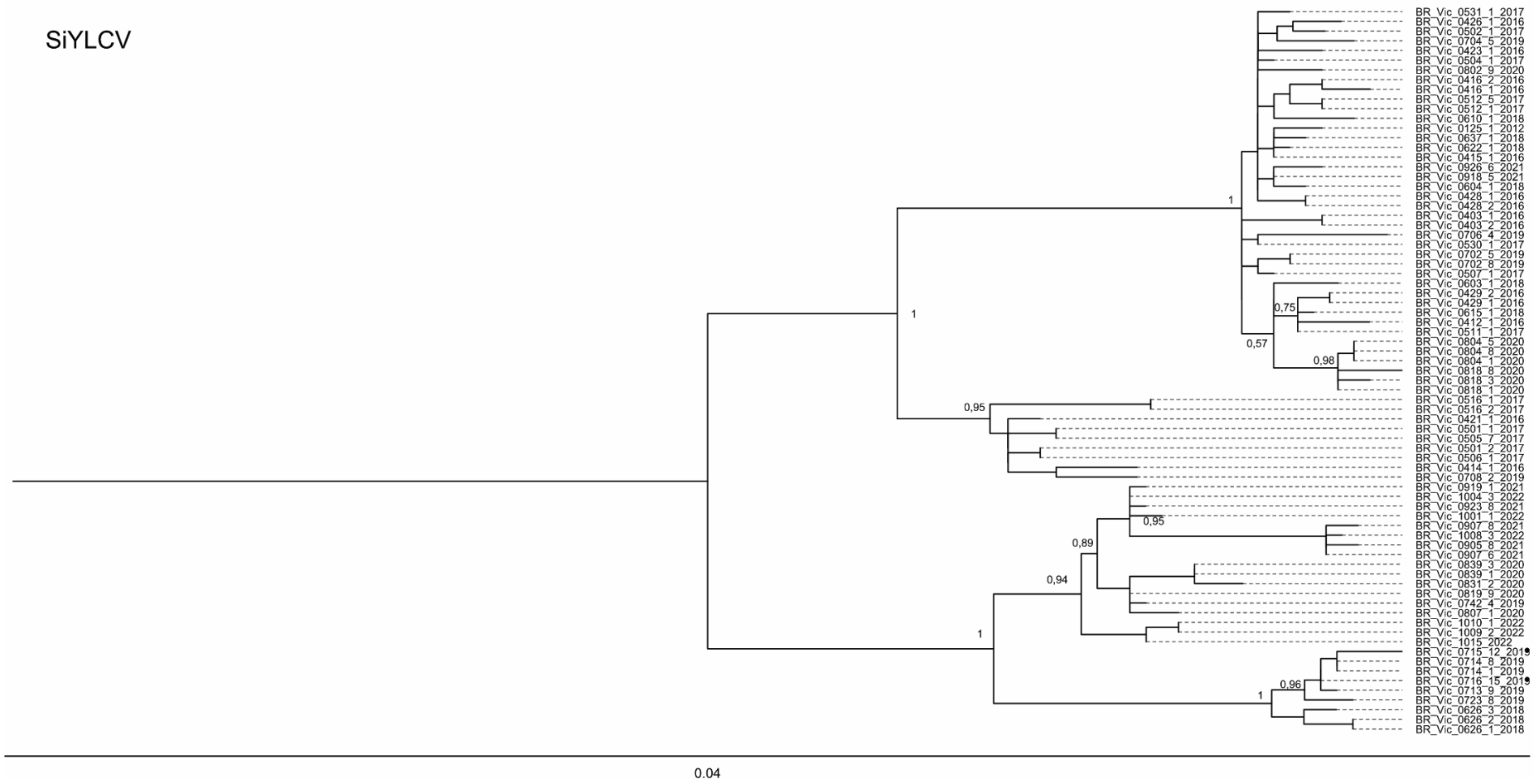

**Suppl. Figure S3**

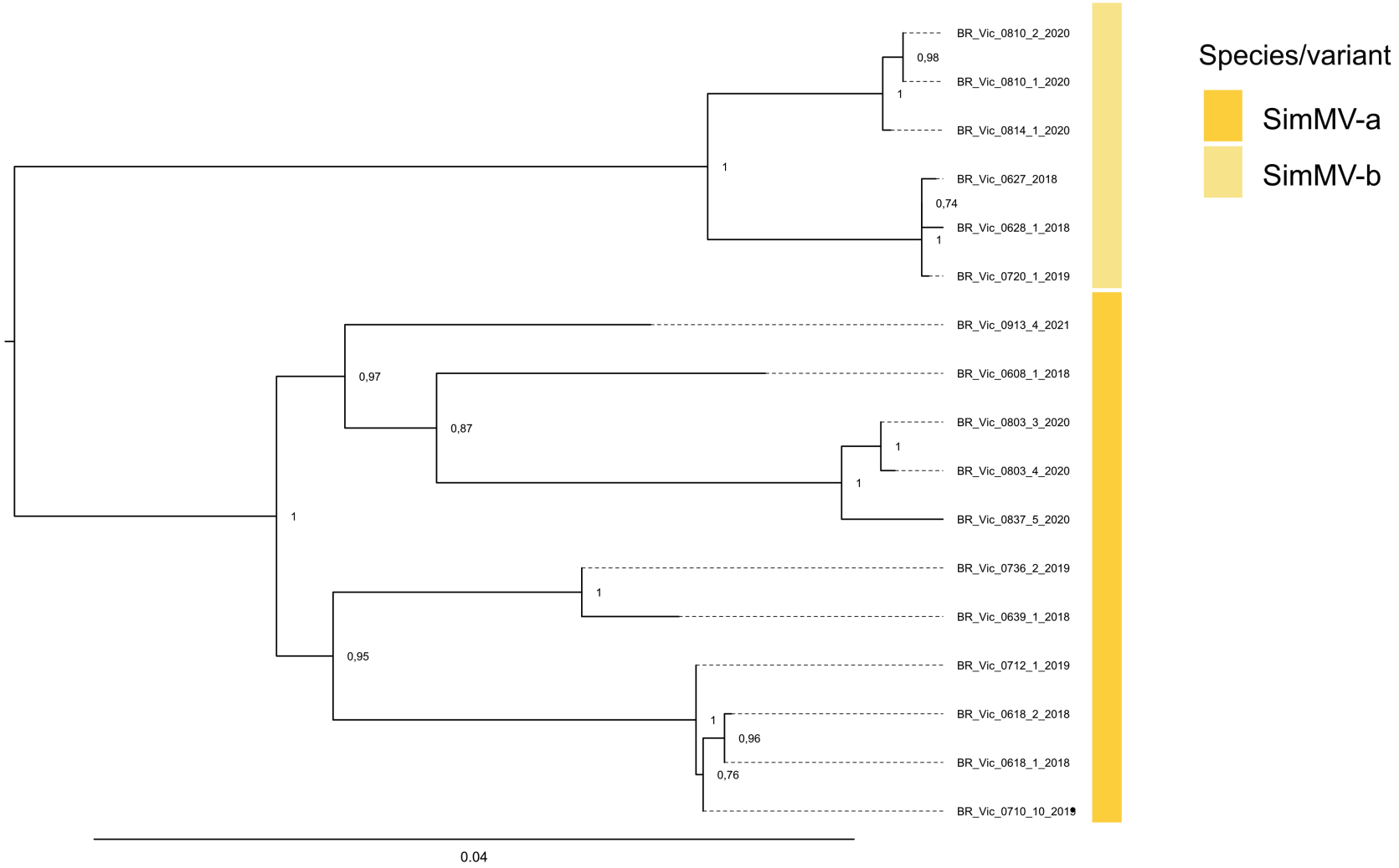

**Suppl. Figure S4**

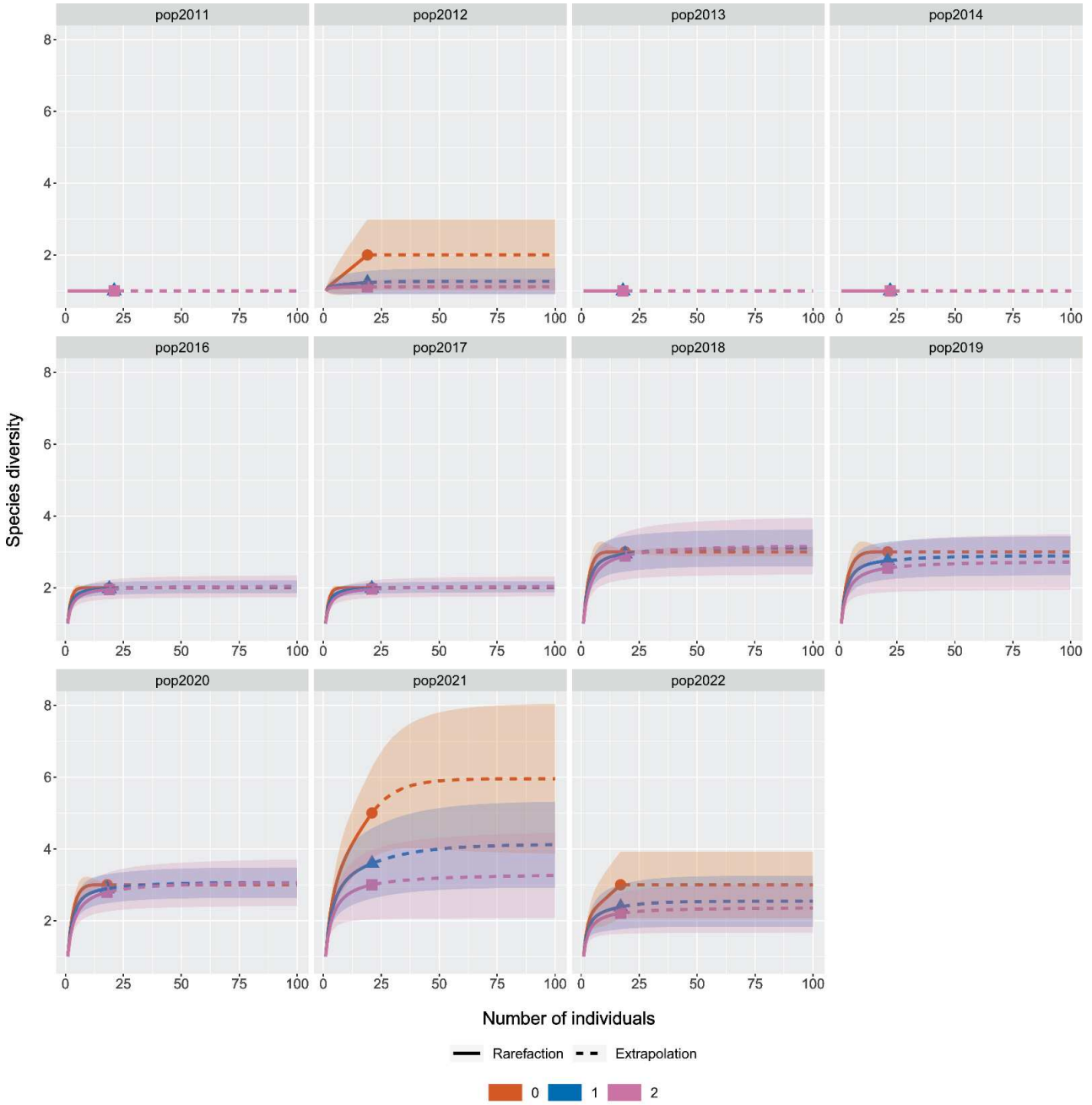

# CHAPTER 2

# DIFFERENTIAL FITNESS OF TWO VARIANTS OF OXALIS YELLOW VEIN VIRUS

Herrera da Silva JP, Xavier CAD, Oliveira PGS, Godinho MT, Lage JB, Orílio AF, Dias RS, Zerbini FM (2024) Differential fitness of two variants of Oxalis yellow vein virus. **Virus Evolution**, *in preparation*.

**Differential fitness of two variants of Oxalis yellow vein virus**

João P. Herrera da Silva[1], César A.D. Xavier[1#], Phedra G.S. Oliveira[1,&], Márcio T. Godinho[1], Júlia B. Lage[1], Anelise F. Orílio[1], Roberto S. Dias[2], F. Murilo Zerbini[1*]

[1]Dep. de Fitopatologia/BIOAGRO, Universidade Federal de Viçosa, Viçosa, MG 36570-900, Brazil

[2]Dep. de Biologia Geral, Universidade Federal de Viçosa, Viçosa, MG 36570-900, Brazil

[#]Present address: Dep. of Entomology and Plant Pathology, North Carolina State University, Raleigh, NC 27695, USA

[&]Present address: Dep. de Microbiologia/BIOAGRO, Universidade Federal de Viçosa, Viçosa, MG 36570-900, Brazil

[*]Corresponding author: Phone: (+55-31) 3612-2423, E-mail: zerbini@ufv.br

**Abstract**

Begomoviruses are important plant pathogens and pose threats to food production worldwide. In recent decades many begomoviruses emerged in different crops and in different regions of the world. A series of ecological and evolutionary factors govern the emergence of new viruses. Wild hosts are sources of viral biodiversity and contribute as a source of inoculum for plants of agricultural interest. Begomoviruses in non-cultivated hosts can coexist as complex populations composed of different variants. In a previous study we explored the temporal dynamics of a begomovirus community in *Sida acuta*. Oxalis yellow vein virus was found in all years of sampling and during most of the sampling time it was the prevalent species. The OxYVV population was subdivided into two strains, OxYVV-S1 and OxYVV-S2, with OxYVV-S1 being prevalent. In turn, OxYVV-S1 showed a pattern of subdivision into five variants. Heterogeneous distribution patterns were observed between the variants, with one variant prevailing over the others most of the time, leading us to hypothesize that there were adaptive differences between them. To test this hypothesis, we attempted to construct infectious clones of the three most abundant variants. Biological assays show clear phenotypic differences between the S1a and S1b variants. Unfortunately, we did not rescue infection with the OxYVV-S1c clone. No significant differences were observed regarding the latent period. Replication fitness was evaluated based on viral load. OxYVV-S1a presented a higher viral load up until 21 days after inoculation (dai) in relation to OxYVV-S1b, but its viral load reduced over time and did not differ statistically from that of OxYVV-S1b at 28 dai. The transmission rate of the two variants was assessed at 28 dai, and were similar. In general, the differential accumulation of the OxYVV-S1a variant at the early stage of infection suggests an adaptive advantage in relation to OxYVV-S1b and could explain the long-term prevalence of this variant.

## Introduction

Plant viruses pose a threat to food production around the world, causing economic losses worth billions of dollars annually (Mumford et al., 2016). It is estimated that at least half of emerging plant diseases are caused by viruses (Anderson et al., 2004).

The *Geminiviridae* family stands out for harboring a great viral diversity, capable of infecting monocots and dicotyledons, causing damage especially in tropical and subtropical regions. The family currently consists of 14 genera, defined based on phylogenetic relationships, genomic organization, type of insect vector and host range. Geminiviruses have a genome composed of one or two components of single-stranded circular DNA (ssDNA) genomes, each approximately 2,600 nucleotides in length, encapsidated in twinned icosahedral particles. The genus *Begomovirus* has the largest number of species, with a total of 445 species formally recognized by the International Committee on Taxonomy of Viruses (ICTV) as of February 2024 (https://ictv.global/taxonomy/). Begomoviruses infect dicots, can have monopartite or bipartite genomes and are transmitted by insects of the *Bemisia tabaci* cryptic species complex (Fiallo-Olive et al., 2021).

Begomoviruses emerged in different areas of the world during the 1980's and 1990's. Dozens of begomoviruses emerged in Latin America infecting tomatoes, peppers and legumes (Morales and Anderson, 2001; Ribeiro et al., 1998), in the African continent in cassava (Legg and Fauquet, 2004), in the Indian subcontinent in cotton and a number of vegetable crops (Borah and Dasgupta, 2012; Briddon and Markham, 2000), and in the Mediterranean basin in vegetable crops (Navas-Castillo et al., 2011). It has been hypothesized that these almost simultaneous emergencies were the result of viral lateral transfer from wild to domesticated hosts mediated by the global dispersal of *Bemisia argentifolii* (previously known as *B. tabaci* biotype B, or *B. tabaci* Middle East-Asia Minor 1) (Gilbertson et al., 2015). The ecological and epidemiological role of wild hosts was demonstrated in a number of studies (Rocha et al., 2013;

Roye et al., 1997; Rybicki and Hughes, 1990). Nevertheless, spillover events almost always fail. For a spillover event to be successful it is necessary for both the virus and its vector(s) to adapt to the new host (Elena et al., 2014; García-Arenal and Zerbini, 2019).

Fitness is the result of a set of components that determine the ability of a population to survive and to achieve reproductive success (Domingo et al., 2019). The complex equation that makes up the adaptive potential is made up of several variables, including replicative capacity, transmission efficiency, ability to overcome host defense pathways, vector resistance against insecticides, imbalance of initial frequencies of viral variants infecting the host, competition or cooperation between replicative entities, epistatic effects, among others (Cervera et al., 2016; Domingo et al., 2019; Wargo and Kurath, 2012).

In a simplified way, we will address two components of fitness: replication and transmission. The replicative component of fitness can be expressed as the relative comparison of viral load between variants in hosts inoculated in parallel, either in the context of single or mixed infections (Nogueira et al., 2023; Wargo and Kurath, 2012). The transmission component of fitness can be measured as the mediated transmission rate. Arthropod vectors mediate the transmission of most plant viruses (Hogenhout et al., 2008; Whitfield et al., 2015).

In 2011, Godinho et al. (2014) described a population of the begomovirus Oxalis yellow vein virus (OxYVV) infecting the non-cultivated plant *Sida acuta*, originally from South America. This population was made up of a complex of three distinct variants, both in the context of simple and mixed infections, named OxYVV-S1a, OxYVV-S1b e OxYVV-S1c, determined based on sequence comparisons and phylogenetic relationships. Later, Silva (2020) and Silva (2024; Chapter 1 of this work) explored the temporal dynamics of the same population, observing variations in terms of frequency distribution of OxYVV variants over time. The OxYVV-S1a variant predominated most of the time, except in 2016, when OxYVV-S1b predominated. The OxYVV-S1c variant was second in terms of frequency until 2014, when

it ceased to be detected. OxYVV-S1b appeared at a lower frequency most of the time, not being detected at some times and re-emerging at others. These observations lead the authors to raise the hypotheses that differential adaptability could explain frequency distribution changes over time and that a bottleneck effect could have caused OxYVV-S1b to outnumber OXYVV-S1a in 2016. Here, our aim was to assess the fitness differences among the three variants based on viral load and transmission rates. The results provide a preliminary idea of the differences between the variants analyzed here and are consistent with observations from previous studies (Silva, 2020; Wander and Silva, 2023)

## Materials and Methods

### Construction of infectious clones

Clones corresponding to the cognate DNA-A and DNA-B components of isolates 1D (OxYVV-S1a), 3D (OxYVV-S1b) and 19D (OxYVV-S1c), originating from *Sida acuta* samples collected in 2011, were used to construct infectious clones of each of the three variants (Godinho, 2014). The complete sequences of each genomic component (DNA-A and DNA-B) were analyzed using the A plasmid Editor (ApE) software (Davis and Jorgensen, 2022) to determine the most appropriate sites for construction of infectious clones. Two strategies were employed: 1.5mer and dimer construction (Suppl. Figure S1).

The strategy of obtaining 1.5mers was used for the DNA-A and DNA-B components of OxYVV-S1a and OxYVV-S1b. For both variants the process started with the release of the full-length copy of the genome from the plasmids by digestion with ClaI (DNA-A) and BamHI (DNA-B), followed by purification from the agarose gel with the Wizard SV Gel and PCR Clean-Up System (Promega) according to the manufacturer's instructions. The purified 1.0mer segments were digested with EcoRV (DNA-A) and KpnI (DNA-B) and purified from the

agarose gel as described above, generating the 0.5mer fragments. The 0.5mers were ligated into the pBluescript II KS+ (pKS+) plasmid vector (Stratagene) and transformed into *E. coli* DHα by electroporation (Sambrook and Russel, 2001). The clones were confirmed by double digestions using the same enzymes used to construct them. In the sequence, the 0.5mer clones were linearized with ClaI (DNA-A) and BamHI (DNA-B) and ligated to the 1.0mer segments. Following transformation of *E. coli* DH5α by electroporation, the 1.5mer constructs were confirmed by digestion with enzymes that cut the viral genome at a single point, previously selected using the ApE software.

The clones of the OxYVV-S1c variant were obtained by the dimer strategy, using Gibson Assembly for the DNA-A and partial digestion of rolling-circle amplification (RCA) products for the DNA-B. For the DNA-A, two pairs of primers were designed to amplify 1.0mers. PCR amplifications were performed using Phusion High-Fidelity DNA Polymerase, with an initial denaturation step at 98°C for 3 minutes followed by 35 cycles of denaturation at 98°C for 30 seconds, annealing at 65°C for 30 seconds and extension at 72°C for 2.5 minutes, with a final extension step at 72°C for 10 minutes. PCR products (0.04 pmol) were recombined using the GeneArt Gibson Assembly Cloning kit (Thermo Scientific) according to the manufacturer's instructions. Following transformation of *E.coli* DH5α by electroporation, the clone was confirmed by digestion with an enzyme that cuts the viral genome at a single point, previously selected using the ApE software. For the DNA-B, initially the complete segment was released from the full-length clone through digestion with the same enzyme used to clone it, religated and subjected to RCA using the phi29 DNA polymerase (Inoue-Nagata et al., 2004). The RCA product was subjected to partial digestion with BamHI at 37° for 30 seconds and the fragment corresponding to two copies of the genome (dimer) was purified from the agarose gel with the Wizard SV Gel and PCR Clean-Up System, ligated to the pKS+ vector and transformed

into *E. coli* DH5α by electroporation. The clone was confirmed as described above for the DNA-A.

**Infectivity assays**

*Sida acuta* seeds were subjected to treatment with concentrated sulfuric acid for five minutes to break dormancy. Healthy plant with two pairs of fully expanded leaves were inoculated with the OxYVV clones by particle bombardment as described by Cabrera-Ponce et al. (1997). For the inoculation assays, 10 micrograms of DNA, 5 mg of each DNA-A and DNA-B component, were used. In total, 12 plants were used per treatment, with each treatment consisting of one of the variants in simple infection context. The experiments were repeated three times, for a total of 36 inoculated plants per treatment. Negative controls consisted of plants inoculated with empty pKS+ vector. The inoculated plants were maintained at 25°C and a photoperiod of 12 hours light/12 hours dark and were monitored daily for the appearance of symptoms for 28 days. Viral infection was confirmed by RCA followed by digestion with MspI.

**Viral load quantification**

We selected 10 plants per treatment of two replications of the infectivity assay to quantify viral accumulation. The youngest, fully expanded leaves of the inoculated plants were collected at 14, 21 and 28 days after inoculation (dai) and used for total DNA extraction (Doyle and Doyle, 1987). Viral load was measured using quantitative-real-time PCR (qPCR) with virus-specific primers. The DNA concentration of each sample was determined by spectrophotometry using a NanoDrop 2000 (Thermo Scientific) and then adjusted to 10 ng/µl. qPCR reactions were performed in triplicates using FastSYBR Green Master Mix (ThermoFisher) in a final volume of 10 µl and 100 mM of each primer. Standard curves were constructed using full-length clones of each of the variants. Serial dilutions containing $1.6x10^1$

to $1.6x10^7$ copies per reaction were prepared. The qPCR cycles consisted of an initial denaturation step at 95°C for 3 min, followed by 35 cycles for 5 sec at 95°C and 30 sec at 60°C. The curves were obtained through linear regression of the cycle threshold (Ct) values of three replications of a given dilution in relation to the log of the number of DNA copies in each dilution. Regression analysis was carried out using the stats package in R software (R Core Team, 2017).

Statistical analysis to assess the level of significance of the latent period and viral load were carried out using the stats package in R software. First, homogeneity of variance was assessed with the Shapiro-Wilk normalization test. To infer the differences in the latent period, a *t*-test was performed to compare the treatment means at a significance level of 0.05%. For viral load, the non-parametric Mann-Whitney test was used.

**Transmission assays**

To assess the transmission component of fitness, transmission assays mediated by *Bemisia argentifolii* were performed with the OxYVV-S1a and OxYVV-S1b variants. *Sida acuta* plants inoculated by particle bombardment as previously described were used as inoculum source. Plant infection was confirmed by RCA and digestion with MspI, which also confirmed the identity of the variant that was infecting each plant. The insects used in the assays came from colonies established at the Virus Ecology and Evolution Laboratory (LEEV) at UFV. The insects are kept on cabbage (*Brassica oleracea*) plants, in cages with whitefly-proof mesh, at 25°C and a photoperiod of 14 hours of light/10 hours of dark. The colonies are periodically tested with universal primers for begomoviruses (Rojas et al., 1993) to confirm that they are aviruliferous.

A total of 15 aviruliferous insects were subjected to a 48-hour acquisition-access period (AAP) on infected plants. Then, the viruliferous insects were transferred to healthy *Sida acuta*

plants for an inoculation-access period (IAP) of 48 hours. After the IAP, the insects were eliminated using acetamiprid (80 mg a.i./L). After 28 days, total DNA was extracted and used for RCA and digestion by MspI to confirm the infection. We used 10 plants per treatment, in a single replication. Replicative fitness was estimated based on successful transmission events, that is, a proportion between the number of times that insects were able to acquire the virus from an infected plant and transmit it to a healthy plant in relation to the total number of plants evaluated in the experiment.

## Results

### Infectivity assays

Healthy *Sida acuta* plants were subjected to viral inoculation by biolistics. In total, 36 plants were used per treatment, and each treatment was comprised of plants infected by one of the variants in a simple infection context. Plants inoculated with the OxYVV-S1a and OxYVV-S1b clones showed symptoms which recalled those observed in the field, and infections were confirmed by RCA followed by MspI digestion (Figure 1). However, no symptoms were observed following inoculation with the OxYVV-S1c clones, and the RCA amplification product was not digested by MspI, indicating that the clones were not infectious.

Of the 36 inoculated plants of each treatment, 10 plants from each of the first two replications were selected for subsequent tests. Regarding infectivity, 18 out of 20 inoculated plants were infected with OxYVV-S1a, and 15 out of 20 were infected with OxYVV-S1b. Both variants induced symptoms of mosaic and vein yellowing, but we observed obvious differences in phenotypes with OxYVV-S1a inducing milder symptoms, while OxYVV-S1b induced more severe symptoms with a more intense yellowing (Figure 2). In general, plants began to show symptoms between 8 and 15 days. A *t*-test was performed to check whether there were

significant differences in latent period (the time from inoculation until the appearance of symptoms) and the variants did not differ (Figure 3).

**Replicative fitness**

To infer the replication component of fitness, we quantified the viral load in the context of single infection at 14, 21 and 28 dai. The experiments were carried out in two replications. *Sida acuta* plants were biolistically inoculated with infectious clones of either the OxYVV-S1a or the OxYVV-S1b variant and leaves from the plants that displayed symptoms were collected. Infections were confirmed by RCA and MspI digestion patterns (Figure 1), and plants that were positive for viral infection were used to assess viral load by qPCR.

The quantification of viral load was based on the accumulation of the DNA-A. For the OxYVV-S1a variant there was no significant difference in viral accumulation between 14 and 21 dai, but there was a significant reduction at 28 dai (Figure 4). For the OxYVV-S1b variant, no accumulation was detected at 14 dai and no significant differences were observed between 21 and 28 dai (Figure 4). In relation to differential accumulation between the two variants, there was a significant difference at 21 dai, with the OxYVV-S1a variant accumulating in greater quantities. However, there was no significant difference between the two variants at 28 dai (Figure 4). Thus, no correlation was observed between symptom severity and viral accumulation. However, it is relevant to check the accumulation kinetics of the DNA-B, which has shown to be a determinant of symptoms in begomovirus infections (Petty et al., 2000).

**Transmission fitness**

*Sida acuta* plants infected with each of the variants served as sources of inoculum for transmission assays with the whitefly vector. Plants were vector-inoculated with either the OxYVV-S1a or the OxYVV-S1b variant and leaves from all inoculated plants were collected

and tested for viral infection by RCA and MspI digestion patterns (Figure 1). For the OxYVV-S1a variant a total of 6 out of 10 inoculated plants were positive, while for the OxYVV-S1b variant 8 out of 10 plants were positive. This assay was conducted only once, the thus the results are considered preliminary.

**Discussion**

Begomoviruses in wild hosts can exist in the form of complex populations made up of different variants (Godinho, 2014; Silva, 2020). Over more than a decade (2011-2022), we monitored *Sida acuta* plants in a small (300 $m^2$) area. During this time, it was observed that the OxYVV population consisted of two strains, OxYVV-S1 and OxYVV-S2, that the OxYVV-S1 strain was the most abundant, and that this strain was subdivided into five variants. Among these variants, three were observed with greater frequency over time, OxYVV-S1a, OxYVV-Sb and OxYVV-S1c. During most of the time the OxYVV-S1a variant prevailed over the others and the OxYVV-S1c variant gradually reduced its frequency until its disappearance (Silva, 2020; this work, Chapter 1). These observations could be explained in several ways, such as a differential adaptation of variants to the host as a result of a long period of coevolution, differential transmission of the variants by the vectors, or antagonistic interactions amongst the variants (Silva, 2020).

To better understand this dynamic and elucidate the factors that may account for the prevalence of a species/strain/variant over the others, we obtained infectious clones of two variants and evaluated fitness-related aspects. We actually attempted to construct infectious clones of the three most common variants (based on the number of clones that were obtained from plants sampled in the area over time) (Silva, 2020). Unfortunately, inoculations with the OxYVV-S1c clone were not successful and as a result we carried out comparisons between the OxYVV-S1a and OxYVV-S1b variants.

We observed marked differences in the symptom patterns of the OxYVV-S1a and OxYVV-S1b variants, with the latter exhibiting more severe symptoms. The DNA-A segments of these variants are very similar, sharing 96.9% identity, but the DNA-B segments are more divergent, with 91% identity (Chapter 1). It is well documented that the begomovirus MP and NSP protein, both encoded by the DNA-B, are pathogenicity factors (Fondong, 2013; Garrido-Ramirez et al., 2000; Martins et al., 2020), and therefore it is possible that differences in these proteins could be responsible for the phenotypic differences between the two variants. Reassortment assays could provide insights into the role of the DNA-B segment as a determinant of symptoms for OxYVV variants. Nevertheless, TrAP and AC4, both encoded by the DNA-A, have also been reported as pathogenicity factors (Mei et al., 2021; Mills-Lujan and Deom, 2010; Park et al., 2010). Thus, constructions of chimeric clones with exchanges of these genes between the variants could also provide clues as to the influence of these genes on the phenotypes observed here.

Several changes in the host caused by viral infection can directly impact the transmission efficiency of viruses. Among these changes are the visual cues that make infected plants more attractive for insects, and it has been suggested that a virus that causes more intense yellowing symptoms is favored by vector attractiveness (Johnston and Martini, 2020; Mauck et al., 2012; Zhang et al., 2022). However, our observations reported in the previous chapter do not support these reports, since the most prevalent variant in the field (S1a) induced yellowing symptoms that were milder than those induced by the least common variant (S1b). Preference tests should be carried out to account for these discrepancies.

Increased replication capacity of a virus can affect prevalence in a location, since the higher the accumulation rate, the greater the probability of the virus contributing infectious offspring to the next generation, as well as the probability of being transmitted by the insect vector. We observed significant differences between the accumulation of the OxYVV-S1a and

OxYVV-S1b variants in the early stages of infection, with OxYVV-S1a showing greater accumulation up to 21 dai compared to OxYVV-S1b. Even though viral load of the two variants did not differ significantly at 28 dai, these results are consistent with the hypothesis that the variants differ in terms of adaptability, and that the most prevalent variant (OxYVV-S1a) is the one with the higher fitness. The period during which the viral load of OxYVV-S1a is higher than that of OxYVV-S1b could increase its chances of being transmitted, enhancing its spread and explaining its prevalence over the other variants. However, the replication rate is just one of the components of fitness and should not be extrapolated to infer the adaptability of a variant.

Our transmission assays, although carried out in a single experiment, seem to indicate that there are no major differences in the transmission efficiency of the two variants by *Bemisia argentifolii*. However, the fact that the observed transmission rates were similar could be due to the fact that the plants used for the assay were at 28 dai, which as mentioned above is a point when there is no statistically significant difference between the accumulation of the two variants. Thus, transmission assays in which plants at 14 or 21 dai are used as inoculum sources should be used to infer whether there the observed differences in viral load could account for a higher transmissibility of one variant compared to the other. Furthermore, our transmission assays were carried out using only one species of vector, and it is known that the efficiency of transmission may differ according to the whitefly species (Jiu et al., 2006). Incidentally, we have not surveyed the composition of whitefly species present in the area. Finally, it must be pointed out that the transmission rate measured under controlled conditions may not be a faithful measure of the real adaptive potential of a virus, as there are other underlying factors that determine the success or failure of transmission. As mentioned above, plant viruses induce phenotypic changes in their hosts that may lead to higher or lower attractiveness for insect vectors, such as the production of visual cues, changes in nutritional quality, synthesis of phytohormones or other volatile compounds that guide vectors, modulation of defense

pathways, increased longevity and fecundity of vectors, among others. In this context (Johnston and Martini, 2020; Mauck et al., 2012; Zhang et al., 2022), behavioral aspects of vectors deserve to be analyzed.

Non-synonymous substitutions throughout the *CP* and *Rep* genes were mapped in previous studies (Godinho, 2014; Silva, 2020). A single amino acid substitution was observed in the *CP* gene, a change from tyrosine (hydrophilic) to phenylalanine (hydrophobic) at position 206 between the OxYVV-S1a and OxYVV-S1b variants (Figure 5). Based on previous studies, the position where this substitution was mapped does not encompass a critical region for transmission of begomoviruses (Caciagli et al., 2009), which is consistent with our preliminary transmission assays.

For the *Rep* gene, there are 15 nucleotide differences between the OxYVV-S1a and OxYVV-S1b variants (Godinho, 2014; Silva, 2020). Among the non-synonymous substitutions observed in the *Rep* gene of OxYVV-S1b isolates, three are in functional motifs: E106D in motif III (the catalytic site for DNA cleavage), G224S located in Walker Motif A (binding to NTP) and V261I located in the Walker B motif (Figure 5). Although all three changes involve an exchange for an amino acid of the same class, these mutations could have incurred adaptive costs for the OXYVV-S1b variant and therefore could explain its lower frequency. Future studies using targeted mutagenesis may clarify whether these substitutions actually account for the fitness differences between the variants. Mutation patterns also differed for the OxYVV-S1c variant, but we were unable to rescue infections with clones of that variant.

We obtained preliminary evidence of the differential adaptability of two OxYVV variants. Some assays need to be repeated and additional ones need to be carried out, such as reassortment tests, vector preference assessments and competition tests between variants in mixed infections, to broaden our view of the fitness landscape of each of these variants.

## References


Anderson, P.K., Cunningham, A.A., Patel, N.G., Morales, F.J., Epstein, P.R., Daszak, P., 2004. Emerging infectious diseases of plants: Pathogen pollution, climate change and agrotechnology drivers. Tr Ecol Evol 19, 535-544.

Borah, B.K., Dasgupta, I., 2012. Begomovirus research in India: A critical appraisal and the way ahead. J Biosc 37, 791-806.

Briddon, R.W., Markham, P.G., 2000. Cotton leaf curl virus disease. Virus Res 71, 151-159.

Cabrera-Ponce, J.L., López, L., Assad-García, N., Medina-Arevalo, C., Bailey, A.M., Herrera-Estrella, L., 1997. An efficient particle bombardment system for the genetic transformation of asparagus (*Asparagus officinalis* L.). Plant Cell Rep 16, 255-260.

Caciagli, P., Piles, V.M., Marian, D., Vecchiati, M., Masenga, V., Mason, G., Falcioni, T., Noris, E., 2009. Virion stability is important for the circulative transmission of tomato yellow leaf curl sardinia virus by *Bemisia tabaci*, but virion access to salivary glands does not guarantee transmissibility. J Virol 83, 5784-5795.

Cervera, H., Lalić, J., Elena, S.F., 2016. Effect of host species on topography of the fitness landscape for a plant RNA virus. J Virol 90, 10160-10169.

Davis, M.W., Jorgensen, E.M., 2022. ApE, A Plasmid Editor: A Freely Available DNA Manipulation and Visualization Program. Frontiers in Bioinformatics 2, 818619.

Domingo, E., de Avila, A.I., Gallego, I., Sheldon, J., Perales, C., 2019. Viral fitness: history and relevance for viral pathogenesis and antiviral interventions. Path Dis 77, ftz021.

Domingo, E., Holland, J.J., 1997. RNA virus mutations and fitness for survival. Annu Rev Microbiol 51, 151-178.

Doyle, J.J., Doyle, J.L., 1987. A rapid DNA isolation procedure for small amounts of fresh leaf tissue. Phytochem Bull 19, 11-15.

Elena, S.F., Fraile, A., Garcia-Arenal, F., 2014. Evolution and emergence of plant viruses. Adv Virus Res 88, 161-191.

Fiallo-Olive, E., Lett, J.M., Martin, D.P., Roumagnac, P., Varsani, A., Zerbini, F.M., Navas-Castillo, J., 2021. ICTV Virus Taxonomy Profile: *Geminiviridae* 2021. J Gen Virol 102, 001696.

Fondong, V.N., 2013. Geminivirus protein structure and function. Mol Plant Pathol 14, 635-649.

García-Arenal, F., Zerbini, F.M., 2019. Life on the edge: geminiviruses at the interface between crops and wild plant hosts. Annu Rev Virol 6, 411-433.

Garrido-Ramirez, E.R., Sudarshana, M.R., Lucas, W.J., Gilbertson, R.L., 2000. Bean dwarf mosaic virus BV1 protein is a determinant of the hypersensitive response and avirulence in *Phaseolus vulgaris*. Mol Plant Microbe In 13, 1184-1194.

Gilbertson, R.L., Batuman, O., Webster, C.G., Adkins, S., 2015. Role of the insect supervectors *Bemisia tabaci* and *Frankliniella occidentalis* in the emergence and global spread of plant viruses. Annu Rev Virol 2, 67-93.

Godinho, M.T., 2014. Coexistência e evolução molecular de populações de begomovírus na planta não-cultivada *Sida acuta*, Dep. de Fitopatologia. Universidade Federal de Viçosa, Viçosa, MG, p. 71.

Hogenhout, S.A., Ammar, E.D., Whitfield, A.E., Redinbaugh, M.G., 2008. Insect vector interactions with persistently transmitted viruses. Annu Rev Phytopathol 46, 327-359.

Inoue-Nagata, A.K., Albuquerque, L.C., Rocha, W.B., Nagata, T., 2004. A simple method for cloning the complete begomovirus genome using the bacteriophage phi29 DNA polymerase. J Virol Met 116, 209-211.

Jiu, M., Zhou, X.P., Liu, S.S., 2006. Acquisition and transmission of two begomoviruses by the B and a non-B biotype of Bemisia tabaci from Zhejiang, China. J Phytopathol 154, 587-591.

Johnston, N., Martini, X., 2020. The influence of visual and olfactory cues in host selection for Bemisia tabaci biotype B in the presence or absence of tomato yellow leaf curl virus. Insects 11, 115.

Legg, J., Fauquet, C., 2004. Cassava mosaic geminiviruses in Africa. Plant Mol Biol 56, 585-599.

Martins, L.G.C., Raimundo, G.A.S., Ribeiro, N.G.A., Silva, J.C.F., Euclydes, N.C., Loriato, V.A.P., Duarte, C.E.M., Fontes, E.P.B., 2020. A Begomovirus Nuclear Shuttle Protein-Interacting Immune Hub: Hijacking Host Transport Activities and Suppressing Incompatible Functions. Front Plant Sci 11, 398.

Mauck, K.E., De Moraes, C.M., Mescher, M.C., 2012. Deceptive chemical signals induced by a plant virus attract insect vectors to inferior hosts. Proc Natl Acad Sci, USA 107, 3600-3605.

Mei, Y., Wang, Y., Hu, T., He, Z., Zhou, X., 2021. The C4 protein encoded by *Tomato leaf curl Yunnan virus* interferes with mitogen-activated protein kinase cascade-related defense responses through inhibiting the dissociation of the ERECTA/BKI1 complex. New Phytol 231, 747-762.

Mills-Lujan, K., Deom, C.M., 2010. Geminivirus C4 protein alters Arabidopsis development. Protoplasma 239, 95-110.

Morales, F.J., Anderson, P.K., 2001. The emergence and dissemination of whitefly-transmitted geminiviruses in Latin America. Arch Virol 146, 415-441.

Mumford, R., Macarthur, R., Boonham, N., 2016. The role and challenges of new diagnostic technology in plant biosecurity. Food Sec 8, 103-109.

Navas-Castillo, J., Fiallo-Olivé, E., Sánchez-Campos, S., 2011. Emerging virus diseases transmitted by whiteflies. Annu Rev Phytopathol 49, 219-248.

Nogueira, A.M., Barbosa, T.M.C., Quadros, A.F.F., Orílio, A.F., Bigão, M.C.J., Xavier, C.A.D., Ferro, C.G., Zerbini, F.M., 2023. Specific nucleotides in the common region of the begomovirus tomato rugose mosaic virus (ToRMV) are responsible for the negative interference over tomato severe rugose virus (ToSRV) in mixed infection. Viruses 15.

Park, J., Hwang, H.S., Buckley, K.J., Park, J.B., Auh, C.K., Kim, D.G., Lee, S., Davis, K.R., 2010. C4 protein of Beet severe curly top virus is a pathomorphogenetic factor in Arabidopsis. Plant Cell Rep 29, 1377-1389.

Petty, I.T., Carter, S.C., Morra, M.R., Jeffrey, J.L., Olivey, H.E., 2000. Bipartite geminivirus host adaptation determined cooperatively by coding and noncoding sequences of the genome. Virology 277, 429-438.

R Core Team, 2017. R: A language and environment for statistical computing. R Foundation for Statistical Computing, Vienna, Austria.

Ribeiro, S.G., Ávila, A.C., Bezerra, I.C., Fernandes, J.J., Faria, J.C., Lima, M.F., Gilbertson, R.L., Zambolim, E.M., Zerbini, F.M., 1998. Widespread occurrence of tomato geminiviruses in Brazil, associated with the new biotype of the whitefly vector. Plant Dis 82, 830.

Rocha, C.S., Castillo-Urquiza, G.P., Lima, A.T.M., Silva, F.N., Xavier, C.A.D., Hora-Junior, B.T., Beserra-Junior, J.E.A., Malta, A.W.O., Martin, D.P., Varsani, A., Alfenas-Zerbini, P., Mizubuti, E.S.G., Zerbini, F.M., 2013. Brazilian begomovirus populations are highly recombinant, rapidly evolving, and segregated based on geographical location. J Virol 87, 5784-5799.

Rojas, M.R., Gilbertson, R.L., Russell, D.R., Maxwell, D.P., 1993. Use of degenerate primers in the polymerase chain reaction to detect whitefly-transmitted geminiviruses. Plant Dis 77, 340-347.

Roye, M.E., McLaughlin, W.A., Nakhla, M.K., Maxwell, D.P., 1997. Genetic diversity among geminiviruses associated with the weed species *Sida* spp., *Macroptilium lathyroides*, and *Wissadula amplissima* from Jamaica. Plant Dis 81, 1251-1258.

Rybicki, E.P., Hughes, F.L., 1990. Detection and typing of maize streak virus and other distantly related geminiviruses of grasses by polymerase chain reaction amplification of conserved viral sequences. J Gen Virol 71, 2519-2526.

Sambrook, J., Russel, D., 2001. Molecular Cloning - A Laboratory Manual (3ª ed.). Cold Spring Harbor Laboratory Press, Cold Spring Harbor, NY.

Silva, J.P., 2020. Evolution of a DNA virus in the natural environment - a journey through time, Dep. de Fitopatologia. Universidade Federal de Viçosa, Viçosa, MG, Brazil.

Wander, A.E., Silva, O.F.S., 2023. Cultivo do Feijão: Estatística da produção. Embrapa Arroz e Feijão.

Wargo, A.R., Kurath, G., 2012. Viral fitness: Definitions, measurement, and current insights. Curr Opin Virol 2, 538-545.

Whitfield, A.E., Falk, B.W., Rotenberg, D., 2015. Insect vector-mediated transmission of plant viruses. Virology 480, 278-289.

Zhang, Z., Zhang, B., He, H., Yan, M., Li, J., Yan, F., 2022. Changes in visual and olfactory cues in virus-infected host plants alter the behavior of *Bemisia tabaci*. Front Ecol Evol 10.

**Figure legends**

**Figure 1. A.** *In silico* restriction patterns for the DNA-A and DNA-B of the three variants (S1a, S1b and S1c) of Oxalis yellow vein virus (OxYVV). **B.** MspI digestion of rolling-circle amplification (RCA) products from *Sida acuta* plants biolistically inoculated with OxYVV-S1a and OxYVV-S1b clones. RCA was performed using total DNA extrated from inoculated plants at 28 days after inoculation (dai). **C.** MspI digestion of RCA products from *Sida acuta* plants inoculated with whiteflies (*Bemisia argentifolii*) with the OxYVV-S1a and OxYVV-S1b variants. RCA was performed using total DNA extrated from inoculated plants at 28 dai.

**Figure 2.** Symptoms in *Sida acuta* plants biolistically inoculated with infectious clones of two variants of Oxalis yelllow vein virus (OxYVV). **A.** Asymptomatic *Sida acuta* plant (negative control). **B.** *Sida acuta* plant infected with the OxYVV-S1a variant exhibiting mild yellow vein symptoms. **C.** *Sida acuta* plant infected with the OxYVV-S1b variant exhibiting severe yellow vein symptoms.

**Figure 3.** Latent period of *Sida acuta* plants inoculated with two variants of Oxalis yellow vein virus, OxYVV-S1a and OxYVV-S1b. The plants were monitored for the appearance of symptoms until 28 days after inoculation. Each point in the boxplots represents one inoculated plant of two independent experiments. Statistical analysis indicated no difference between the latent period of the two variants.

**Figure 4.** Accumulation of two variants of Oxalis yellow vein virus, OxYVV-S1a and OxYVV-S1b, in *Sida acuta* plants. Absolute quantification of viral DNA was carried out by real-time quantitative PCR at 14, 21 and 28 days after inoculation. Each point in the boxplots represents

one inoculated plant of two independent experiments. Different top bars indicate statistically significant differences between groups according to the Mann Whitney non-parametric test ($p$<0.05).

**Figure 5. A.** Schematic representation of the OxYVV coat protein (CP). Yellow boxes represent non-synonymous sites that allow differentiation between variants. The letters represent amino acid changes. **B.** Schematic representation of the OxYVV replication-associated protein (Rep). Yellow boxes represent non-synonymous sites that allow differentiation between variants. Pink boxes represent conserved motifs in the coding sequence. The letters represent amino acid changes; U represents any hydrophobic amino acid and X represents any amino acid. The numbers represent amino acid positions in the protein sequence. The letters in parentheses represent amino acids present in each variant (OxYVV-S1a/b/c).

**Suppl. Figure S1.** *In silico* digestion carried out to construct 1.5mer clones of the **(A)** DNA-A and **(B)** DNA-B components of the OxYVV-S1a and OxYVV-S1b variants, and dimeric clones of the **(C)** DNA-A and **(D)** DNA-B of the OxYVV-S1c variant.

**Figure 1**

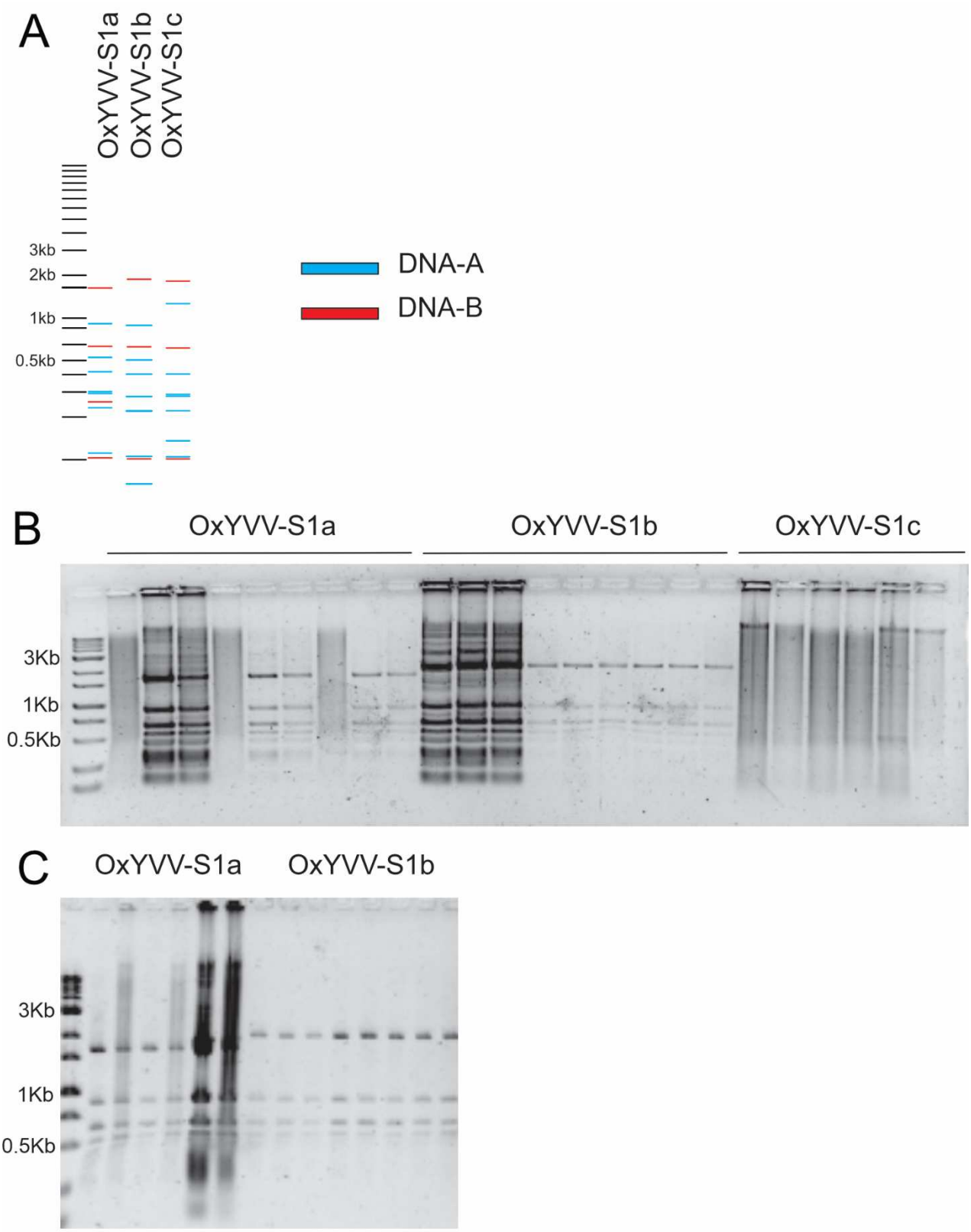
A
OxYVV-S1a
OxYVV-S1b
OxYVV-S1c
3kb
2kb
1kb
0.5kb
DNA-A
DNA-B
B
OxYVV-S1a
OxYVV-S1b
OxYVV-S1c
3Kb
1Kb
0.5Kb
C
OxYVV-S1a
OxYVV-S1b
3Kb
1Kb
0.5Kb

**Figure 2**

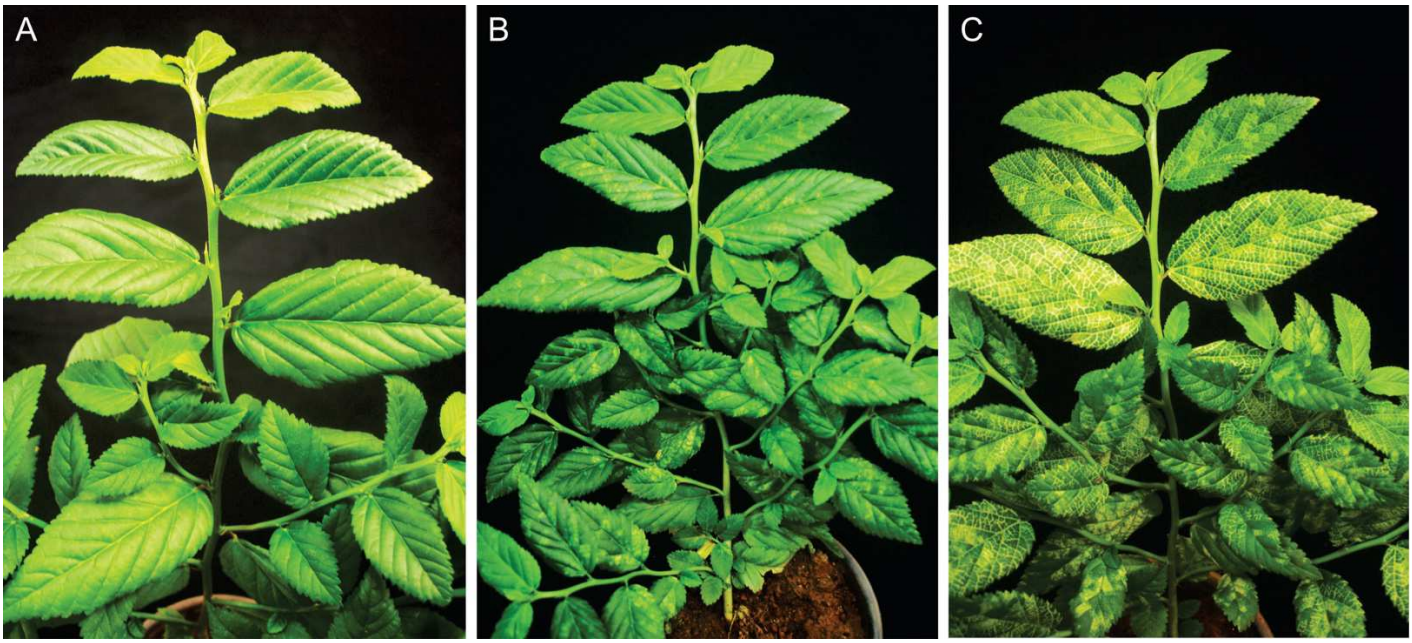

**Figure 3**

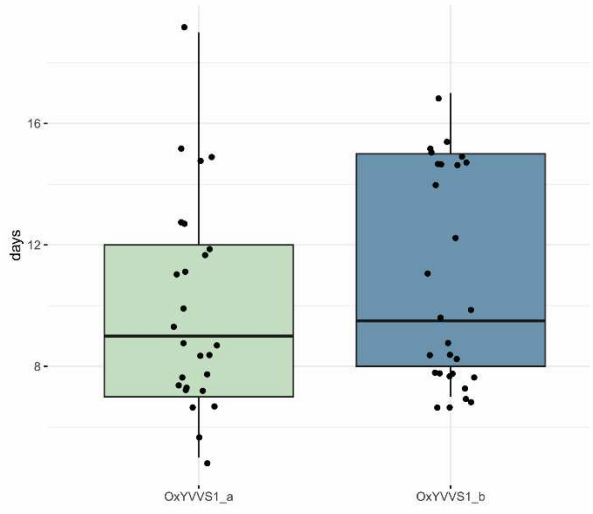

**Figure 4**

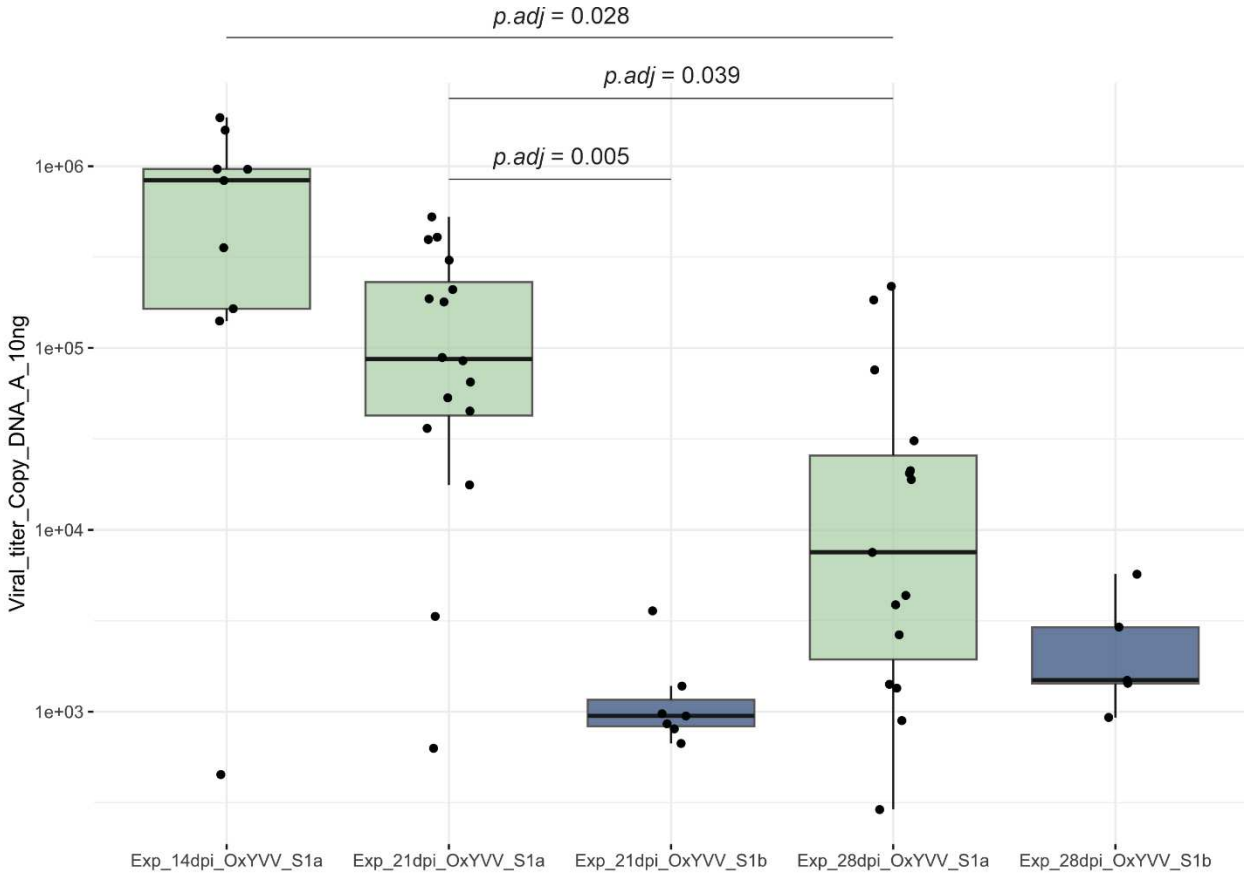
p.adj = 0.028
p.adj = 0.039
p.adj = 0.005
1e+06
1e+05
1e+04
1e+03
Viral_titer_Copy_DNA_A_10ng
Exp_14dpi_OxYVV_S1a
Exp_21dpi_OxYVV_S1a
Exp_21dpi_OxYVV_S1b
Exp_28dpi_OxYVV_S1a
Exp_28dpi_OxYVV_S1b

**Figure 5**

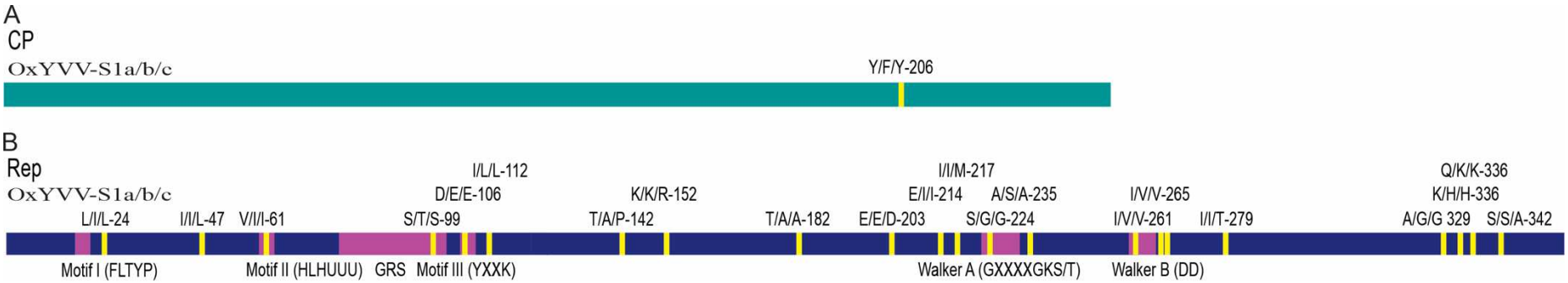
A
CP
OxYVV-S1a/b/c
Y/F/Y-206
B
Rep
OxYVV-S1a/b/c
L/I/L-24
I/I/L-47
V/I/I-61
S/T/S-99
I/L/L-112
D/E/E-106
K/K/R-152
T/A/P-142
T/A/A-182
E/E/D-203
I/I/M-217
E/I/I-214
A/S/A-235
S/G/G-224
I/V/V-265
I/V/V-261
I/I/T-279
Q/K/K-336
K/H/H-336
A/G/G 329
S/S/A-342
Motif I (FLTYP)
Motif II (HLHUUU)
GRS
Motif III (YXXK)
Walker A (GXXXXGKS/T)
Walker B (DD)

**Suppl. Figure S1**

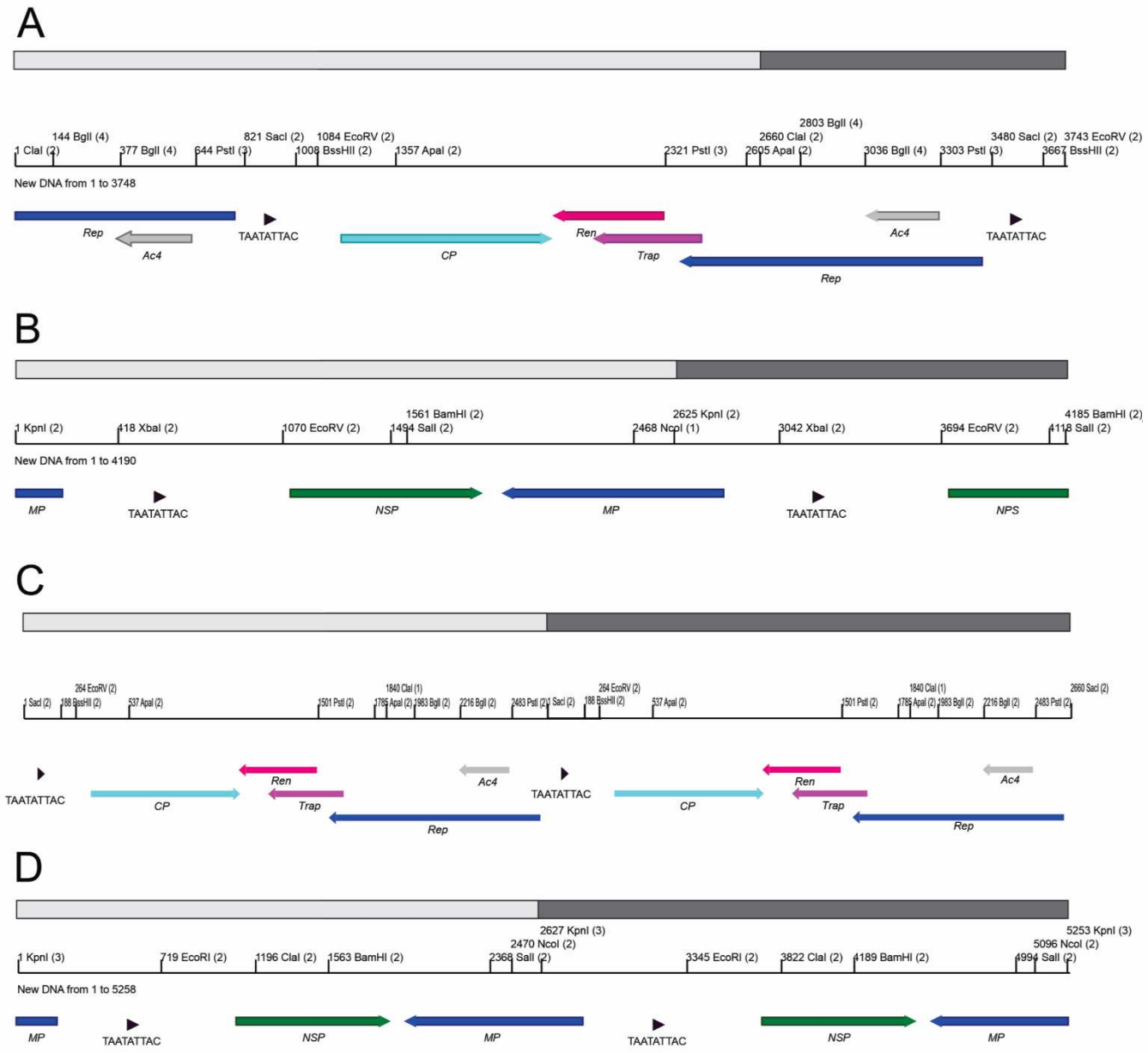

# GENERAL CONCLUSIONS

- Begomoviruses infecting *Sida acuta* plants coexist as complex communities, with populations formed by different variants, which makes these hosts an important reservoir of biodiversity.
- The level of genetic variability observed among different species suggest different evolutionary rates intrinsic to each species. It also reinforces differences in variability between the DNA-A and DNA-B components, suggesting that both have distinct evolutionary histories.
- The intensity with which natural selection acts on each region differs, and we identified that the *AC4* gene is under positive selection.
- Differences in terms of frequency distribution between species and their respective variants suggest differences in fitness.
- Although begomoviruses are prone to recombination, we found that in each species these events occur at different frequencies, leading us to believe that some viruses could be more prone to recombination than others. Furthermore, the recombination events detected in DNA-A and DNA-B of SiYLCV reveal a close evolutionary history with OxYVV.
- Our biological assays using infectious clones of two variants of OxYVV support the hypothesis of differential adaptability between the variants.
- As the OxYVV-S1a variant presents greater accumulation at the beginning of the infection compared to the OxYVV-S1b variant, this would increase its chances of being transmitted more efficiently.